

ROBOTIZATION OF HAND WOVEN CARPET TECHNOLOGY PROCESS

**A Thesis Submitted to
the Graduate School of Engineering and Sciences of
İzmir Institute of Technology
in Partial Fulfillment of the Requirements for the Degree of**

MASTER OF SCIENCE

in Mechanical Engineering

**by
Özgün SELVİ**

**January 2008
İZMİR**

We approve the thesis of **Özgün SELVİ**

Prof. Dr. Tech. Sc. Rasim ALİZADE
Supervisor

Asst. Prof. Dr. H. Seçil Altundağ ARTEM
Committee Member

Dr. Özgür KİLİT
Committee Member

02 January 2008

DATE

Assoc. Prof. Dr. Metin TANOĞLU
Head of the Department of
Mechanical Engineering

Prof. Dr. Hasan BÖKE
Dean of the Graduate School of
Engineering and Sciences

Learn from yesterday, live for today, hope for tomorrow.

The important thing is not to stop questioning...

Albert Einstein

ACKNOWLEDGMENTS

I would like to express my appreciation to my supervisor Prof. Dr. Tech. Sc. Rasim ALIZADE for his endless support and trust, encourage, ideas and comments throughout the all steps of this study. I would like to acknowledge to my parents for their support and patience. Also, I would like to thank to my colleagues in Intelligent Machines Laboratory for their help throughout this study.

ABSTRACT

ROBOTIZATION OF HAND WOVEN CARPET TECHNOLOGY PROCESS

This thesis covers a study on the structural design of new overconstrained mechanisms and manipulators and their application to the robotization of hand woven carpet technology process.

Moreover, recurrent vector equations are investigated for the synthesis of linkages, and used for the design of new mechanisms with linear-angular conditions in the subspace with general constraint one. These conditions are generalized for defining the structural groups of subspace $\lambda=5$ and these structural groups are used both for the creation of new parallel manipulators and new serial-parallel platform manipulators.

After investigating hand woven carpets, the knowledge gained during the structural design of mechanisms is applied to the robotization of hand woven carpet technology process. Finally, design of carpet weaving robot is introduced.

ÖZET

EL DOKUMA HALI TEKNOLOJİ PROSESİNİN ROBOTİZASYONU

Bu tez yeni kısıtlı mekanizmaların ve manipulatörlerin yapısal tasarımı üzerine bir çalışma ve el dokuma halı teknoloji prosesinin robotizasyonu üzerine uygulanmasını kapsamaktadır.

Linklerin sentezi için ardışık vektör denklemleri geliştirilmiş ve bir genel kısıtlı alt uzaydaki doğrusal ve açısal koşullu yeni mekanizmaların tasarımı için kullanılmıştır. Bu koşullar $\lambda=5$ alt uzayındaki yapısal grupların tanımlanması için genellenmiştir ve bu yapısal gruplar yeni paralel manipulatörlerin ve yeni seri-paralel platform tipli manipulatörlerin yaratılması için kullanılmıştır.

El dokuma halıları incelendikten sonra, mekanizmaların yapısal tasarımı sırasında edinilen bilgiler el dokuma halı teknoloji prosesinin robotizasyonu için uygulanmıştır. Son olarak halı dokuma robotunun tasarımı sunulmuştur.

TABLE OF CONTENTS

LIST OF FIGURES	ix
LIST OF TABLES	xi
CHAPTER 1. INTRODUCTION	1
1.1. Survey of Structural Design of Mechanism with General Constraint One	2
1.2. History of Carpet Manufacturing	6
1.3. Research on the Robotization of Hand Woven Carpet Technology Process	12
CHAPTER 2. THEORY OF UNIT VECTORS IN SPACE	14
2.1. Definition of a Unit Vector	14
2.2. Geometry of Two Unit Vectors	15
2.3. Geometry of Three Unit Vectors	16
CHAPTER 3. STRUCTURAL SYNTHESIS OF MECHANISMS WITH GENERAL CONSTRAINT ONE	20
3.1. Displacement of the Rigid Body in Space and Subspaces	20
3.1.1. Displacement of the Rigid Body in Space	21
3.1.2. Displacement of the Spherical RB on Planar Surface	22
3.1.3. Displacement of the Spherical RB on Spherical Surface	23
3.1.4. Displacement of the Planar RB with Constant Twist Angle on Planar Surface	24
3.1.5. Displacement of the Spherical RB on an Elliptic Torus	25
3.1.6. Displacement of the Planar RB on an Elliptic Torus	26
3.1.7. Displacement of the Elliptic Torus RB on an Elliptic Torus	26
3.2. Serial Manipulators in Subspaces with General Constraint One	27
3.3. Analytical Approach for the Overconstrained Mechanisms with General Constraint One	29
3.4. Overconstrained Mechanisms with General Constraint One	34

CHAPTER 4. STRUCTURAL SYNTHESIS OF MANIPULATORS WITH GENERAL CONSTRAINT ONE	41
4.1. Structural Synthesis of Overconstrained Parallel Manipulators	42
4.2. Structural Synthesis of Overconstrained Serial-Parallel Platform Manipulators	53
CHAPTER 5. HAND WOVEN CARPET TECHNOLOGY PROCESS.....	57
5.1. Terminology and Definitions.....	57
5.2. Technology Process of Hand Woven Carpets	59
5.3. Pattern Study for the Turkish Hand Woven Carpets	61
CHAPTER 6. DESIGN OF MECHANISMS FOR HAND WOVEN CARPET TECHNOLOGY PROCESS.....	65
6.1. Structural Design of Carpet Robot.....	66
6.2. Design of Mechanisms for the Carpet Weaving Process.....	66
6.1.1. Design of Mechanisms for Heddle Motion.....	67
6.1.2. Design of Mechanisms for Weft and Sley Motions.....	69
6.1.3. Design of Weaver Arm	73
6.1.4. Design of Weaver System.....	75
6.3. Design of Carpet Weaving Robot.....	80
CHAPTER 7. CONCLUSION	84
REFERENCES	85
APPENDIX A. Force and Strength Calculations of Carpet Loom.....	92

LIST OF FIGURES

<u>Figure</u>	<u>Page</u>
Figure 1.1. Pazırık Carpet	7
Figure 1.2. Types of Knots	8
Figure 1.3. Principle of Face to Face Weaving	9
Figure 1.4. Gripper Assembly for the Axminster Weaving.....	10
Figure 1.5. Tufting Mechanism	11
Figure 2.1. Elements of a Unit Vector	14
Figure 2.2. Geometry of Two Arbitrary Unit Vectors in Space	15
Figure 2.3 Geometry of Three Arbitrary Unit Vectors in Space	16
Figure 2.4. Joint and Link Parameters of a Spatial Link	18
Figure 3.1. Displacement of Rigid Body in Space	21
Figure 3.2. Sphere on Plane Motion	22
Figure 3.3. Sphere on Sphere Motion	24
Figure 3.4. Plane on Plane Motion with Constant Twist Angle	24
Figure 3.5. Motion of a Sphere on an Elliptic Torus	25
Figure 3.6. Motion of Plane on an Elliptic Torus	26
Figure 3.7. Elliptic Torus on Elliptic Torus.....	27
Figure 3.8 Parameters for RRRS Linkage	28
Figure 3.9. New 3D Overconstraint RRRS Linkage with Linear and Angular Constraint.....	33
Figure 4.1. End Effector Chain with Branch Loop.....	47
Figure 4.2. The Motion of End Effector	54
Figure 4.3. Structure of Overconstrained Serial Platform Manipulator	56
Figure 5.1. Carpet Structure.....	57
Figure 5.2. Loom Structure.....	58
Figure 5.3. Heddle Motions	58
Figure 5.4. Knot Types	59
Figure 5.5. General Design Structure for Turkish Carpets.....	64
Figure 5.6. Unique Carpet Pattern	64
Figure 6.1. Schematic Structure of the Carpet Weaving Robot.....	65
Figure 6.2. Forces Acting on the Loom	66

Figure 6.3. Double Slider Crank Mechanism	67
Figure 6.4. Slotted Slider Mechanism	68
Figure 6.5. Sprocket and Roller Chain	68
Figure 6.6. Rack and Pinion Mechanism.....	69
Figure 6.7. Holder and the Positions of the Holder	69
Figure 6.8. Double Four-Bar Mechanisms	70
Figure 6.9. Extension Mechanisms.....	70
Figure 6.10. Paths of the Mobile Robot System.....	72
Figure 6.11. The Robots for Wefting.....	72
Figure 6.12. Sley Mechanisms.....	73
Figure 6.13. Path for Sley Mechanism	73
Figure 6.14. Serial Robot Arms	74
Figure 6.15. Parallel Manipulator	74
Figure 6.16. Hybrid Manipulator	75
Figure 6.17. System for Preparing the Pile.....	76
Figure 6.18. Mechanism for Holding the Warps	76
Figure 6.19. Mechanism for Holding the Warps	77
Figure 6.20. The Path of the Pile	77
Figure 6.21. Four-Bar Mechanisms	78
Figure 6.22. Serial Fingers.....	78
Figure 6.23. Cylindrical Manipulator	79
Figure 6.24. Gripper for Grasping the Pile Ends	79
Figure 6.25. Positions of Mechanisms on the Loom	80
Figure 6.26. Work Order of the Carpet Robot.....	81
Figure 6.27. Detail of the Mobile Robot.....	81
Figure 6.28. Cylindrical Manipulators.....	82
Figure 6.29. The Weaver	83
Figure 6.30. Carpet Weaving Robot	83
Figure A.1. Free Body Diagram of the Cylindrical Beam.....	92
Figure A.2. Beam Loading and Boundary Conditions	93
Figure A.3. Outer and Inner Radius of the Cylindrical Beam	94
Figure A.4. Equilibrium of Warp Thread at Working Position.....	96

LIST OF TABLES

<u>Table</u>	<u>Page</u>
Table 3.1. Serial Manipulators.....	28
Table 3.2. Structural Bonding of Joint Axes	34
Table 3.3. 6R Mechanisms with General Constraint One	35
Table 3.4. Overconstrained 6R Mechanisms	39
Table 3.5. New Overconstrained 6R Mechanisms with Linear and Angular Conditions.....	40
Table 4.1. Possible Angular Conditions for the Subspace $\lambda=5$	42
Table 4.2. Possible Linear-Angular Conditions for the Subspace $\lambda=5$	43
Table 4.3. Simple Structural Groups with General Constraint one Respect to Angular and Linear-Angular Conditions	44
Table 4.4. Structural Bonding of Overconstrained Parallel Manipulators with Angular Conditions $\lambda=5, c_1=2$	49
Table 4.5. Structural Bonding of Overconstrained Parallel Manipulators with Linear-Angular Conditions $\lambda=5, c_1=2$	50
Table 4.7. New Angular and Linear-Angular Parallel Manipulators	52
Table 4.8. Steps for Constructing Overconstrained Manipulators.....	55
Table 4.9. Construction Steps for Overconstrained Serial Platform Manipulator.....	56
Table 5.1. Animal Figures Seen in Turkish Carpets.....	61
Table 5.2. Plant Figures Seen in Turkish Carpets.....	62
Table 5.3. Non-Living Figures Seen in Turkish Carpets.....	63
Table 6.1. Gripper Designs for the Holder	71
Table A.1. Moment of Inertia and Elastic Modulus Values for Different Materials ($L = 2$ m).	95
Table A.2. Alternatives of Inner and Outer Radii for Different Materials ($L = 2$ m)	95
Table A.3. Bearing Types From ORS Catalog.....	96

CHAPTER 1

INTRODUCTION

One of the definitions of a robotic system can be given as a re-programmable multi-functional manipulator that is designed to move materials, parts, tools or devices through variable programmed motions for desired tasks. A robotic system usually consists of a mechanical manipulator, a controller, a computer, external sensing devices and an end effector, which is a mechanical interface between the manipulator and its environment. A manipulator can be classified as a machine as it can transform external energy into useful work. Similar with machines, it is an assemblage of one or more mechanisms with other electrical, hydraulic or pneumatic components. Mechanisms are the vital parts of the machines. A mechanism is the combination of gears, cams, linkages, springs, and etc. Linkages can be defined as the collection of links that are connected with joints. Beside others, the linkage systems are the elementary subject of manipulators. By the help of knowing constraints imposed by the linkages, the subspace of the mechanism and the movement of mechanism could easily be described. Thus the relations of these linkages, their mobility effect on manipulators and over constraint conditions are investigated in this study as structural synthesis of manipulators with general constraint one. The reason for describing only one general constrained mechanism is the fact that it is one of the steps for defining the conditions of a mechanism in subspace as defined in the section titled analytical approach for overconstrained mechanisms. When a constraint is imposed on a space then the movements of rigid body in this space are restricted due to the configurations of linkages and this system is called as subspace. When a mechanism belongs to a subspace it can be defined as overconstrained mechanism. Note the sum of subspace and constraint numbers for the mechanism is always equal to the movements in spatial environment. Introducing the definition, the structural mobility can be defined as the difference between the sum of the mobility of joints in the system and the sum of subspaces of independent loops.

Although there are many definitions for a robot, the best one describes it as a mechanical being built to do routine manual work for human beings. These works can be exemplified as carrying loads, pick and place operations, welding, assembly and other industrial operations. In this thesis hand woven carpet process is selected as a subject for the new application area of robots; due to the fact that, there is no machine designed to do this work up to now thanks to the complicated structure of hand weaving operation and also making it manually takes much time and effort for a human being when compared with a robot.

1.1. Literature Survey of Structural Design of Mechanism with General Constraint One

A mechanism can be defined as a system that transmits mechanical motion via joints and links. If the DoF of a mechanism or manipulator is zero, it can be defined as a structural group, which can not be splitted into other groups with zero mobility. This property is related with one of the main problems of the linkage systems; that is, to determine whether a linkage is a mechanism or a structural group. Referring to the formula of Freudenstein and Alizade (1975), any 6R linkage has zero mobility for a spatial environment $\lambda=6$. When this linkage has any mobilities, it becomes an overconstrained mechanism that belongs to a lower environment, which is referred as subspace ($\lambda<6$).

Throughout the literature several overconstrained mechanisms with angular conditions has been discovered. First time Sarrus (1853) introduced an overconstrained mechanism which is a special case of planar-hybrid linkage that has six axes intersecting by pairs of three distinct points. Bennett (1905) introduced spherical-hybrid linkage and plano-spherical hybrid linkage with the criteria of intersecting six axes by pairs in two different points.

Also seven types of mobile 6R linkage with linear and angular conditions were discovered by Bricard (1927) and Goldberg (1943) constructed two Goldberg 6R overconstrained linkage by combining three Bennett loops with linear and angular conditions. As an inversion of Bricard's orthogonal 6R linkage, the "wirbelkette" overconstrained mechanism with equal links and zero offset of all joints was introduced by Franke (1951). Altmann (1954) presented a 6R linkage, which is actually special

case of the Bricard line symmetric linkage. The general model of the six link mechanism with six skew orthogonal axis and equality of link and offset lengths separately described by Harrisberger and Soni (1966). Waldron (1967-1969) proposed a family of overconstrained hybrid linkages and some of them are created by combining Bennett overconstrained linkages. Wohlhart (1987, 91) combined double Goldberg linkages to construct new over constrained hybrid 6R linkage. A special trihedral Bricard linkage was described by Schatz (1998) and a new asymmetrical 6R linkage has been obtained with single degrees of freedom.

Note that in these investigations geometric reasoning has been used and derivation of closed loop equations is not included in the search of new mechanisms. Later throughout the design the closed loop equations of overconstrained mechanisms have been obtained by using algebraic methods that are specialized to the geometry of overconstrained mechanisms. Starting with Bennett (1903), Baker (1993-2005) Mavroidis and Roth (1994, 1995), Karger (1998), Shih and Yan (2002), Lerbet (2005), Jin and Yang (2002), Dietmeier (1995), Alizade et al. (2007) deal with analytical methods. In these studies Bennett (1903) firstly gives analytical formulations for defining an overconstrained four bar mechanism and this research has many contributions to the mechanism science. Baker (1993-2005), investigated the analysis of the overconstrained Altmann's linkage by using geometric and algebraic ways and the determination of existence criteria of overconstrained five and six bar linkages analytically by using loop closure equations and screw algebra. A systematic approach is defined by Mavroidis and Roth (1994, 1995) in order to obtain and solve overconstrained mechanisms by analyzing a certain matrix to prove the overconstraint conditions of special structures as well as to obtain the input output equations of the mechanisms in analytical form and solve them algebraically. Also an overconstrained mechanism with two Bennett joints with no common axis is constructed by them. After classifying and describing all 5R overconstrained mechanisms with mobility one, Karger (1998) obtained another class of 5R closed kinematic chains with non-zero offsets by an analytical method that uses loop closure equations. Shih and Yan (2002) built up the geometric constraints and the steps for mechanisms dimensional synthesis based on the descriptive and analytical geometry and applied to 6R linkage mechanisms for the guidance of a cylindrical body between two positions. Likewise, Lerbet (2005) introduces mechanism analysis based on analytical geometry to analyze classical overconstrained mechanisms by using both the loop closure equations and explicitly the

relations of singularity, and creates a coordinate free method via Lie algebra. Jin and Yang (2002) verify the overconstraint conditions of the Bricard trihedral mechanism and derive closure conditions of a known 4R2P overconstrained mechanism based on an analytical method by using only four basic equations combined with a new technique in order to reduce the complexity of overconstraint analysis of the 6 link mechanism presented by them. Dietmeier (1995) has discovered a new family of overconstrained 6R linkages to solve the loop closure equation by using the algebraic and the numerical methods. Moreover, Huang and Sun (2000) investigated the finite displacements of all known Bennett based 6R overconstrained linkages by the help of numerical solutions and they found that every Bennett based 6R linkage, except the isomerization of Wohlhart's hybrid linkage, relates with the properties of the Bennett mechanism. Lastly Alizade et al. (2007) presented not only the way to determine conditions of overconstrained mechanisms with analytical methods are given but also new mechanisms are proposed for these conditions, the recurrent unit vector relations are used in the calculations of this study.

Furthermore, Dai et al. 2006 propose a new approach to the mobility analysis based on the motion decompositions and constraints in screw systems. To predict the platform degrees of freedom accurately and to eliminate the redundant constraints, they present new versions of mobility criterion. Similarly a symmetry-extended mobility rule for mechanical linkages is proposed, where the traditional mobility rules for a linkage is included and strengthened with a new equation by Guest and Fowler (2005) and applied to the overconstrained mechanisms

A parallel manipulator is defined as a platform connected to the ground at least with two legs and motors that are distributed to these legs. One of the few investigations about parallel manipulators with two legs is done by Li et al. (2006) is related to a 2 DoF parallel mechanism with spherical output. They also applied a workspace analysis for the mechanism. The only investigation known to us about overconstrained parallel manipulators with two legs is done by Gogu (2005). An approach for structural synthesis of overconstrained parallel wrists with 2 DoF has been proposed in his study. The property of the overconstrained mechanism is the fact that it gives a spherical output with a singularity free and fully isotropic structure.

Neville and Sanderson (1996) investigates the synthesis of unit cells which could be used in creating structures for building up parallel robots and gives the way for the computation of kinematics for the control of actuated system. In their study Tishler et

al. (2001) inspected the selection of an appropriate kinematic chain from the many by describing variety and its relationship with the motion capabilities of mechanisms. New families of translational parallel manipulators with independent constraints are represented by Gregorio (2002), where manipulators have three identical limbs with no rotation singularity. The synthesis topology of parallel manipulators and the use of qualitative reasoning was interpreted in the study of Angeles (2002) and new kinematic bonds producing Schönflies motion were proposed with various examples. After describing several types of composite pairs and new kinds of sub-chains with specific degrees of freedom, Gao et al. (2002) gives the principle for design of sub 6 DoF parallel manipulator based on the special Plücker coordinates that describes the displacement of sub-chains. Huang and Li (2002) proposed a general constraint synthesis method for the type synthesis of lower mobility by using a reciprocal screw system for the mechanism and the limbs. Via the proposed method they presented some novel lower mobility manipulators with 3, 4 and 5 DoF. By using the properties of planar-spherical kinematic bonds and Lie groups Herve (2007) gather many known and novel parallel mechanisms. Fang and Tsai (2004) interpreted a systematic methodology for the structural synthesis of a class of 3 DoF rotational parallel manipulators and the enumeration of kinematic structures is done via theory of reciprocal screws in their research. Also they proposed a systematic methodology for the structural synthesis of general and overconstrained 3 DoF translational parallel manipulators. A novel method for generating classes of orthogonal Gough-Stewart Platforms is described by Yi et al. (2004). Also redundant isotropic manipulators with even number of studs are derived in their study. In the research of Meng et al. (2005), a geometric theory is developed for the synthesis and analysis of sub-6 DoF parallel manipulators, where the set of desired end effector motions fit a Lie subgroup or a regular sub manifold. 3 DoF translational parallel manipulators are introduced by Lee and Herve (2006) by using the Lie group algebraic properties of the displacement set. All possible 5 DoF limbs generating double-planar bonds are enumerated for spatial translational motion.

The structural formula for parallel manipulators working in space or subspaces is given by Alizade and Bayram (2004). While giving a procedure for the synthesizing of structures of parallel manipulators using simple structural groups they also define a classification for parallel manipulators based on the number of mobile platforms, number of joints, number of legs and branches. After revising all structural formulations for parallel manipulators, Alizade et al. (2006) give a new formulation for

not only the creation of new manipulators such as Cartesian and serial platform manipulators, but also for the calculation of pre-designed manipulators. Moreover, Alizade et al. (2007) proposed a method for the structural synthesis of Euclidean platform robot manipulators with general constraints. Also the new structural classification of simple structural groups with variable general constraints including platforms, hinges, legs and branch loops from different subspaces and space is introduced by them. Furthermore in the scientific work of Alizade et al. (2007) Euclidean, overconstrained parallel platform manipulators, and serial-parallel platform manipulators with variable general constraints are presented and structural formulations are proposed.

1.2. History of Carpet Manufacturing

Carpet is a thick loom-woven textile floor covering which is firstly started to use by nomads. Carpets can be categorized in three types as woven, tufted and needle-felt carpets. Hand woven carpets are produced on a loom by knotting many different colored yarns one by one, thus this type of carpet is the most valuable and durable one. Tufted and needle-felt types are the machine made carpets with faster production lines. Note that needle-felt type carpets are the nearest simulation of hand made carpets.

We get the information about when, by whom and how hand-woven carpets are weaved from the archeological excavations and the researches of scientists studying in this area. From the pieces that found in the archeological excavations gives information about the age and the quality of that carpet. The results of these researches show us that, hand woven carpet technology improved by color, size and ornament knotting styles till this day from old times. Hand-woven carpet is the only product that preserves its importance and basic structure till 3000 years in the world textile history.

The oldest hand-woven carpet is found in the mounds at Pazırık in the foothills of the Altai Mountains by Russian archeologist Rudenko (Figure 1.1). The carpet is almost square (1.83 x 2 meters) and displayed in the Hermitage museum in Leningrad. The material of the Pazırık carpet is wool and it is weaved by Turkish knotting technique. It is interesting that this carpet has a good quality with respect to its period and has 3600 knots per dm^2 (Ellis 1976).

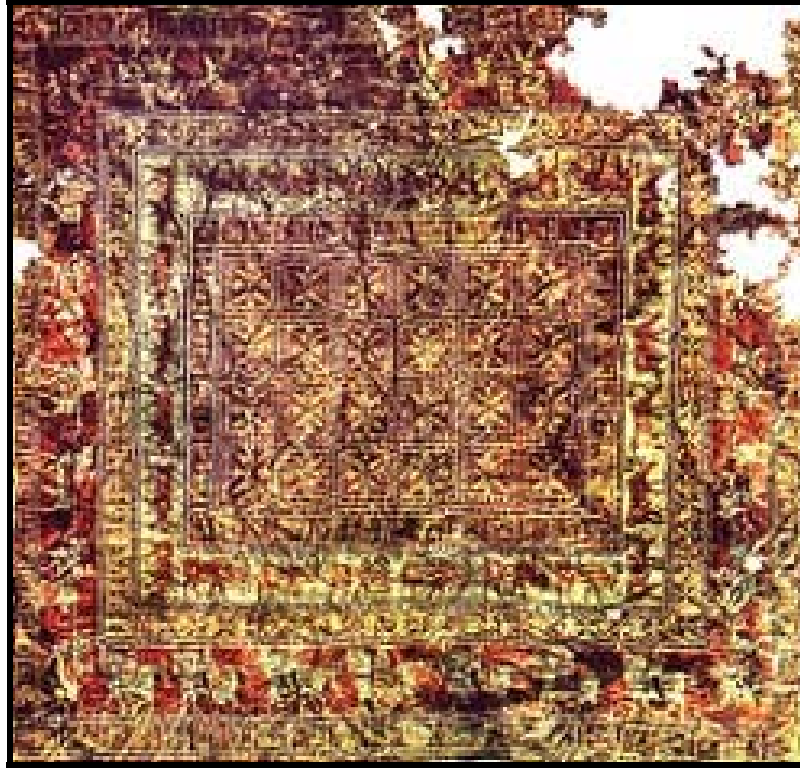


Figure 1.1. Pazırık Carpet.
(Source : Best Iran Travel 2007)

The history of the carpet is closely linked to the Turkish people, who are most probably originates the pile technique. Also carpet weaving is one of the most important subjects of Turkish art history (Yetkin 1981). The carpet is used firstly for floor covering and some other issues however, later it becomes a valuable art and used in the castles, palaces and chateaus. It should be noted that carpet making is one of the oldest weaving arts.

The carpet with knots is occurred in the presence of the Seljuk reign in the 11th century. The centers of carpet weaving in 11th century are Konya, Kayseri, and Sivas. The property of Seljuk carpets is that they have patterns with geometric motifs. Main characteristic of these carpets are the big kufic writings on the borders. The heritage of Seljuk carpets can be seen at the Yahyalı region of Kayseri. In the 13th and 14th century Carpet weaving in Anatolia is reached its maximum potential. In 12th century carpets are produced at homes but in 13th century carpets are started to woven in big sizes at the workshops. These valuable carpets can be seen across the museums of Europe. In 14th century small squared geometric motifs are weaved. Unfortunately the 15th century is a dark period for carpet making. After a 200-year history of carpet making

during the Seljuk reign carpet weaving is nearly disappeared at 15th century in Ottoman Empire. The 16th and the 17th centuries were second bright period for carpet weaving. In this period lots of carpets are weaved for supplying the requirements of Ottoman palaces and mosques so the Ottoman architecture traces can be seen in the patterns of this period. Although the carpets are rich about the motifs and has high quality, they could not reach to the Seljuk period. In the 18th and 19th centuries export directed carpet manufacturing is started so during this period the carpet get an importance as an economic subject thus the art property fall in to the second plan. Till today the carpet produced as an economic material. Today in some regions of Anatolia partially consequent to the art tradition but trade dependent carpet weaving continues.

Knot types used in hand-woven carpets (Figure 1.2) can be classified with respect to their usage in two general forms as Ghordes knot, also known as symmetrical knot or double knot and Persian knot (non-symmetrical knot or single knot). Although the knot types are classified with respect to the regions, these knot types are widely used in all regions. There is also many kind of knots that are used in some regions of Europe and Asia but they are neither broad nor effective. As stated in the researches of Kühnel (1958) and Deniz (2000) a weaver can tie 15 knots per minute so that a weaver can tie 900 knots per hour and the maximum number of knots for a weaver in one day is 7000 knots.

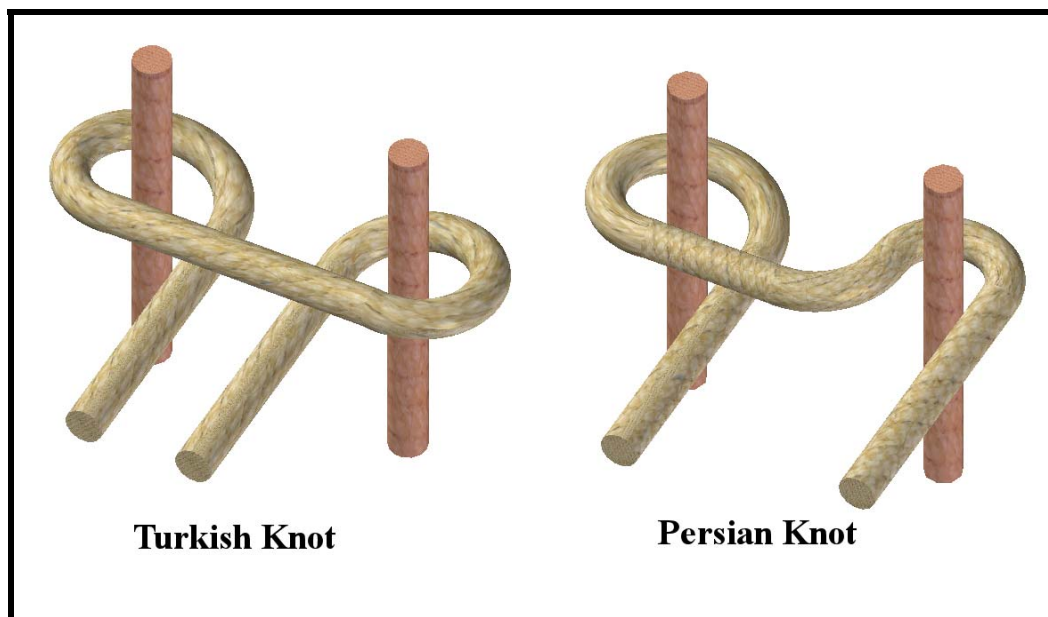


Figure1.2. Types of Knots.

The quality factor is an important subject for hand woven carpets. The knot density, defined as knots per a unit square usually 1 dm² is the first thing to be considered. In high quality carpets knot density gets up to 80Vx80H knots per decimeter square. The knot density is not the only factor for deciding the quality. The quality of the raw material, the quality of dye and the experience of carpet weaver also affect the final quality. Another thing is that the yarns used in weaving process must be specially prepared. Warp threads must be placed straight and piles must be cut at each two rows.

At the beginning of 1900's, when the developing technology and enhanced of industry affect the textile industry, carpet making is started to be made by machines. The main properties of this type of carpets are their faster production rates and low costs however the disadvantage of machine made carpets is the fact that the producers concede from quality and use easy produced materials. Also the durability of hand woven carpets can not be reached by machine weaving. Note that there is no machine in textile industry that can make one-to-one copy of hand-woven carpet. Machine made carpets can be divided in to two main categories, such as weaved and tufted carpets. Weaved carpets are classified as face to face weaving, Axminster weaving and Wilton construction. Between these methods face to face weaving is the most productive method currently available (Figure 1.3). In this method pile warps are connected to the backing fabric which is woven one above the other under strong tension. After the beat-up of the loom the pile warps are cut by a knife mechanism with a reciprocating motion to separate the two fabrics for creating two carpets. The pile height of carpet is determined by the distance between the top and bottom cloths. Heald shafts are moved by cams or other devices on the side of the loom and ground warps are drawn in to these.

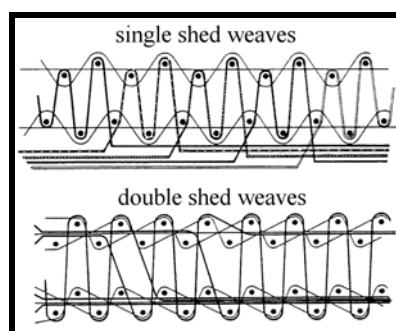


Figure 1.3. Principle of Face to Face Weaving.

(Source: Grawshaw 1987)

Another weaving type, Axminster weaving, has an ease of operation and it is possible to simulate hand-knotted products by using a gripper system for the selection of piles (Figure 1.4). One of the important properties of this type of weaving is the fact that it can apply patterns to the carpets by using different colors of pre-dyed piles. Spool Axminster weaving is used for producing the highly patterned multi color (up to 50 color). But they are no longer produced because of high labor cost and generation of waste pile yarn. The last type of carpet weaving machines, Wilton construction. It is also a multi colored type and has the properties of combining different yarns or different pile structures such as cut pile and loop pile. So, carved or sculptured effects are produced.

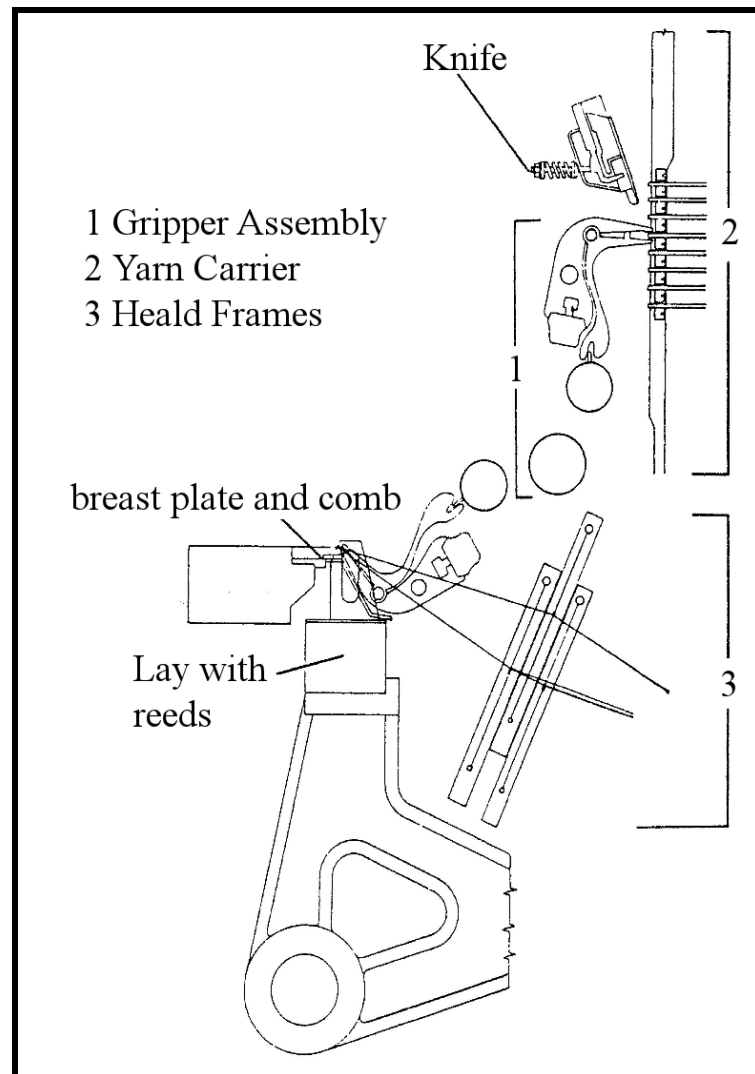


Figure 1.4. Gripper Assembly for the Axminster Weaving.

(Source: Grawshaw 1987)

Mechanized tufting machine is developed in 1930's at USA, Dalton. In this machine the yarn that is fed from a supply creel enters the ends of the guide tubes which leads all the individual yarns to the top of the tufting machine. There are guide bars that feed yarns to the positively driven feed rollers. The yarn is then get through a movable yarn guide and a further yarn guide, which is attached to the needle bar. The bar next to the needle bar moves up and down with the needle bar during insertion and withdrawal of the needles. At last the yarn is get to its needle. A vertical reciprocating motion is given to the row of vertical needles that are arranged transversely across the machine. Then the needles pass through the slots of a reed plate. After this operation, the needle pierces the backing fabric, which is drawn by a spiked roller. During the insertion of the needle a looper is actuated by the looper shaft and passes between the yarn and the needle. A presser bar prevents backing from rising as the needles are withdrawn (Figure 1.5) (Grawshaw 1987).

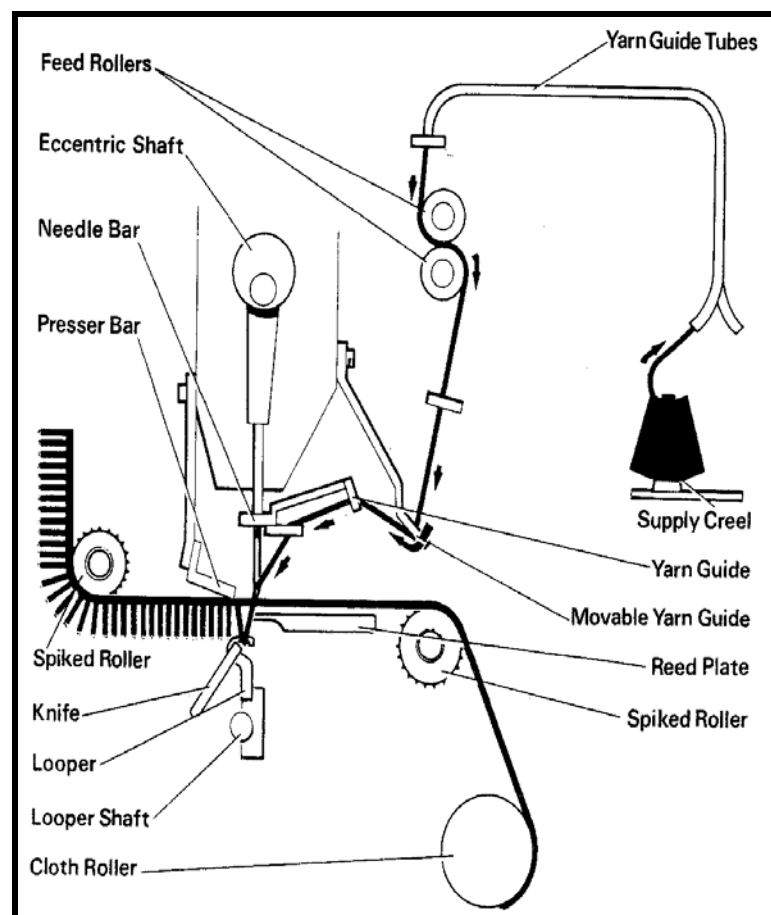


Figure 1.5. Tufting Mechanism.

(Source: Grawshaw 1987)

As it is difficult to make a one-to-one copy of hand-woven carpet and hand-woven knot there is only one research we know throughout the literature that is done by Topalbekiroğlu et al. (2005). In this investigation, the electro-pneumatic knotting system is proposed pattern study is examined and a control system is represented.

1.3. Research on Robotization of Hand Woven Carpet Technology

Process

Over constrained linkages are examined and researches in this area are considered. It is seen that defining the parameter of linkages by analytical methods is an important subject that is not investigated enough. The need for defining a method for the determination of linear-angular constraints of overconstrained mechanisms is vital. Also, after examining the literature about parallel manipulators, mobility analysis and platform manipulators, it is seen that there is not such a definition that describes the overconstrained parallel and platform manipulators and the structural design of these types of manipulators is not found in the literature. After these researches, the subject for robotization is selected as the carpet technology process for the industrial and social reasons in this area such as necessity of machinery that simulates the woven carpets as humans do, lack of labor in this area, negative effects on human health and child labor. Then history of hand woven carpets is introduced to clearly define the process of hand woven carpets. Finally machine made carpets are represented for the comparison with the hand woven ones.

To apply kinematics on linkage systems, a tool is needed such as unit vector algebra, screw theory, transformation matrices, quaternion, biquaternion and etc. Each method has its advantages and disadvantages. Because of the simplicity, improvability, adaptability and applicability properties, the unit vector algebra is selected. In second chapter of this study, definitions for a unit vector, two unit vectors and three unit vectors are given. The method for the calculations of third unit vector from given two unit vectors, where each vector is recurrent, is defined as well as the application of this method on linkage systems.

After defining the geometrical properties and relations of unit vectors in space in the third chapter, not only an analytical method for finding new overconstrained mechanisms with general constraint one is given but also all the mechanisms with

general constraint one with revolute joints are given for further uses in the design of parallel manipulators. The method proposed in this study can be summarized as the derivation of parameters that turns an RRRS structure in space to a novel RRRS mechanism in subspace with general constraint one by using newly proposed recurrent unit vector equations with loop closure equations. And new mechanisms with linear-angular conditions are presented.

Subsequent to the definition of all the mechanisms in subspace with general constraint one, in the fourth chapter the structural groups that can be generated as parallel manipulators are given. Moreover the calculation of mobility not only for all the manipulators but also for one general constrained parallel manipulators is explained. After defining all single loop parallel manipulators and expressing the way to construct overconstrained parallel manipulators. The proposed method is applied to the serial and parallel platform manipulators with loops of same or different conditions. Application is also supported with example.

In chapter five, firstly the terminology and the definitions of the carpet technology process that are needed to be known are summarized. Then the steps of the process are detailed in three main groups as pre-weaving operations, weaving operations and finishing operations. Furthermore the ornaments of Turkish hand woven carpets are tabulated with definitions to describe a way of combining these ornaments and getting new patterns.

In the sixth chapter, the motions of carpet weaving process are defined. These motions can be listed as heddle motion, motion of wefting, sley motion and motions in the weaving of the knot. Then some mechanisms are proposed for each motion and the best available ones are detailed for construction. Also additional mechanisms that can be used either in this research or in other robotic subjects are given.

CHAPTER 2

THEORY OF UNIT VECTORS IN SPACE

In this thesis, unit vectors and their relations in space are used as a tool for defining new mechanisms. In this chapter some information about unit vectors, vector calculations and vector equations will be given.

2.1. Definition of a Unit Vector

The components of a unit vector in space can be described with parameters l , m , n which are belong to the x , y , z coordinates of Cartesian system O as shown in Figure 2.1

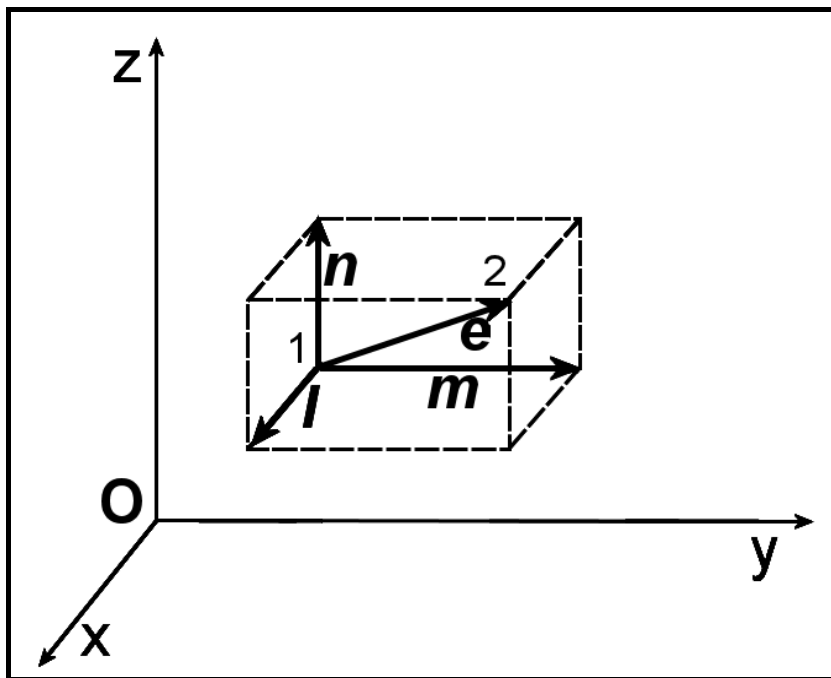


Figure 2.1. Elements of a Unit Vector.

Let the direction ratios of e_{21} be l , m , n as shown in Equation (2.1).

$$l = x_2 - x_1, \quad m = y_2 - y_1, \quad n = z_2 - z_1 \quad (2.1)$$

Finally calculations for unit vector algebra can be given as follows,

- $\mathbf{e}_1 \pm \mathbf{e}_2 = [l_1 \pm l_2, m_1 \pm m_2, n_1 \pm n_2]^T$
- $\mathbf{e}_1 \cdot \mathbf{e}_2 = \text{Cos}\alpha_{12} = l_1 l_2 + m_1 m_2 + n_1 n_2$
- $\mathbf{e}_1 \times \mathbf{e}_2 = \text{Sin}\alpha_{12} \mathbf{n}$
- $\frac{\mathbf{e}_1}{e_1} = \frac{\mathbf{e}_1 \cdot \mathbf{e}_2}{e_2^2}$

(2.2)

2.2 Geometry of Two Unit Vectors

A rigid body in space can be described by two unit vectors \mathbf{e}_1 and \mathbf{e}_2 (Figure 2.2). The angle and the minimum distance between these two unit vectors is defined with α_{12} and a_{12} consequently.

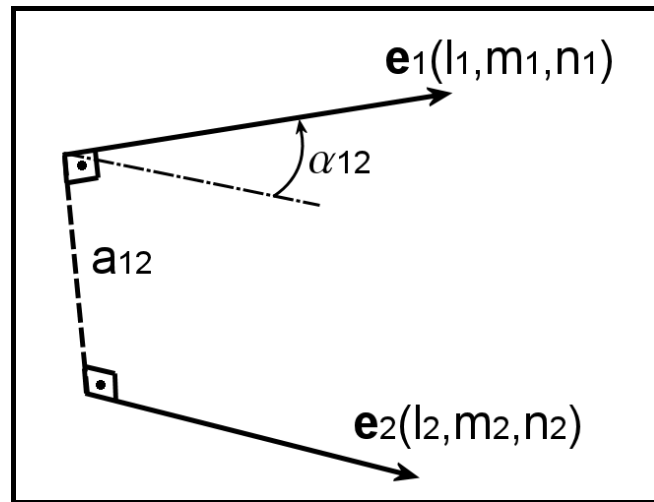


Figure 2.2. Geometry of Two Arbitrary Unit Vectors in Space.

For these two unit vectors, one can write the following equations:

$$\begin{aligned} \mathbf{e}_1 \cdot \mathbf{e}_1 &= e_1^2 = l_1^2 + m_1^2 + n_1^2 = 1 \\ \mathbf{e}_2 \cdot \mathbf{e}_2 &= e_2^2 = l_2^2 + m_2^2 + n_2^2 = 1 \\ \mathbf{e}_1 \cdot \mathbf{e}_2 &= l_1 l_2 + m_1 m_2 + n_1 n_2 = \text{Cos}\alpha_{12} \end{aligned}$$
(2.3)

Note that if the angle $\alpha_{12} = 0^\circ, 180^\circ$ that means these unit vectors are said to be parallel and when $\alpha_{12} = 90^\circ, 270^\circ$ that means these unit vectors are said to be skew diagonal.

2.3 Geometry of Three Unit Vectors

Three arbitrary unit vectors in space $\mathbf{e}_i, \mathbf{e}_j, \mathbf{e}_k$ are shown in Figure 2.3

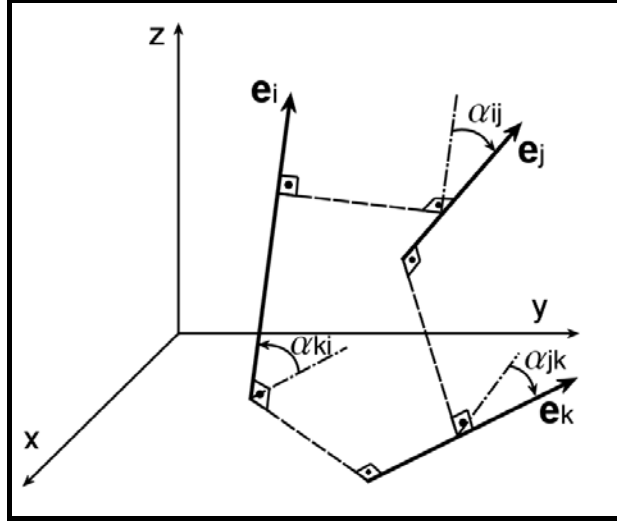


Figure 2.3 Geometry of Three Arbitrary Unit Vectors in Space.

To define $\mathbf{e}_k(l_k, m_k, n_k)$ from given unit vectors $\mathbf{e}_i(l_i, m_i, n_i)$ and $\mathbf{e}_j(l_j, m_j, n_j)$, some calculations should be carried out. Firstly the unit vector \mathbf{e}_k can be defined by the following equations

$$\begin{aligned} \mathbf{e}_k \cdot (\mathbf{e}_i \times \mathbf{e}_j) &= C\alpha_{kn} S\alpha_{ij} \\ \mathbf{e}_k \cdot \mathbf{e}_i &= C\alpha_{ki} \\ \mathbf{e}_j \cdot \mathbf{e}_k &= C\alpha_{jk} \end{aligned} \quad (2.4)$$

where, C stands for Cosine and S stands for Sine, α_{kn} stands for the angle between \mathbf{e}_k and the plane constructed by \mathbf{e}_i and \mathbf{e}_j . Writing Equation (2.4) in coordinate form we have

$$\begin{aligned} l_k l_{ij} + m_k m_{ij} + n_k n_{ij} &= C\alpha_{kn} S\alpha_{ij} \\ l_k l_i + m_k m_i + n_k n_i &= C\alpha_{ki} \\ l_k l_j + m_k m_j + n_k n_j &= C\alpha_{jk} \end{aligned} \quad (2.5)$$

where, $l_{ij} = m_i n_j - n_i m_j$, $m_{ij} = n_i l_j - l_i n_j$, $n_{ij} = l_i m_j - m_i l_j$

Solving the three linear equations (2.5) will result in the parameters of \mathbf{e}_k

$$\begin{aligned} l_k &= (l_i A_1 + l_j A_2 + l_{ij} S \alpha_{ij} C \alpha_{kn}) S^{-2} \alpha_{ij} \\ m_k &= (m_i A_1 + m_j A_2 + m_{ij} S \alpha_{ij} C \alpha_{kn}) S^{-2} \alpha_{ij} \\ n_k &= (n_i A_1 + n_j A_2 + n_{ij} S \alpha_{ij} C \alpha_{kn}) S^{-2} \alpha_{ij} \end{aligned} \quad (2.6)$$

where, $A_1 = C \alpha_{ki} - C \alpha_{jk} C \alpha_{ij}$, $A_2 = C \alpha_{jk} - C \alpha_{ij} C \alpha_{ki}$

As we know the condition for a unit vector $\mathbf{e}_k \cdot \mathbf{e}_k = l_k^2 + m_k^2 + n_k^2 = 1$, by substituting quantities of l_k, m_k, n_k to this equation we can define angle α_{kn} as a function of α_{ki} and α_{jk}

$$\alpha_{kn} = \text{Cos}^{-1} \left(\pm \frac{\left(S^2 \alpha_{ij} - C^2 \alpha_{ij} - C^2 \alpha_{jk} + 2C \alpha_{ki} C \alpha_{jk} C \alpha_{ij} \right)^{1/2}}{S \alpha_{ij}} \right) \quad (2.7)$$

Sign (\pm) indicates the two possible directions of vector \mathbf{e}_k with respect to the plane constructed by \mathbf{e}_i and \mathbf{e}_j . Considering Equation (2.7) generalized form of $\mathbf{e}_k (l_k, m_k, n_k)$ can be written as follows;

$$\begin{aligned} l_k &= (l_i A_1 + l_j A_2 + l_{ij} A_3) S^{-2} \alpha_{ij} \\ m_k &= (m_i A_1 + m_j A_2 + m_{ij} A_3) S^{-2} \alpha_{ij} \\ n_k &= (n_i A_1 + n_j A_2 + n_{ij} A_3) S^{-2} \alpha_{ij} \end{aligned} \quad (2.8)$$

where, $A_3 = \left(S^2 \alpha_{ij} - C^2 \alpha_{ij} - C^2 \alpha_{jk} + 2C \alpha_{ki} C \alpha_{jk} C \alpha_{ij} \right)^{1/2}$

After defining geometry of three unit vector in space we will define geometry of three recurrent unit vectors. These recurrent unit vectors will describe links and joints of the mechanisms including link and kinematic pair parameters.

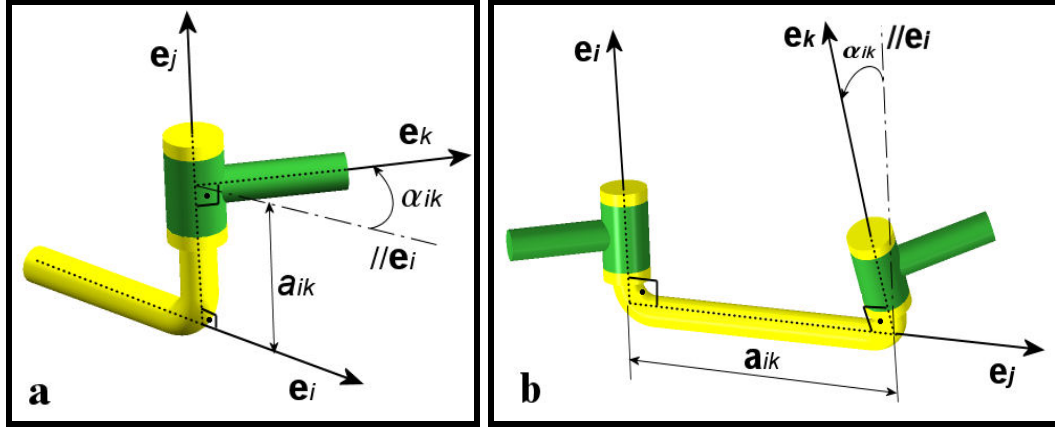


Figure 2.4. Joint and Link Parameters of a Spatial Link.

As shown in Figure 2.4 the components of three independent vectors \mathbf{e}_i , \mathbf{e}_j , \mathbf{e}_k describe the joint parameters as $d_j = a_{ik}$ and $\theta_j = \alpha_{ik}$ (Figure 2.4a), and also the link parameters as $a_j = a_{ik}$ and $\alpha_j = \alpha_{ik}$ (Figure 2.4b). In any case, two unit vectors $\mathbf{e}_i = [l_i, m_i, n_i]^T$ and $\mathbf{e}_k = [l_k, m_k, n_k]^T$ will describe the directions of links for joint parameters and the directions of joints for link parameters. The directions of joint and link are a unit vector, $\mathbf{e}_j = [l_j, m_j, n_j]^T$ as shown in Figure 2.4a and Figure 2.4b, respectively. Note that, for revolute pair, parameters α_{ik} is variable while a_{ik} is constant (Figure 2.4a), but for prismatic pair, while parameters α_{ik} is constant a_{ik} is variable.

Now let the directions of two unit vectors \mathbf{e}_i and \mathbf{e}_j are known. Knowing the two of the directions, our problem is to compute the direction of the third unit vector \mathbf{e}_k . Throughout the solution of this problem, first we will describe the vector equations of the three unit vectors as,

$$\begin{aligned}
 1) \quad & \mathbf{e}_i \times \mathbf{e}_k = \mathbf{e}_j \text{Sin}\alpha_{ik} \\
 2) \quad & \mathbf{e}_i \cdot \mathbf{e}_k = l_i l_k + m_i m_k + n_i n_k = \text{Cos}\alpha_{ik} \\
 3) \quad & \mathbf{e}_j \cdot \mathbf{e}_k = l_j l_k + m_j m_k + n_j n_k = 0
 \end{aligned} \tag{2.9}$$

The first equation of Equations (2.9) can be expressed in algebraic form as

$$(l_j \mathbf{i} + m_j \mathbf{j} + n_j \mathbf{k}) \text{Sin}\alpha_{ik} = (m_i n_k - n_i m_k) \mathbf{i} + (n_i l_k - l_i n_k) \mathbf{j} + (l_i m_k - m_i l_k) \mathbf{k} \tag{2.10}$$

where, \mathbf{i} , \mathbf{j} , \mathbf{k} are unit vectors along three orthogonal axes, x, y and z, respectively.

Expanding Equation (2.10) yields,

$$\left. \begin{aligned} l_j \text{Sin}\alpha_{ik} &= 0l_k - n_i m_k + m_i n_k \\ m_j \text{Sin}\alpha_{ik} &= n_i l_k + 0m_k - l_i n_k \\ n_j \text{Sin}\alpha_{ik} &= -m_i l_k + l_i m_k + 0n_k \end{aligned} \right\} \quad \text{or} \quad \mathbf{e}_j \text{Sin}\alpha_{ik} = \mathbf{A}_i \mathbf{e}_k, \quad (2.11)$$

$$\text{where, } \mathbf{A}_i = \begin{bmatrix} 0 & -n_i & m_i \\ n_i & 0 & -l_i \\ -m_i & l_i & 0 \end{bmatrix}, \quad \mathbf{e}_k = \begin{bmatrix} l_k \\ m_k \\ n_k \end{bmatrix}, \quad \mathbf{e}_j = \begin{bmatrix} l_j \\ m_j \\ n_j \end{bmatrix}$$

If both sides of the Equation (2.11) are multiplied by \mathbf{e}_j^T , the result will be

$$\mathbf{e}_j^T \mathbf{e}_j \text{Sin}\alpha_{ik} = \mathbf{e}_j^T \mathbf{A}_i \mathbf{e}_k \quad \text{or} \quad \text{Sin}\alpha_{ik} = \mathbf{B}^T \mathbf{e}_k \quad (2.12)$$

$$\text{where, } \mathbf{e}_j^T \mathbf{e}_j = 1, \quad \mathbf{B}^T = \mathbf{e}_j^T \mathbf{A}_i, \quad \mathbf{B}^T = [l_{ij} \ m_{ij} \ n_{ij}]^T,$$

$$l_{ij} = m_j n_i - n_j m_i, \quad m_{ij} = n_j l_i - l_j n_i, \quad n_{ij} = l_j m_i - m_j l_i$$

Using Equation (2.12), the set of Equations (2.9) will be converted to the following form,

$$\mathbf{B}^T \mathbf{e}_k = \text{Sin}\alpha_{ik}, \quad \mathbf{e}_i \cdot \mathbf{e}_k = \text{Cos}\alpha_{ik}, \quad \mathbf{e}_j \cdot \mathbf{e}_k = 0 \quad (2.13)$$

Solution of the set of Equations (2.13) results in,

$$\mathbf{C}\mathbf{b} = \mathbf{e}_k \quad (2.14)$$

$$\text{where, } \mathbf{b} = [\text{Sin}\alpha_{ik} \ \text{Cos}\alpha_{ik} \ 0]^T, \quad \mathbf{C} = [\mathbf{B} \ \mathbf{e}_i \ \mathbf{e}_j]$$

Finally Equation (2.14) gives us the recurrent unit vector equations as;

$$\begin{aligned} l_k &= l_{ij} \text{Sin}\alpha_{ik} + l_i \text{Cos}\alpha_{ik} \\ m_k &= m_{ij} \text{Sin}\alpha_{ik} + m_i \text{Cos}\alpha_{ik} \\ n_k &= n_{ij} \text{Sin}\alpha_{ik} + n_i \text{Cos}\alpha_{ik} \end{aligned} \quad (2.15)$$

Recurrent unit vector equations, Equations (2.15), can be used to describe an orientation of a rigid body with respect to reference frame.

CHAPTER 3

STRUCTURAL SYNTHESIS OF MECHANISMS WITH GENERAL CONSTRAINT ONE

Since Bennett (1903) defined a new overconstrained mechanisms with linear-angular conditions there has been a wide interest on this type of linkages during the history of mechanisms, and many overconstrained mechanisms have discovered. These linkages are tabulated in Table 3.2. However during the synthesis of these linkages, only angular conditions are used. Not only the mechanisms with linear-angular conditions are relatively rare, but also they are synthesized by combinations of Bennett and angular conditions. During the research of new overconstrained mechanisms, the interest is concentrated only on mechanisms with revolute joints, for the fact that this research is a step for determining overconstrained mechanisms. The method proposed in this study might be applied not only to the mechanisms with prismatic or screw pairs but also some overconstrained mechanisms with more constraints.

3.1. Displacement of the Rigid Body in Space and Subspaces

In structural synthesis of robot manipulators the definition of motion of rigid body (RB) has vital importance. Theoretical model of a solid body, in which the distances between points are considered to be constant regardless of any forces acting upon the body, is called RB. To create the space and subspaces with the space number λ for the motion of rigid body (work organ or gripper), the term general constraint $d = (0, 1, 2, 3, 4, 5)$ should be clearly defined as the first step.

In fact, the general constraint of the manipulators refers to the difference between the maximum possible achievable motion of their single link that is assumed to be moving freely in general space ($\lambda=6$) and the maximum possible achievable free motion of the same link in the space or subspace ($\lambda=5, 4, 3, 2, 1$), in which the manipulator is actually moving. Note that this definition only valid for the manipulators, where the general constraint is constant throughout the manipulator. Due to the fact that,

the maximum possible achievable motion of any single link is equal to its space or subspace number (λ), the general constraint can be formulated as,

$$d = 6 - \lambda \quad (3.1)$$

where, in Equation (3.1), 6 represents the full motion of rigid body in space, three translations along and three rotations about orthogonal Cartesian coordinate system.

3.1.1. Displacement of the Rigid Body in Space

Displacement of the rigid body in space (Figure 3.1) with space number $\lambda=6$ and general constraint $d=0$ is examined by six independent coordinates, three parameters are describing position $\rho=[x_A, y_A, z_A]^T$, and three parameters of two orthogonal unit vectors are describing orientation $e_1=[l_1, m_1, n_1]^T$ and $e_2=[l_2, m_2, n_2]^T$.

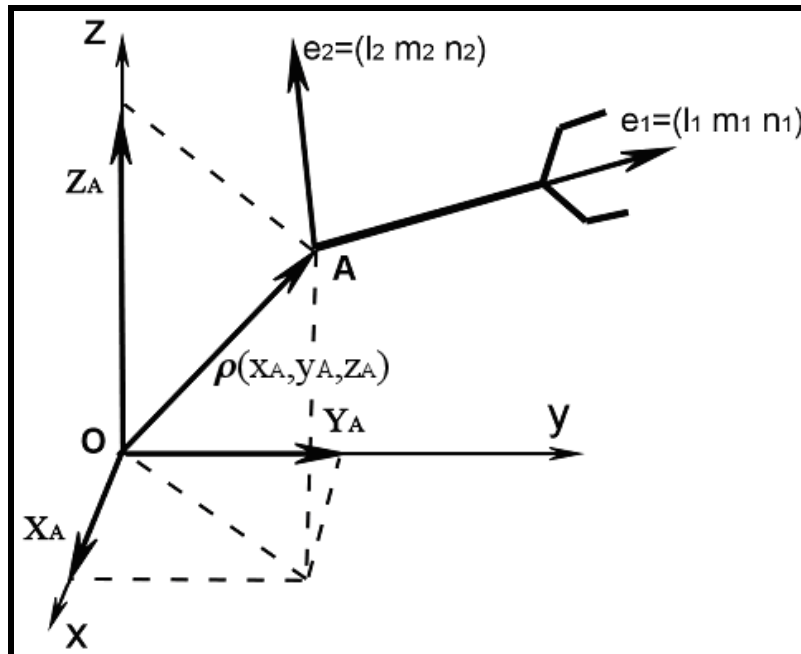


Figure 3.1. Displacement of Rigid Body in Space.

For defining rigid body in space we have nine parameters that six of them are independent and the remaining three parameters are obtained by using the following conditions shown in Equations (3.2-3.4)

$$e_1^2 = |\mathbf{e}_1|^2 = \mathbf{e}_1 \cdot \mathbf{e}_1 = l_1^2 + m_1^2 + n_1^2 = 1 \quad (3.2)$$

$$e_2^2 = |\mathbf{e}_2|^2 = \mathbf{e}_2 \cdot \mathbf{e}_2 = l_2^2 + m_2^2 + n_2^2 = 1 \quad (3.3)$$

$$\mathbf{e}_1 \cdot \mathbf{e}_2 = l_1 l_2 + m_1 m_2 + n_1 n_2 = 0 \quad (3.4)$$

Thus displacement of the rigid body (RB) in space $\lambda=6$ and $d=0$ can be introduced in the following matrix vector form,

$$\mathbf{D} = \begin{bmatrix} \boldsymbol{\rho} \\ \mathbf{e} \end{bmatrix}, \quad \mathbf{e} = [l_1 \quad m_1 \quad n_1]^T, \quad \boldsymbol{\rho} = [x_A \quad y_A \quad z_A]^T \quad (3.5)$$

Notice that the components of vector \mathbf{e} can be chosen from any combinations of three parameters of the vector components \mathbf{e}_1 and \mathbf{e}_2 .

3.1.2. Displacement of the Spherical RB on Planar Surface

After defining the motion of the RB in space $\lambda=6$ we can define subspace as $\lambda=5$ by imposing general constraint one to this space. As seen in Figure 3.2 the motion of the rigid body is constrained with the contact of a spherical surface and a planar surface at one point. Rigid body can be defined by position parameters $\boldsymbol{\rho}(x, y)$ and orientation parameters $\mathbf{e}_1 = [l_1 \quad m_1 \quad n_1]^T$ and $\mathbf{e}_2 = [l_2 \quad m_2 \quad n_2]^T$.

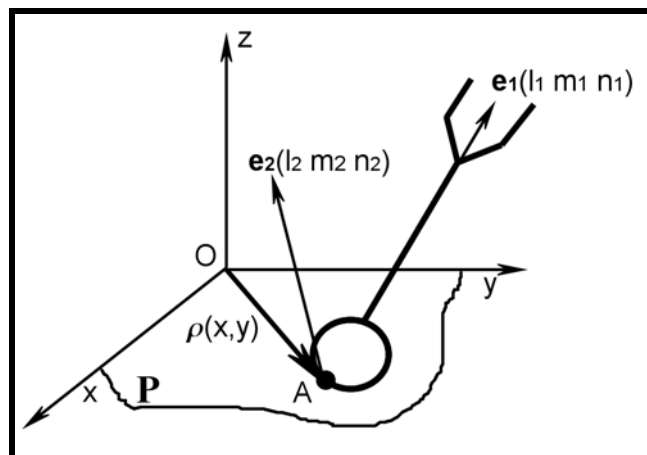


Figure 3.2. Sphere on Plane Motion.

In here, eight parameters are defining the motion of our rigid body and five of them are independent and three is dependent by the equations $\mathbf{e}_1 \cdot \mathbf{e}_1 = 1$, $\mathbf{e}_2 \cdot \mathbf{e}_2 = 1$, and, $\mathbf{e}_1 \cdot \mathbf{e}_2 = 0$. Thus the displacement of the rigid body in subspace with space number $\lambda=5$ and general constraint $d=1$ is defined by five independent parameters and can be described in the matrix vector form as in Equation (3.6).

$$\mathbf{D} = \begin{bmatrix} \boldsymbol{\rho} \\ \mathbf{e} \end{bmatrix}, \quad \mathbf{e} = [l_1 \quad m_2 \quad n_2]^T, \quad \boldsymbol{\rho} = [x \quad y \quad 0]^T \quad (3.6)$$

Notice, that the components of vector $\boldsymbol{\rho}$ can be chosen by other Cartesian planes $[x \ 0 \ z]^T$, $[0 \ y \ z]^T$ or planes parallel to them $[c \ y \ z]^T$, $[x \ c \ z]^T$, $[x \ y \ c]^T$. Also the plane can be inclined, by $\boldsymbol{\rho} [x \ y \ z]^T$ and the normal $\mathbf{n}[l \ m \ n]^T$, where five cut of six parameters are independent by the condition shown in Equation (3.7).

$$|\mathbf{n}| = l^2 + m^2 + n^2 = 1 \quad (3.7)$$

3.1.3. Displacement of the Spherical RB on Spherical Surface

If the constraint imposed to rigid body by the contact of two spherical surfaces as shown in Figure 3.3, the position of the rigid body on sphere with unit radius r be described by two parameters (ψ, ϕ) and $\mathbf{e}_1 = [l_1 \quad m_1 \quad n_1]^T$, while $\mathbf{e}_2 = [l_2 \quad m_2 \quad n_2]^T$ describes the orientation. Thus we have eight parameters and three of them are dependent because of the conditions $\mathbf{e}_1 \cdot \mathbf{e}_1 = 1$, $\mathbf{e}_2 \cdot \mathbf{e}_2 = 1$, and, $\mathbf{e}_1 \cdot \mathbf{e}_2 = 0$.

The displacement of the rigid body in vector form can be described as in Equation (3.8).

$$\mathbf{D} = \begin{bmatrix} \boldsymbol{\rho} \\ \mathbf{e} \end{bmatrix}, \quad \mathbf{e} = [l_1 \quad m_2 \quad n_2]^T, \quad \boldsymbol{\rho} = \begin{bmatrix} r \cos \phi \sin \varphi \\ r \sin \phi \sin \varphi \\ r \cos \varphi \end{bmatrix}^T \quad (3.8)$$

where, r is a constant value.

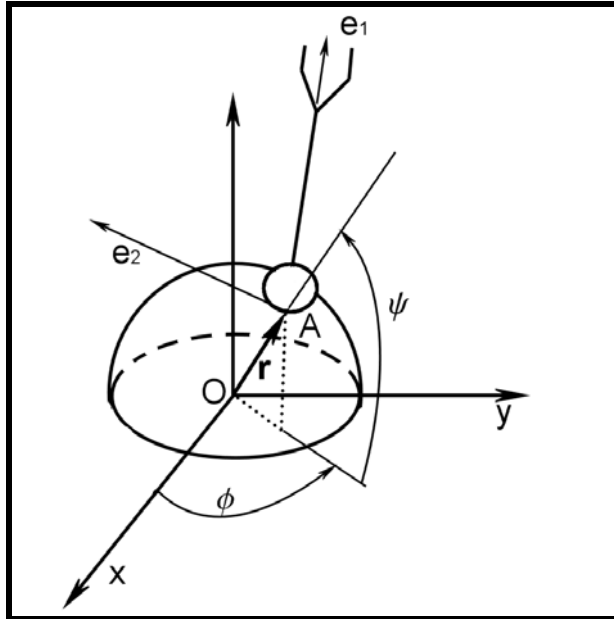


Figure 3.3. Sphere on Sphere Motion.

3.1.4. Displacement of the Planar RB with Constant Twist Angle on Planar Surface

When the motion of RB is constrained by the motions of two planes with a constant twist angle α as shown in Figure 3.4, the grounding plane P_1 is defined by the normal $\mathbf{n}_1 = [0 \ m_1 \ 0]^T$ and the moving plane P_2 is defined by the normal $\mathbf{n}_2 = [l_2 \ m_2 \ n_2]^T$.

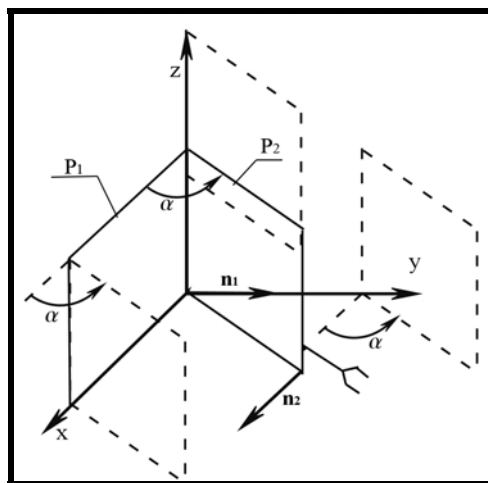


Figure 3.4. Plane on Plane Motion with Constant Twist Angle.

The position of the RB is described by the vector $\mathbf{P} = [x \ y \ z]^T$ and two rotations around two normal are defining the orientation, so we have seven parameters defining the displacement of the rigid body that five of them are independent and remaining are calculated from two conditions (Equation(3.9)), first condition comes from, $\mathbf{e}_2 \cdot \mathbf{e}_2 = 1$ and the second one comes from $\mathbf{n}_1 \cdot \mathbf{n}_2$

$$\begin{aligned} l_2^2 + m_2^2 + n_2^2 &= 1 \\ m_1 m_2 &= \text{Cos}\alpha \end{aligned} \quad (3.9)$$

3.1.5. Displacement of the Spherical RB on an Elliptic Torus

Another constraint can be imposed to the rigid body by the contact of a spherical surface and the surface of an elliptic torus as shown in Figure 3.5. Surface of the elliptic torus is generated by the rotation of an ellipse in x-z plane about the z axis and given by the parametric Equations (3.10)

$$\begin{aligned} x(u, v) &= (a + b \text{Sin } v) \text{Cos } u \\ y(u, v) &= (a + b \text{Sin } v) \text{Sin } u \\ z(u, v) &= c \text{Cos } v \end{aligned} \quad (3.10)$$

Where parameters b and c are belong to ellipse, a is torus radius, v and u are rotating axes of ellipse around z and z_1 of reference coordinate systems x, y, z and x_1, y_1, z_1 respectively.

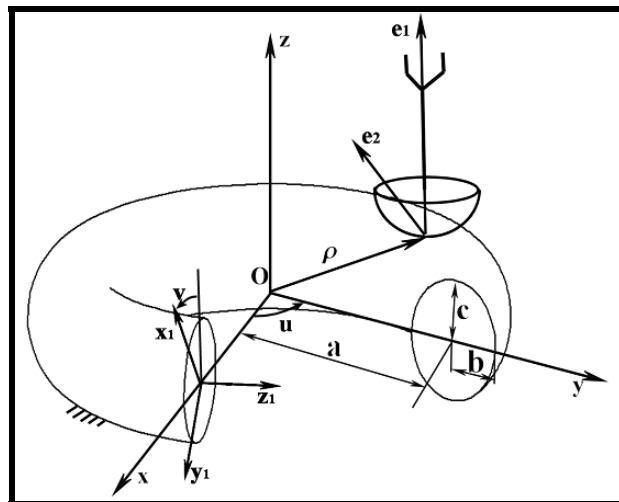


Figure 3.5. Motion of a Sphere on an Elliptic Torus.

The displacement of a rigid body then defined by spherical parameters $S(r, \theta, \phi)$ and by parametric Equations (3.10), which describe contact point by two independent parameter $\rho(u, v)$. Thus five independent parameters describe subspace with space number $\lambda=5$ and general constraint parameter $d=1$.

3.1.6. Displacement of the RB with a Planar Face on an Elliptic Torus

The displacement of the rigid body with a planar face on an elliptic torus (Figure 3.6) can be found by the help of position parameters $\rho(u, v)$ with respect to the Equations(3.10) and orientation parameters of plane normal $\mathbf{n} = [l \ m \ n]^T$ and a tangential vector $\mathbf{t} = [l_1 \ m_1 \ n_1]^T$ on the contact point. Eight parameters and three conditions $\mathbf{n} \cdot \mathbf{n} = 1$, $\mathbf{t} \cdot \mathbf{t} = 1$, $\mathbf{n} \cdot \mathbf{t} = 0$ describe five independent parameters in subspace $\lambda=5$.

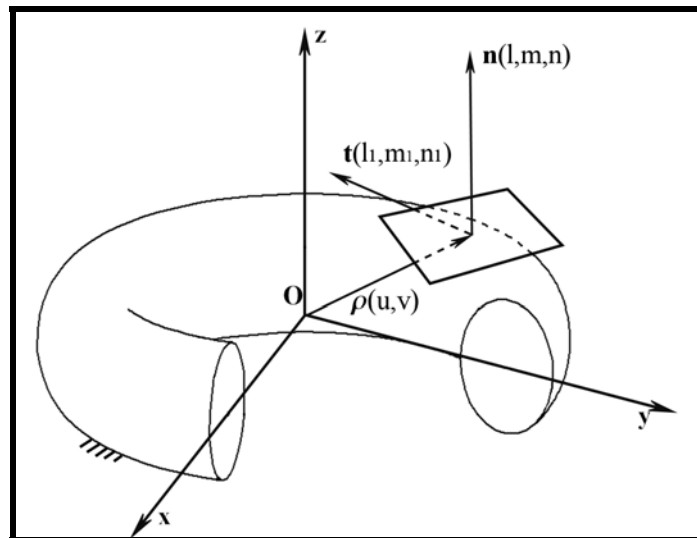


Figure 3.6. Motion of Plane on an Elliptic Torus.

3.1.7. Displacement of the Elliptic Torus RB on an Elliptic Torus

As shown in Figure 3.7 the constraint defined by the contact of two elliptic torus surfaces can be described by the position $\rho(u, v)$ and orientation of tangential

vector $\mathbf{t} = [l_1 \ m_1 \ n_1]^T$ and normal vector $\mathbf{n} = [l \ m \ n]^T$ with the following conditions $\mathbf{n} \cdot \mathbf{n} = 1$, $\mathbf{t} \cdot \mathbf{t} = 1$, $\mathbf{n} \cdot \mathbf{t} = 0$. Note that from eight parameters, five are independent and three are dependent.

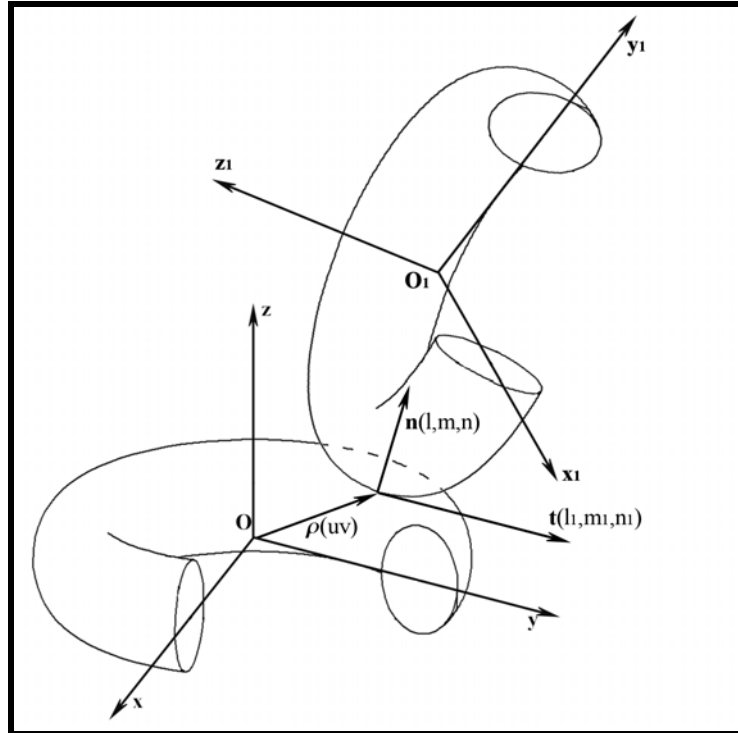


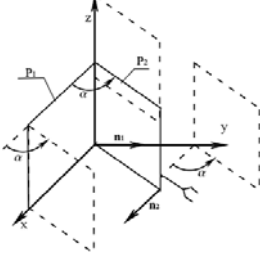
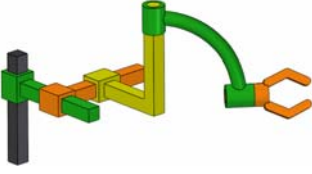

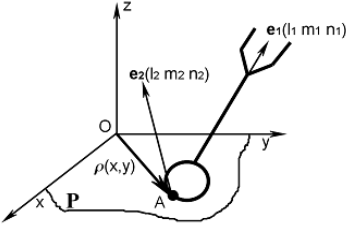
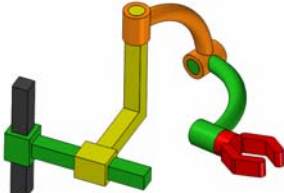

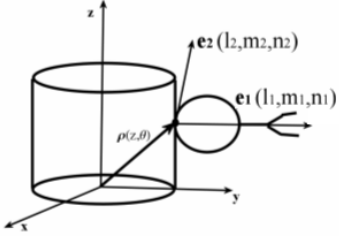
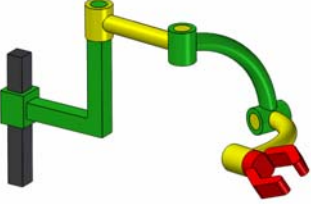

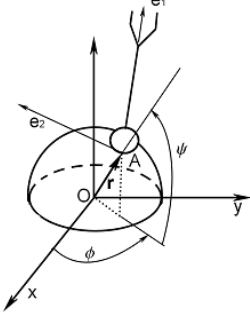
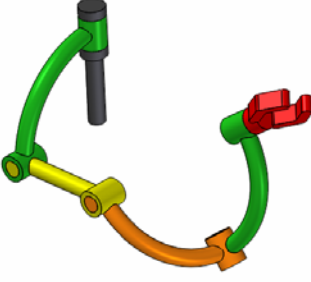

Figure 3.7. Elliptic Torus on Elliptic Torus.

As a summary, when the displacement of the rigid body is constrained by a condition, such as contact of two surfaces as exemplified in this section then it is said to belong to a subspace.

3.2 Serial Manipulators in Subspaces with General Constraint One

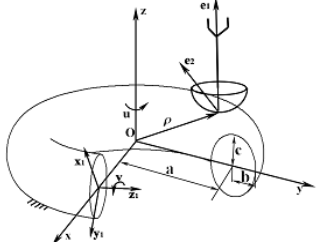
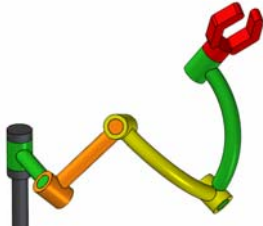

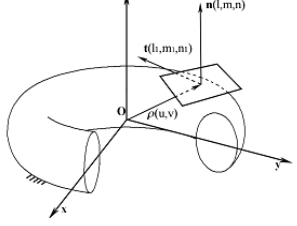


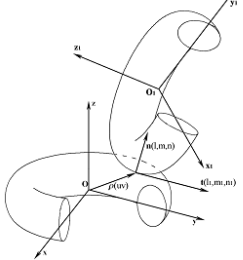


In this section we design serial manipulators in subspace with general constraint one. The maximum serial manipulators describing the motions of rigid body on different surfaces are seven. As shown in Table 3.1 the seven geometries of rigid body motions are generated by serial manipulators. Structural bonding and geometry of joint axis are illustrated by Table 3.1 also.

Table 3.1. Serial Manipulators.

#	Motion	Serial Manipulator	Geometry of Joint Axes
1	 <p>PPRRR</p>	 <p>\$\underline{\\$}(\overline{\\$})</p>	
2	 <p>PPRRR</p>	 <p>\$\overline{\\$}(\overline{\\$})</p>	
3	 <p>PRRRR</p>	 <p>\$\underline{\\$}(\overline{\\$})</p>	
4	 <p>RRRRR</p>	 <p>(\overline{\\$})(\overline{\\$})</p>	

(cont. on next page)

Table 3.1 Serial Manipulators. (cont.)

5	 <p style="text-align: center;">RRRRR</p>	 <p style="text-align: center;">\$\$(\$\$\$)</p>	
6	 <p style="text-align: center;">RRRPP</p>	 <p style="text-align: center;">\$\$\$\$\$</p>	
7	 <p style="text-align: center;">RRRRR</p>	 <p style="text-align: center;">\$\$\$\$\$</p>	

3.3. Analytical Approach for the Overconstrained Mechanisms with General Constraint One

If a spatial 6R linkage mechanism has any motion then it is said to be overconstrained. Thus, an analytical approach can be described for finding a new RRRS linkage shown in Figure 3.8. Here, S is denoted for spherical joint that is equivalent of three revolute joints (R) with intersecting axes. The revolute joints 1, 2 and 3 with arbitrary directions \mathbf{e}_2 , \mathbf{e}_4 and \mathbf{e}_6 are described by joint parameters $\{a_{13}, \alpha_{13}\}$, $\{a_{35}, \alpha_{35}\}$ and $\{a_{57}, \alpha_{57}\}$, so that the remaining link parameters will be $\{a_{24}, \alpha_{24}\}$, $\{a_{46}, \alpha_{46}\}$ and a_{68} . Note that, the spherical joint and the first revolute joint are connected to the fixed frame. As shown in Figure 3.8, the vector loop-closure equation for the mentioned overconstrained mechanism can be written as follows;

$$\sum_{i=2}^7 \mathbf{e}_i a_{i-1,i+1} = \boldsymbol{\rho}_c \quad \text{where} \quad \boldsymbol{\rho}_c = [x_c, y_c, z_c]^T, \quad \mathbf{e}_i = [l_i, m_i, n_i]^T \quad (3.11)$$

The vector equation (Equation (3.11)) can also be written in the coordinate form as,

$$\begin{aligned} l_2 a_{13} + l_3 a_{24} + l_4 a_{35} + l_5 a_{46} + l_6 a_{57} + l_7 a_{68} &= x_c \\ m_2 a_{13} + m_3 a_{24} + m_4 a_{35} + m_5 a_{46} + m_6 a_{57} + m_7 a_{68} &= y_c \\ n_2 a_{13} + n_3 a_{24} + n_4 a_{35} + n_5 a_{46} + n_6 a_{57} + n_7 a_{68} &= z_c \end{aligned} \quad (3.12)$$

The vectors $\{\mathbf{e}_i\}_3^7$ can be calculated by using recurrent unit vector equations (Equations (2.16)) with given vectors $\mathbf{e}_1 = [1, 0, 0]^T$ and $\mathbf{e}_2 = [0, 0, 1]^T$ as below,

$$\begin{aligned} \mathbf{e}_3 &= \begin{pmatrix} C_{13} \\ S_{13} \\ 0 \end{pmatrix}, \quad \mathbf{e}_4 = \begin{pmatrix} S_{13} S_{24} \\ -C_{13} S_{24} \\ C_{24} \end{pmatrix}, \quad \mathbf{e}_5 = \begin{pmatrix} C_{13} C_{35} - C_{24} S_{13} S_{35} \\ S_{13} C_{35} + C_{24} C_{13} S_{35} \\ S_{24} S_{35} \end{pmatrix}, \quad \mathbf{e}_6 = \begin{pmatrix} C_{46} S_{13} S_{24} + (C_{24} S_{13} C_{35} + C_{13} S_{35}) S_{46} \\ S_{35} S_{13} S_{46} - (C_{24} S_{46} C_{35} + C_{46} S_{24}) C_{13} \\ C_{24} C_{46} - C_{35} S_{24} S_{46} \end{pmatrix} \\ \mathbf{e}_7 &= \begin{pmatrix} C_{13}(C_{35} C_{57} - C_{46} S_{35} S_{57}) - S_{13}(-S_{24} S_{46} S_{57} + C_{24}(C_{57} S_{35} + C_{35} C_{46} S_{57})) \\ C_{57}(C_{35} S_{13} + C_{13} C_{24} S_{35}) + S_{57}(-C_{46} S_{13} S_{35} + C_{13}(C_{35} C_{46} C_{24} - S_{24} S_{46})) \\ C_{57} S_{24} S_{35} + S_{57}(C_{35} S_{24} C_{46} + C_{24} S_{46}) \end{pmatrix} \end{aligned} \quad (3.13)$$

where, C_{ik} and S_{ik} represent the cosine and sine of the angle α_{ik} , respectively.

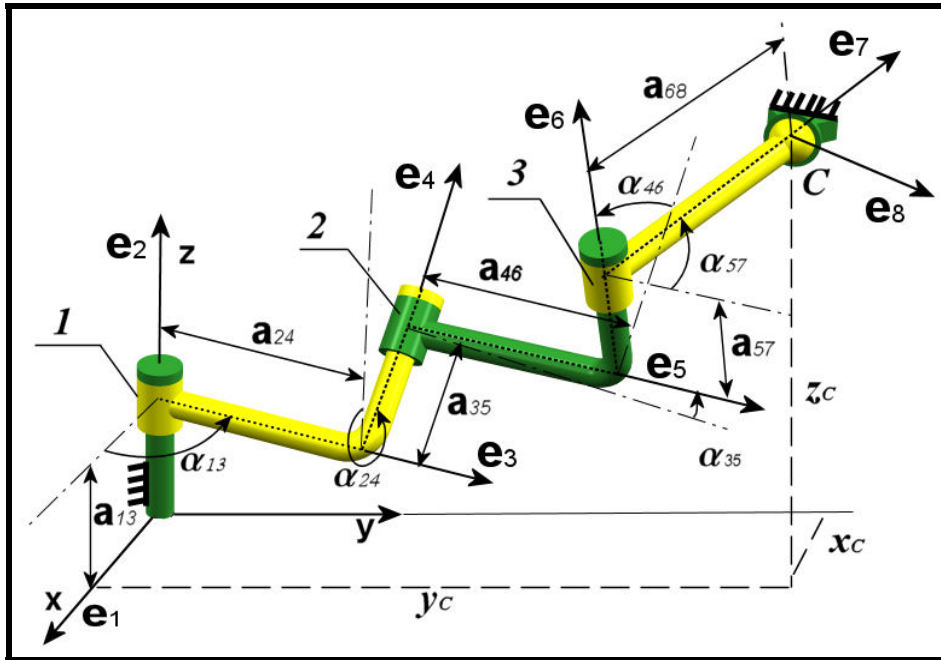


Figure 3.8 Parameters for RRRS Linkage.

Substitution of the elements of the vector values from Equations (3.13) into Equations (3.12) yields,

$$p C_{13} + q S_{13} = x_c \quad (3.14)$$

$$p S_{13} - q C_{13} = y_c \quad (3.15)$$

$$r + a_{13} = z_c \quad (3.16)$$

where,

$$\begin{aligned} p &= a_{24} + C_{35}(a_{46} + a_{68}C_{57}) + S_{35}(a_{57}S_{46} - a_{68}C_{46}S_{57}), \\ q &= S_{24}(a_{35} + a_{57}C_{46} + a_{68}S_{46}S_{57}) - C_{24}(S_{35}(a_{46} + a_{68}C_{57}) + C_{35}(a_{68}C_{46}S_{57} - a_{57}S_{46})), \\ r &= C_{24}(a_{35} + a_{57}C_{46} + a_{68}S_{46}S_{57}) + S_{24}(S_{35}(a_{46} + a_{68}C_{57}) + C_{35}(a_{68}C_{46}S_{57} - a_{57}S_{46})) \end{aligned}$$

After this point the following operations are carried on the Equations (3.14-3.16) for the ease of use. First Equation (3.14) and Equation (3.15) are multiplied by S_{13} and C_{13} respectively and then subtracted from each other. Second the same equations are multiplied by C_{13} and S_{13} respectively and then added to each other. Finally, after rearranging the Equation (3.16) the results yield,

$$x_c S_{13} - y_c C_{13} = q \quad (3.17)$$

$$x_c C_{13} + y_c S_{13} = p \quad (3.18)$$

$$z_c - a_{13} = r \quad (3.19)$$

Expanding Equations (3.18) and (3.19) with respect to C_{35} and S_{35} , we can get the following equations

$$p_1 C_{35} + q_1 S_{35} = r_1 \quad (3.20)$$

$$-q_1 C_{35} + p_1 S_{35} = r_2 \quad (3.21)$$

where, $p_1 = a_{46} + a_{68}C_{57}$, $q_1 = a_{57}S_{46} - a_{68}C_{46}S_{57}$, $r_1 = x_c C_{13} + y_c S_{13} - a_{24}$,

$$r_2 = z_c - a_{13} - C_{24}(a_{35} + a_{57}C_{46} + a_{68}S_{46}S_{57})$$

After solving Equations (3.20) and (3.21), we will find,

$$C_{35} = \Delta_1 \Delta^{-1} = \begin{vmatrix} r_1 & q_1 \\ r_2 & p_1 \end{vmatrix} \begin{vmatrix} p_1 & q_1 \\ -q_1 & p_1 \end{vmatrix}^{-1}, \quad S_{35} = \Delta_2 \Delta^{-1} = \begin{vmatrix} p_1 & r_1 \\ -q_1 & r_2 \end{vmatrix} \begin{vmatrix} p_1 & q_1 \\ -q_1 & p_1 \end{vmatrix}^{-1} \quad (3.22)$$

By using S_{35} and C_{35} values that are found in Equations(3.22), a unique value for $\alpha_{35} = \text{Atan2}(S_{35}, C_{35})$ is obtained.

We may consider S_{ik} and C_{ik} as two independent variables and add following trigonometric identities as supplementary equations of constraint,

$$S_{35}^2 + C_{35}^2 = 1, \quad S_{57}^2 + C_{57}^2 = 1, \quad (x_c S_{13} - y_c C_{13})^2 + (y_c S_{13} + x_c C_{13})^2 = x_c^2 + y_c^2 \quad (3.23)$$

After summing the squares of Equations. (3.17-3.19) by taking into account Equations. (3.23) and substituting Equations (3.22) into Equation (3.17), we obtain the following equations with respect to the unknowns C_{57} and S_{57} as,

$$C_{57} = [r_3 - 2a_{35}S_{24}(x_c S_{13} - y_c C_{13}) - 2a_{24}(y_c S_{13} + x_c C_{13})] p_2^{-1} \quad (3.24)$$

$$S_{57} = [r_4 + S_{24}(x_c S_{13} - y_c C_{13})] q_2^{-1} \quad (3.25)$$

where: $r_3 = x_c^2 + y_c^2 + (z_c - a_{13})^2 + a_{24}^2 + a_{35}^2 - a_{46}^2 - a_{57}^2 - a_{68}^2 - 2a_{35}(z_c - a_{13})C_{24}$,

$$r_4 = C_{24}(z_c - a_{13}) - a_{57}C_{46} - a_{35}, \quad p_2 = 2a_{46}a_{68}, \quad \text{and} \quad q_2 = a_{68}S_{46}$$

Equations (3.24) and (3.25) both represent a unique solution for $\alpha_{57} = \text{Atan2}(S_{57}, C_{57})$. Due to the fact that S_{57} and C_{57} are found, by using the trigonometric identities in Equation (3.23) we can reach the following overconstraint equation,

$$4a_{46}^2 [r_4 + (x_c S_{13} - y_c C_{13})S_{24}]^2 + S_{46} [r_3 - 2a_{35}S_{24}(x_c S_{13} - y_c C_{13}) - 2a_{24}(y_c S_{13} + x_c C_{13})]^2 - 4a_{46}^2 a_{68}^2 S_{46}^2 = 0 \quad (3.26)$$

Arranging overconstraint Equation (3.26), the following polynomial equation can be constructed as,

$$A\alpha^2 + B\alpha + C\beta + D\alpha\beta + E = 0 \quad (3.27)$$

where, $\alpha = x_c S_{13} - y_c C_{13}$, $\beta = y_c S_{13} + x_c C_{13}$, $A = 4a_{46}^2 S_{24}^2 + 4a_{35}^2 S_{24}^2 S_{46}^2 - 4a_{24}^2 S_{46}^2$,
 $B = 8a_{46}^2 r_4 x_c S_{24} + 4a_{35} r_3 S_{24} S_{46}^2$, $C = 4a_{24} r_3 S_{46}^2$, $D = 8a_{24} a_{35} S_{24} S_{46}^2$,
 $E = 4a_{46}^2 r_4^2 + S_{46}^2 r_3^2 - 4a_{46}^2 a_{68}^2 S_{46}^2 + (x_c^2 + y_c^2) 4a_{24}^2 S_{46}^2$

In the case of mobile mechanism, the functions $\alpha = f(\alpha_{13})$, $\beta = f(\alpha_{13})$ can not be equal to zero, thus coefficients of polynomial Equation (3.27) must be equal to zero ($A = B = C = D = E = 0$). As a result, we will get the following linear and angular overconstraint conditions for the spatial mechanism RRR-(RRR) as,

$$\begin{aligned} a_{46}^2 S_{24}^2 + a_{35}^2 S_{24}^2 S_{46}^2 - a_{24}^2 S_{46}^2 = 0 \quad , \quad 2a_{46}^2 r_4 S_{24} - a_{35} r_3 S_{24} S_{46}^2 = 0 \quad , \quad a_{24} r_3 S_{46}^2 = 0 \\ a_{24} a_{35} S_{24} S_{46}^2 = 0 \quad , \quad 4a_{46}^2 r_4^2 + S_{46}^2 r_3^2 - 4a_{46}^2 a_{68}^2 S_{46}^2 + (x_c^2 + y_c^2) 4a_{24}^2 S_{46}^2 = 0 \end{aligned} \quad (3.28)$$

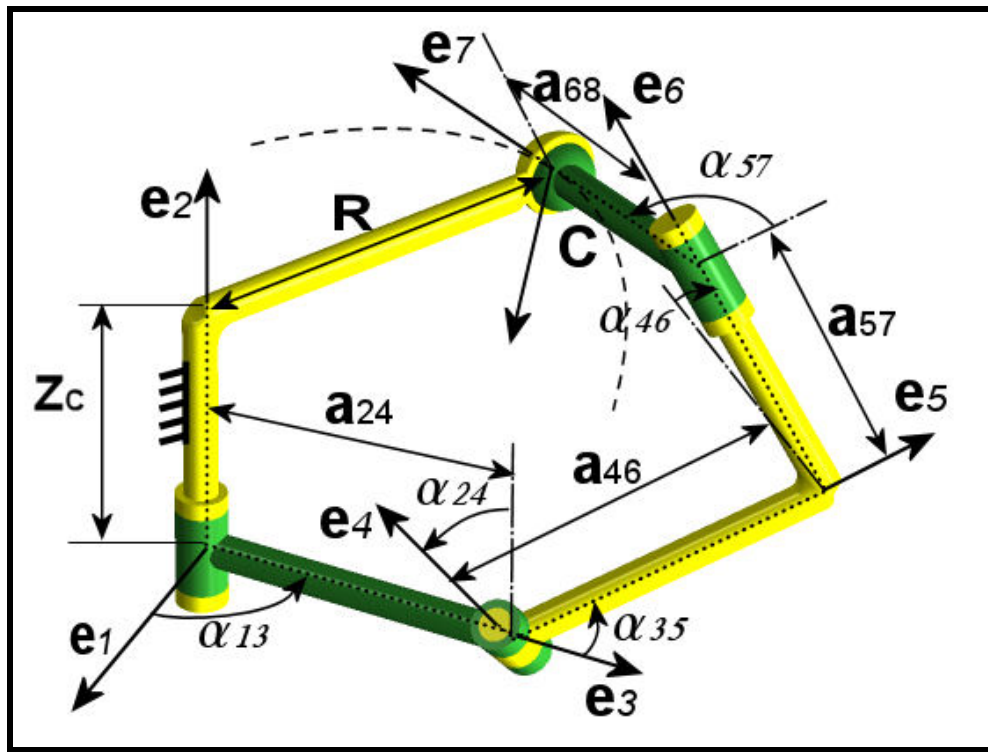


Figure 3.9. New 3D Overconstraint RRRS Linkage with Linear and Angular Constraint.

Now for simplification, let the joint offset parameters a_{35} and a_{13} be zero. Thus solving Equations (3.28) gives us both the linear and angular constraints and the coordinates of the spherical joint for the RRR-(RRR) mechanism with mobility $M=1$.

$$a_{46} = a_{24}S_{46}S_{24}^{-1} \quad , \quad z_c = a_{57}C_{46}C_{24}^{-1} \quad , \quad x_c^2 + y_c^2 = R^2 = a_{46}^2 a_{68}^2 a_{24}^{-2} \quad (3.29)$$


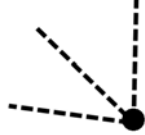


$$a_{68} = (a_{24}^2 + a_{57}^2 \tan^2 \alpha_{24})^{0.5}$$

Note that, the first overconstrained mechanism with linear-angular constraint have been presented by Bennett in 1903 the RRRS overconstraint mechanism is the second overconstrained mechanism with linear-angular constraint in the history of mechanism and machine science. The new RRRS overconstraint mechanism is called Alizade mechanism.

3.4. Overconstrained Mechanisms with General Constraint One

Overconstrained mechanisms are usually created by using either angular conditions, such as intersecting joint axes in one point, and joints with parallel axes, or linear-angular conditions, such as joints with skew perpendicular axes and arbitrary axes. as illustrated in Table 3.2 with structural bonding.

Table 3.2. Structural Bonding of Joint Axes.

Structural Bonding	Structural Properties of Joint Axes	Geometry of Joint Axes
$\overline{\text{\$}\text{\$}\text{\$}}$	Joint axes are parallel	
$(\text{\$}\text{\$}\text{\$})$	Joint axes are intersecting in one point	
$\text{\$}\perp\text{\$}\perp\text{\$}$	Joint axes are skew perpendicular to each other	
$\text{\$}/\text{\$}/\text{\$}$	Joint axes are arbitrary	

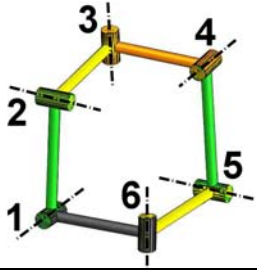
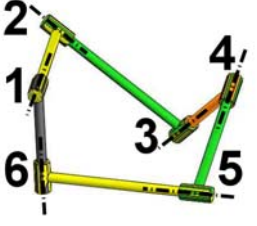
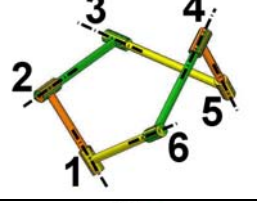
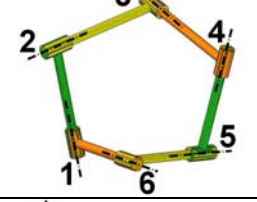
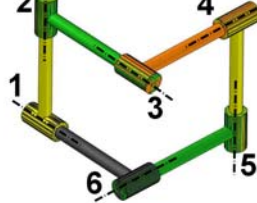
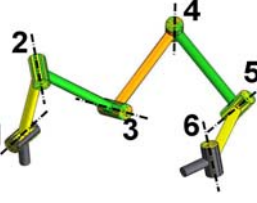
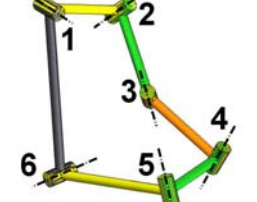
In Table 3.3 all known 6R mechanisms are listed with structural bonding of mechanisms. These mechanisms will be used for constructing multi loop overconstrained manipulators

Table 3.3. 6R Mechanisms with General Constraint One.

#	Authors	Linkage Name & Structural Bonding	Denavit- Hartenberg Parameters	Figure
1	Sarrus 1853	Planar-Hybrid \$\$\$-\$\$\$	$\alpha_{12} = \alpha_{23} = 0$ $\alpha_{45} = \alpha_{56} = 0$	
2	Bennett 1905	Spherical Hybrid (\$\$\$)-(\$\$\$)	$a_{12} = a_{23} = 0$ $a_{45} = a_{56} = 0$ $a_{34} = a_{61}$ $d_1 = d_2 = d_3$ $d_4 = d_5 = d_6$	
		Plano-Spherical Hybrid (\$\$\$)-\$\$\$	$a_{45} = a_{56} = 0$ $d_1 = d_2 = 0$ $d_4 = d_5 = d_6 = 0$ $\alpha_{12} = \alpha_{23} = 0$	
3	Bricard 1927	Line-Symmetric Loop \$\$\$\$\$\$	$a_{12} = a_{45}, a_{23} = a_{56},$ $a_{34} = a_{61}$ $\alpha_{12} = \alpha_{45}, \alpha_{23} = \alpha_{56},$ $\alpha_{34} = \alpha_{61}$ $d_1 = d_4, d_2 = d_5, d_3 = d_6$	
		Plane-Symmetric Loop \$\$\$\$\$\$	$a_{12} = a_{61}, a_{23} = a_{56}$ $a_{34} = a_{45}$ $\alpha_{12} + \alpha_{61} = \alpha_{23} + \alpha_{56} = \alpha_{34} + \alpha_{45} = \pi$ $d_2 = d_6, d_3 = d_5$ $d_1 = d_4 = 0$	

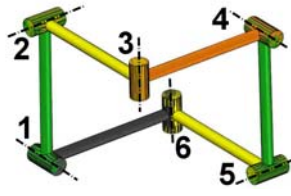
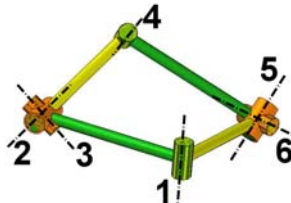
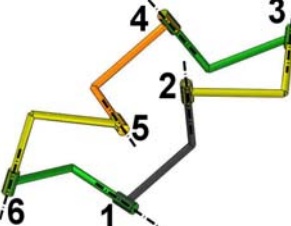
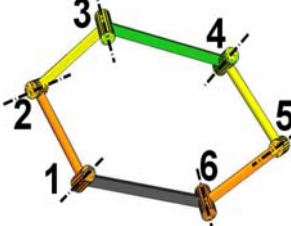
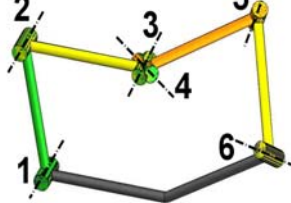
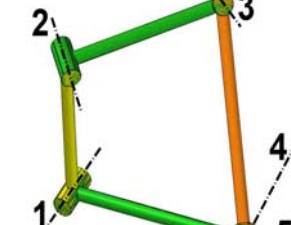
(cont. on next page)

Table 3.3. 6R Mechanisms with General Constraint One (cont.).

3	Bricard (Cont.)	Trihedral \$\$\$\$\$	$a_{12}^2 + a_{34}^2 + a_{56}^2 = a_{23}^2 + a_{45}^2 + a_{61}^2$ $\alpha_{12} = \alpha_{34} = \alpha_{56} = \pi / 2$ $\alpha_{23} = \alpha_{45} = \alpha_{61} = 3\pi / 2$ $d_1 = d_2 = d_3 = d_4 = d_5 = d_6 = 0$	
		Plane-Symmetric Octahedral \$\$\$\$\$	$a_{12} = a_{23} = a_{34} = a_{45} = a_{56} = a_{61} = 0$ $d_4 = -d_1$ $d_2 = -d_1 S\alpha_{12} / S\alpha_{(12+34)}$ $d_5 = -d_1 S\alpha_{61} / S\alpha_{(45+61)}$ $d_3 = -d_1 S\alpha_{34} / S\alpha_{(12+34)}$ $d_6 = -d_1 S\alpha_{61} / S\alpha_{(45+61)}$	
		Line-Symmetric Octahedral \$\$\$\$\$	$a_{12} = a_{23} = a_{34} = a_{45} = a_{56} = a_{61} = 0$ $d_1 + d_4 = d_2 + d_5 = d_3 + d_6$	
		Doubly-Collapsible Octahedral \$\$\$\$\$	$a_{12} = a_{23} = a_{34} = a_{45} = a_{56} = a_{61} = 0$ $d_1 d_3 d_5 = d_2 d_4 d_6$	
		Orthogonal \$\$\$\$\$	$a_{12} = a_{23} = a_{34} = a_{45} = a_{56} = a_{61} = 0$ $d_1 = d_2 = d_3 = d_4 = d_5 = d_6 = d$	
4	Goldberg 1943	Series 6R \$\$\$\$\$	$a_{61} = a_{12} + a_{23} + a_{34} + a_{45} + a_{56}$ $S\alpha_{i,i+1} / a_{i,i+1} = k (i = 1, 2, \dots, 6)$ $d_1 = d_2 = d_3 = d_4 = d_5 = d_6 = 0$	
		L-Shaped 6R \$\$\$\$\$	$a_{12} = a_{23} + a_{34}, a_{61} = a_{45} + a_{56}$ $S\alpha_{i,i+1} / a_{i,i+1} = k (i = 1, 2, \dots, 6)$ $d_1 = d_2 = d_3 = d_4 = d_5 = d_6 = 0$	

(cont. on next page)

Table 3.3. 6R Mechanisms with General Constraint One (cont.).

5	Franke 1951	Wirbelkette \$!\$!\$!\$!\$!\$	$a_{12} = a_{23} = a_{34} = a_{45} = a_{56} = a_{61} = a$ $d_1 = d_2 = d_3 = d_4 = d_5 = d_6 = 0$ $\alpha_{12} = \alpha_{23} = \alpha_{34} = \alpha_{45} = \alpha_{56} = \alpha_{61} = \frac{\pi}{2}$	
6	Altmann 1954	Line-Symmetric Loop \$!\$!\$!\$!\$!\$	$a_{12} = a_{45} = a, a_{23} = a_{56} = 0$ $a_{34} = a_{61} = b$ $\alpha_{12} = \alpha_{23} = \alpha_{34} = \alpha_{45} = \alpha_{56} = \alpha_{61} = \frac{\pi}{2}$ $d_1 = d_2 = d_3 = d_4 = d_5 = d_6 = 0$	
7	Harrisberger Soni 1966	Orthogonal \$\$\$\$\$\$	$a_{12} = a_{23} = a_{34} = a_{45} = a_{56} = a_{61} = a$ $d_1 = d_2 = d_3 = d_4 = d_5 = d_6 = d$	
8		Double-Bennett Hybrid \$\$\$\$\$\$	$S\alpha_{i,i+1} / a_{i,i+1} = k (i = 1, 2, \dots, 6)$ $d_1 = d_2 = d_3 = d_4 = d_5 = d_6 = 0$	
	Waldron 1967, 1968 1969	Plano-Bennett Hybrid \$\$\$-\$\$\$	$\alpha_{12} = \alpha_{23} = 0$ $a_{61} = a_{12} + a_{45}$ $S\alpha_{i,i+1} / a_{i,i+1} = k (i = 1, 2, \dots, 6)$ $d_1 = d_2 = d_3 = d_4 = d_5 = d_6 = 0$	
		Spherico-Bennett Hybrid (\$\$\$)-\$\$\$	$a_{56} = a_{45} = 0$ $\alpha_{12} = \alpha_{23} = 0$ $S\alpha_{i,i+1} / a_{i,i+1} = k (i = 1, 2, \dots, 6)$ $d_1 = d_2 = d_3 = 0$	

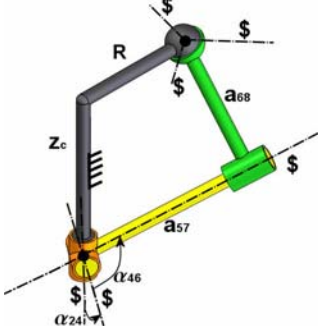
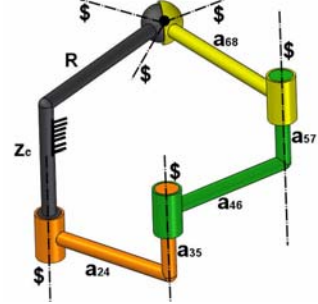
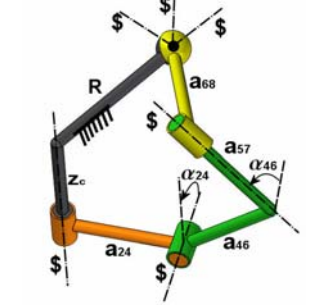
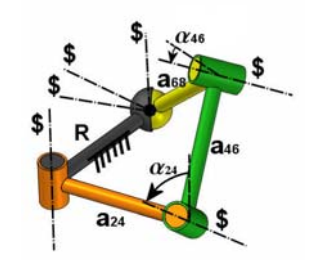
(cont. on next page)

Table 3.3. 6R Mechanisms with General Constraint One (cont.).

9	Wohlhart 1987,1991	Double Goldberg hybrid \$\$\$\$\$\$	$S\alpha_{i,i+1}/a_{i,i+1} = k (i = 1, 2, \dots, 6)$ $d_1 = d_2 = d_3 = d_4 = d_5 = d_6 = 0$	
		Triple-Part- Symmetric \$\$\$\$\$\$	$a_{12} = a_{23}, a_{34} = a_{45}, a_{56} = a_{61}$ $\alpha_{12} = -\alpha_{23}, \alpha_{34} = -\alpha_{45}, \alpha_{56} = -\alpha_{61}$ $d_6 = -d_2 - d_4, d_1 = d_3 = d_5 = 0$	
10	Mavroidis Roth 1995	Bennett-Joint \$\$\$\$\$\$	$a_{12} = a_{34}, a_{23} = a_{56}, a_{45} = a_{61}$ $\alpha_{12} = \alpha_{34}, \alpha_{56} = \alpha_{23}, \alpha_{45} = \alpha_{61}$ $S\alpha_{i,i+1}/a_{i,i+1} = k (i = 1, 2, \dots, 6)$ $d_1 = d_4 = 0, d_5 = d_2, d_6 = d_3$	
11	Dietmaier 1995	Skew-Plane Symmetric \$\$\$\$\$\$	$a_{12} = a_{45}, \alpha_{12} = \alpha_{45}$ $a_{34}/S\alpha_{34} = a_{23}/S\alpha_{23}$ $a_{61}/S\alpha_{61} = a_{56}/S\alpha_{56}$ $a_{23}(C\alpha_{23} + C\alpha_{34})/S\alpha_{23} =$ $a_{56}(C\alpha_{56} + C\alpha_{61})/S\alpha_{56}$ $d_3 = d_1, d_6 = d_4, d_5 = d_2 = 0$	
12	Schatz 1998	Schatz \$1\$1\$1\$1\$1\$	$a_{12} = a_{56} = 0$ $a_{23} = a_{34} = a_{45} = a, a_{61} = a\sqrt{3}$ $\alpha_{12} = \alpha_{34} = \alpha_{56} = \alpha_{23} = \alpha_{45} = \frac{\pi}{2}$ $\alpha_{61} = 0$ $d_1 = -d_6, d_2 = d_3 = d_4 = d_5 = 0$	
13	Alizade Can Gezgin Selvi 2007	Alizade- symmetric (\$\$\$)-\$\$\$	$d_1 = d_2 = 0, d_6 = d_3$ $a_{12} = a_{23}, a_{61} = a_{34}$ $a_{34} = (a_{23}^2 + d_3^2 \tan^2 \alpha_{12})^{0.5}$	
14	Alizade Selvi Gezgin 2007	Alizade (\$\$\$)-\$\$\$	$d_1 = d_2 = 0, a_{61} = a_{34}$ $a_{23} = a_{12} S\alpha_{23} S\alpha_{12}^{-1}$ $d_6 = d_3 C\alpha_{23} C\alpha_{12}^{-1}$ $a_{34} = (a_{23}^2 + d_3^2 \tan^2 \alpha_{12})^{0.5}$	

After representing the mechanisms in literature, in the light of analytical approach, we can list four old mechanisms with angular and linear-angular conditions that are proved by the Equation (3.29) as illustrated in Table 3.4.

Table 3.4. Overconstrained 6R Mechanisms

Structural Bonding and Conditions	Mechanism
$(\$ \$ \$) - (\$ \$ \$)$ $a_{24} = 0, a_{46} = 0$ $a_{35} = 0, a_{13} = 0$ $z = a_{57}, R = a_{68}$	
$(\$ \$ \$) - \overline{\$ \$ \$}$ $\alpha_{24} = 0, \alpha_{46} = 0$ $(z - a_{13} - a_{57} - a_{35}) = 0$	
$(\$ \$ \$) - \$ \perp \$ \perp \$$ $\alpha_{24} = 90^\circ, \alpha_{46} = 90^\circ$ $a_{13} = 0, a_{35} = 0$ $a_{46} = a_{24}, R = a_{68}$ $z = a_{57}$	
$(\$ \$ \$) - \$ / \$ / \$$ $a_{13} = a_{35} = a_{57} = z_c = 0$ $R = a_{46} a_{68} a_{24}^{-1}$ $a_{46} \text{Sin} \alpha_{24} = a_{24} \text{Sin} \alpha_{46}$	

Two new 6R mechanisms with general constraint one are represented in Table 3.5 by using linear and angular conditions with respect to the Equations (3.29). As shown in Table 3.5 the first mechanism is the symmetrical overconstrained 6R mechanism and the second is the nonsymmetrical 6R mechanism with linear and angular constraint. Several new 6R mechanisms can be generated with different values of link and joint parameters considering the relations described in Equation (3.29).

Table 3.5. New Overconstrained 6R Mechanisms with Linear and Angular Conditions.

Structural Bonding and Conditions	Mechanism
<p style="text-align: center;">(\$\$\$)-\$/\$/\$</p> $a_{13} = a_{35} = 0$ $a_{46} = a_{24}$ $\alpha_{46} = \alpha_{24}$ $z_c = a_{57}$ $x_c^2 + y_c^2 = R^2 = a_{68}^2$ $a_{68} = (a_{24}^2 + a_{57}^2 \tan^2 \alpha_{24})^{0.5}$	
<p style="text-align: center;">(\$\$\$)-\$/\$/\$</p> $a_{13} = a_{35} = 0$ $a_{46} = a_{24} S_{46} S_{24}^{-1}$ $z_c = a_{57} C_{46} C_{24}^{-1}$ $x_c^2 + y_c^2 = R^2 = a_{46}^2 a_{68}^2 a_{24}^{-2}$ $a_{68} = (a_{24}^2 + a_{57}^2 \tan^2 \alpha_{24})^{0.5}$	

CHAPTER 4

STRUCTURAL SYNTHESIS OF MANIPULATORS WITH GENERAL CONSTRAINT ONE

A parallel manipulator can be defined as a closed loop mechanism with an end effector also called as platform. In parallel manipulators the link of the end effector must be connected to the base by at least two independent kinematic chains where each chain contains one actuator at minimum. Parallel manipulators have some advantages with respect to serial manipulators such as higher precision, robustness, stiffness, and load carrying capacity.

Creation of structural groups is the main step in structural design of robot manipulators, where simple structural groups are defined as the kinematic chains that have zero mobility and that can not be split into other structural groups with smaller number of links. Introducing the definition, the general structural mobility formula for the manipulators with general constraint can now be introduced in the following form,

$$M = (d - 6)L + \sum_{i=1}^j f_i \quad (4.1)$$

where, M is the mobility of the manipulator, j is the number of joints, f_i is the degrees of freedom of the i^{th} joint, and L is the number of independent loops of the manipulator. As the mobility of any simple structural group is zero, by using Equation (4.1), the objective function of the simple structural groups with general constraint can be given as,

$$\sum_{i=1}^j f_i = (6 - d)L \quad (4.2)$$

If only one DoF pairs are to be used in the pre-design Equation 4.2 will be reduced to

$$j = (6 - d)L \quad (4.3)$$

Using the objective function given in Equation (4.3), any designer can easily create simple structural groups for the manipulators with general constraint in the pre-manipulator designs by following the procedure below.

- Determine the moving space or subspace (λ) of the desired manipulator that will be designed for the specific task.
- Determine the number of independent loops (L) of the desired manipulator that will be designed for the specific task.
- Calculate the general constraint (d) of the manipulator by using Equation (3.1).
- Calculate the number of joints $j = \sum f_i$ by using Equation (4.3).
- By using appropriate and desired angular and linear-angular conditions of the selected space or subspace, combine the joints together with the links to create the simple structural groups.

4.1 Structural Synthesis of Overconstrained Parallel Manipulators

Due to the fact that there are not many investigations in the literature about the overconstrained parallel manipulators, this study will focus on the creation of the simple structural groups with general constraint one. The descriptions of angular and linear-angular conditions for the subspace $\lambda=5$ will also be given in this section of the study.

As the parameters, general constraint and the number of loops, are pre-determined ($d=1, L=1$), the objective function Equation (4.2) for the current task will result in the number of joints equals to five ($j = \sum f_i = 5$). Calculating the number of joints, the appropriate angular (Table 4.1) and linear-angular conditions (Table 4.2) should be considered in order to combine the joints with links.

Table 4.1. Possible Angular Conditions for the Subspace $\lambda=5$





a	b	c	d
			
Two spheres with constant distance	Sphere on plane or plane on sphere		Two planes with constant twist angle

Table (4.1) shows the four possible angular conditions for $\lambda=5$. The geometry of the condition (Table 4.1a) can be created by the rotation of two spheres with one coincident axis through the centers that have the constant distance between each other. The conditions (Table 4.1b) and (Table 4.1c) describe the motion of the sphere on the plane or plane on the sphere. And the last condition (Table 4.1d) consists of two sets of parallel axes that give us two planes with constant twist angle.

Table 4.2. Possible Linear-Angular Conditions for the Subspace $\lambda=5$.


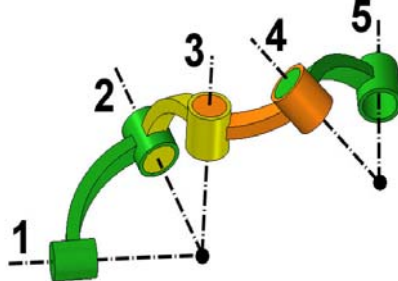

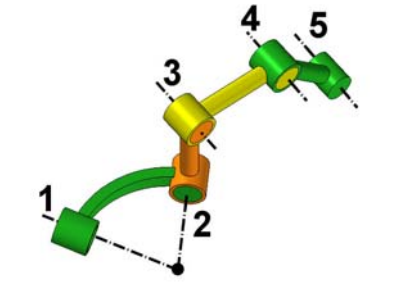

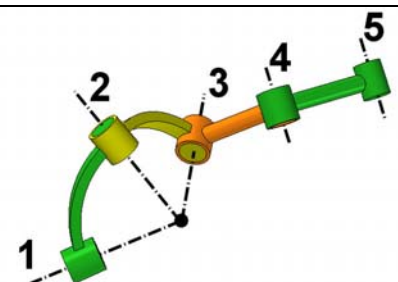

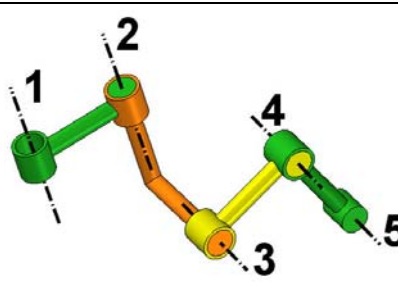
a	b	c	d
Plane on elliptic torus		Sphere on elliptic torus	
e	f	g	h
Sphere on torus		Sphere on elliptic torus	Torus on elliptic torus

Table (4.2) demonstrates the eight possible linear-angular conditions for $\lambda=5$. The conditions (Table 4.2a) and (Table 4.2b) describe the motion of a plane on an elliptic torus and vice versa. The elliptic torus in Cartesian coordinate system is a quadratic surface generated by two revolute joints that are placed arbitrarily. The formula of the elliptic torus is defined in Equation(3.10)

The conditions (Table 4.2c) through (Table 4.2f) can be generated by the motion of a sphere on an elliptic torus and vice versa, where the geometry of the elliptic torus differentiates due to the joint and link parameters. Note that, in conditions (Table 4.2e) and (Table 4.2f) the elliptic torus shifts in to torus because of the perpendicular joints. The condition (Table 4.2g) is the basis for the motion of an elliptical torus on an elliptical torus and the last condition (Table 4.2h) is similar to the former with the contact of a torus on elliptic torus

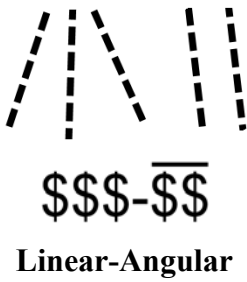
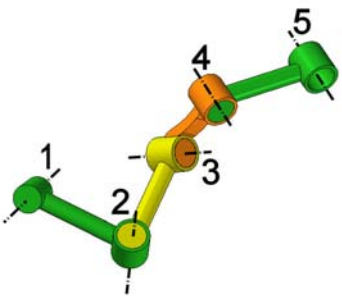
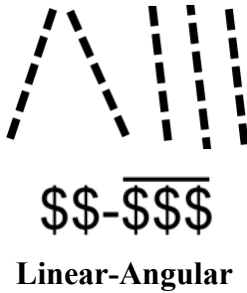
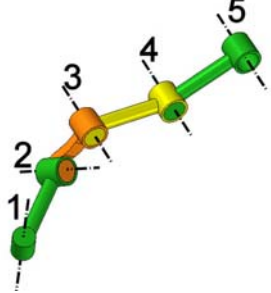
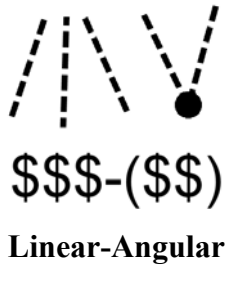
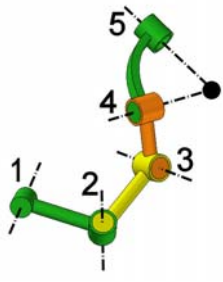
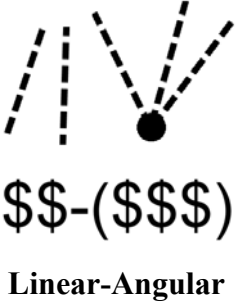
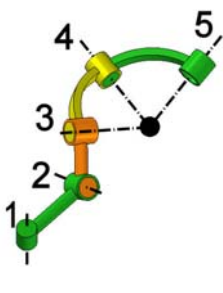
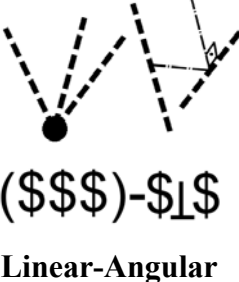
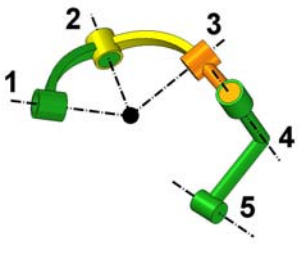
Finally, using each of the conditions that are described above, the calculated joints can be combined in 14 possible different ways that results in the simple structural groups with general constraint one (Table 4.3).

Table 4.3. Simple Structural Groups with General Constraint One Respect to Angular and Linear-Angular Conditions.

#	Structural Bonding and Condition	Structural group	Link-joint parameters
1	 <p>(\$\$\$)-(\$\$) Angular</p>		$a_{12} = a_{23} = a_{45} = 0$ $a_{34} = a_{51}$ $d_1 = d_2 = d_3$ $d_4 = d_5$
2	 <p>\$\$\$-((\$\$) Angular</p>		$a_{12} = 0$ $\alpha_{34} = \alpha_{45} = 0$
3	 <p>\$\$-((\$\$\$) Angular</p>		$a_{12} = a_{23} = 0$ $\alpha_{45} = 0$ $d_1 = d_2 = d_3$
4	 <p>\$\$-\$\$\$ Angular</p>		$\alpha_{12} = \alpha_{34} = \alpha_{45} = 0$

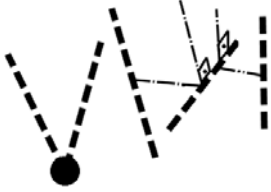
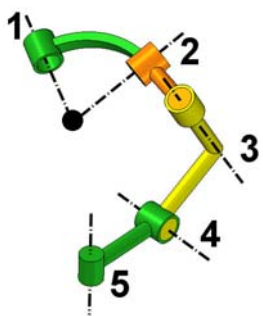

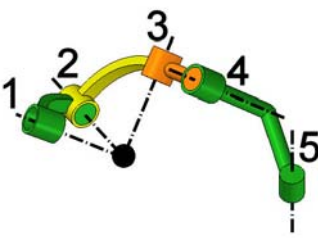
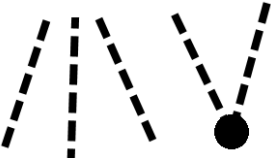
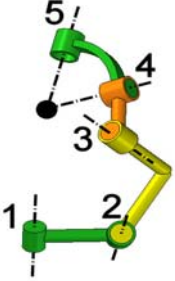

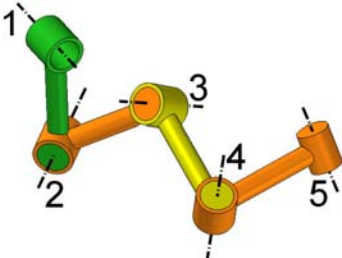

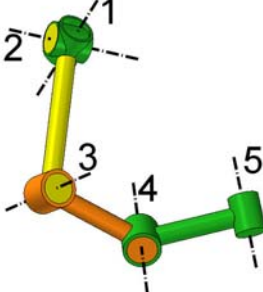
(cont. on next page)

Table 4.3 Simple Structural Groups with General Constraint One Respect to Angular and Linear-Angular Conditions (cont.).

5	 <p>Linear-Angular</p>		$a_{12} / S\alpha_{12} = a_{23} / S\alpha_{23}$ $\alpha_{45} = 0$ $d_1 = d_2 = d_3 = 0$
6	 <p>Linear-Angular</p>		$\alpha_{34} = \alpha_{45} = 0$ $d_1 = d_2 = 0$
7	 <p>Linear-Angular</p>		$a_{12} / S\alpha_{12} = a_{23} / S\alpha_{23}$ $a_{45} = 0$ $d_1 = d_2 = d_3 = 0$ $d_4 = d_5$
8	 <p>Linear-Angular</p>		$a_{34} = a_{45} = 0$ $d_1 = d_2 = 0$ $d_3 = d_4 = d_5$
9	 <p>Linear-Angular</p>		$a_{12} = a_{23} = 0$ $d_5 = 0$ $\alpha_{45} = \pi / 2$ $d_1 = d_2 = d_3$

(cont. on next page)

Table 4.3 Simple Structural Groups with General Constraint One Respect to Angular and Linear-Angular Conditions (cont.).

10	 <p>$(\\$\\$)-\\$L\\$L\\$ Linear-Angular</p>		$a_{12} = 0$ $d_4 = d_5 = 0$ $\alpha_{34} = \alpha_{45} = \pi/2$ $a_{34} = a_{45}$
11	 <p>$(\\$ \\$ \\$)-\\$ \\$ Linear-Angular</p>		$a_{12} = a_{23} = 0$ $d_5 = 0$
12	 <p>$\\$ \\$ \\$-(\\$ \\$)$ Linear-Angular</p>		$d_1 = d_2 = 0$ $a_{12} / S\alpha_{12} = a_{23} / S\alpha_{23}$ $a_{34} = (a_{23}^2 + d_3^2 \tan^2 \alpha_{12})^{0.5}$
13	 <p>$\\$ \\$ \\$ \\$ \\$ Linear-Angular</p>		$d_1 = d_2 = d_3 = d_4 = d_5 = 0$ $a_{12} / S\alpha_{12} = a_{23} / S\alpha_{23}$ $a_{23} = a_{34} = a_{45}$
14	 <p>$(\\$ \\$)-\\$ \\$ \\$ \\$ Linear-Angular</p>		$d_1 = d_2 = d_3 = d_4 = d_5 = 0$ $a_{12} / S\alpha_{12} = a_{23} / S\alpha_{23}$ $a_{34} / S\alpha_{34} = a_{45} / S\alpha_{45}$ $\alpha_{12} = \pi - \alpha_{34}, \alpha_{23} = \pi/2$

Describing the creation of simple structural groups of robot manipulators with general constraint, an important procedure should be followed to give the desired mobilities to the robot manipulators. In the light of this, creation of the end effector chains gains great importance.

By adding the joints and the branch loops to the end effector that is freely moving in space or any subspace, different end effector chains can be formed (Figure 4.1). With respect to their pair and branch loop properties, each of these end effector chains has its own mobility. The formed end effector chains will then be combined appropriately with the zero mobility structural groups to create robot manipulators with various mobilities.

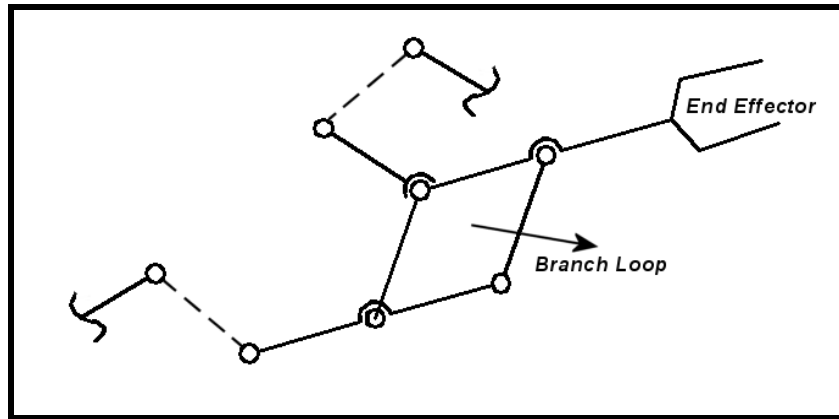


Figure 4.1. End Effector Chain with Branch Loop.

In general, a single end effector moving free in space or any subspace λ has mobility equals to the same space or subspace number. However, when connected with pairs and branch loops, mobility of the resultant end effector chain will become,

$$M_e = \lambda_e + \sum f_s + \sum_{L=1}^n (f_L - \lambda_L) \quad (4.3)$$

where, λ_e is the space or subspace of the end effector, $\sum f_s$ is the total degrees of freedom of the single pairs; that is, the pairs outside the branch loops, n is the number of branch loops, f_L is the total degrees of freedom of the pairs of the L^{th} branch loop and λ_L is the space or subspace of the L^{th} branch loop.

As it is clear that, $\sum f_s = \sum_{i=1}^k f_i - \sum_{L=1}^n f_L$ the Equation (4.3) will be reduced to,

$$M_e = \lambda_e + \sum_{i=1}^k f_i - \sum_{L=1}^n \lambda_L \quad (4.4)$$

where, k is the number of pairs in the end effector chain.

Finally, after the proper connection between the structural group and the end effector chain, the total mobility of the resultant robot manipulator will become,

$$M = M_e - \lambda \quad (4.5)$$

where, λ is the space or subspace of the base structural group.

In order to proceed in the design of parallel manipulators with general constraint one, current study considers only the simple end effector chains without branch loops in subspace $\lambda=5$. As there are no branch loops and the subspace of the end effector is $\lambda_e = 5$, Equation (4.4) will be reduced to,

$$M_e = 5 + \sum_{i=1}^k f_i \quad (4.6)$$

During the design of overconstrained manipulators the first thing to consider the motion of the end effector that will move in a suitable subspace as described in the section 3.2. The motion of displacement of the rigid body is equivalent to the end effector for the parallel manipulators. The subspace can be selected from Table 4.1 or Table 4.2. If the end effector has insufficient mobility, more than one subspace geometry can be used for that motion.

After deciding the mobility and the subspace of the parallel manipulator the design parameters as number of joints, configuration of links and joints can be calculated. Due to the fact that, the mobility is known the number of joints on the parallel manipulator can easily calculated by Equation (4.6). Next to calculation of joints one must select a structural group and design parameters that fit the desired subspace from Table 4.3. The mobility then will be added to the structural group with conditions such as spherical, parallel, or arbitrary in contribution with parameters of


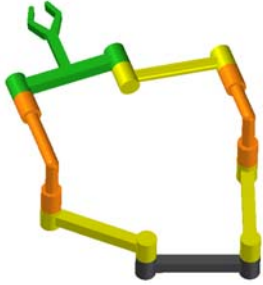
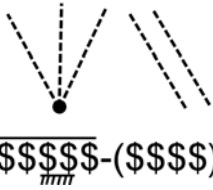
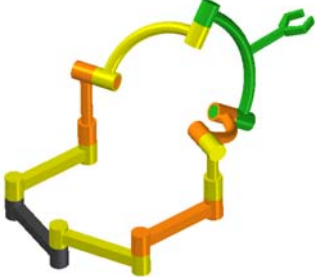


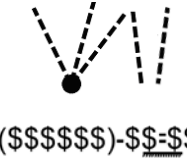
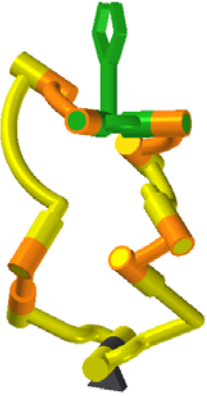
A) For the first overconstrained manipulator an end effector with mobility two is decided with subspace as shown in Table 4.1d. Thus number of joints is calculated as $\sum f_i = 2 + 5 = 7$. The structural group of this manipulator is picked from Table 4.3 as (4). The number of joints should be increased to the calculated value by adding 2 joints with conditions related to the selected subspace. The overconstrained manipulator will result in structural bondings of $\overline{\text{---}}-\overline{\text{---}}$, $\overline{\text{---}}-\overline{\text{---}}$, $\overline{\text{---}}-\overline{\text{---}}$ as shown in Table 4.4 a for mobility two. Structural bonding $\overline{\text{---}}-\overline{\text{---}}$ is selected for construction and the placement of end effector and actuated joints are shown in Table 4.7a.

B) For the second overconstrained manipulator the mobility of the end effector for the subspace Table 4.1 b is decided as four. Total number of joints will be $\sum f_i = 4 + 5 = 9$. After selecting the structural group from Table 4.3 as (2) four joints are added considering the conditions of subspace. Then the overconstrained manipulator will result in structural bondings shown in Table 4.4 b for mobility four and $\overline{\text{---}}-(\text{---})$ is selected for construction. The end effector is placed according to the rule defined and the actuated joints are shown in Table 4.7 (b).

C) For the third overconstrained manipulator the mobility of the end effector for subspace shown in Table 4.2 h is decided as three. Thus total number of joints will be calculated as $\sum f_i = 3 + 5 = 8$. The structural group decided Table 4.3 as (13). Three joints will be added for the actuation with in the conditions of subspace. Then the overconstrained manipulator will result in the structural bondings shown in Table 4.5e for mobility three as $\overline{\text{---}}\overline{\text{---}}\overline{\text{---}}$. The link of the end effector and the joints to be actuated are shown in Table 4.7(c).

D) For the Fourth overconstrained manipulator an end effector with mobility five in subspace Table 4.2c is decided. Total number of joints for this manipulator is calculated as $\sum f_i = 5 + 5 = 10$. The structural group is selected Table 4.3 as (12). After adding five joints to this structural group the manipulator ends with a structural bonding of $(\text{---})-\overline{\text{---}}$ is shown in Table 4.5(d). The end effector placement and selection of actuated joints are also shown in Table 4.5(d)

Table 4.7. New Angular and Linear-Angular Parallel Manipulators.

	Structural Group/Structure	DoF	Figure
a		2	
b		4	
c		3	
d		5	

4.2 Structural Synthesis of Overconstrained Serial-Parallel Platform Manipulators

Platform type manipulators can be referred as the manipulators that have more than two legs and consist of either one platform or many platforms connected by hinges or branches. Overconstrained term for the manipulator can be described by looking to the end effector which is moving in a subspace. During the structural synthesis of overconstrained serial-parallel platform manipulators, both legs of the manipulator and the loops of the manipulator are considered. Note that, in serial-parallel platform manipulators there should exist minimum two platforms connected by hinges or minimum two platforms connected by branch loops. . The mobility formula for platform manipulators can be given as in Equation (4.7)

$$M = (B - c) \lambda + \sum_{i=1}^c f_i \quad (4.7)$$

where, B is the number of platforms and c is equal to total number of legs, branches.

The algorithm of structural synthesis of parallel platform manipulators with no branch loops in subspace with general constraint one ($\lambda=5$) can be given as,

1. Select the motion for the end effector
2. Decide mobility of system (M)
3. Decide number of legs (c)
4. Decide number of platforms (B)
5. Select motions of the platforms
6. Calculate total number of joints $\sum_{i=1}^c f_i = M + (c - B) \lambda$
7. Selecting the subspace conditions for first loop (Table 4.4 or Table 4.5.)
8. Add legs/loops to the first loop with the same or new subspace conditions.
9. Decide the actuated joints

Example 2: Let us design an overconstrained parallel platform manipulator for a desired motion. Firstly an overconstrained manipulator with 3 DoF will be designed where the end effector motion can be prescribed by two orientations along a circular arc

as shown in Figure 4.2. Numbers of legs are depicted as three and one platform is decided. Total number of joints calculated as $\sum f_i = M + (c - B)\lambda = 3 + (3 - 1)5 = 13$. Joints will be distributed to the legs as 4-4-5. The subspace condition of loop 1 which is formed by the legs 1 and 2 is selected as shown in Table 4.5d for 3 DoF $(\text{---})\text{---}$ depicted as Table 4.8 a. Then a leg is attached to the platform as shown in Table 4.8b that will compose a loop that belongs to subspace $\lambda=5$ with leg 1. Note that leg 2 can also be selected. Finally all the actuated joints are selected as shown in Table 4.8c.

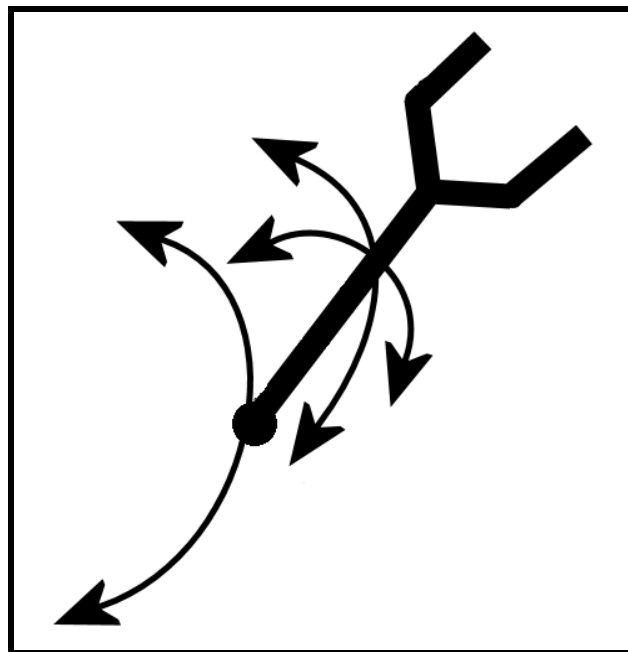
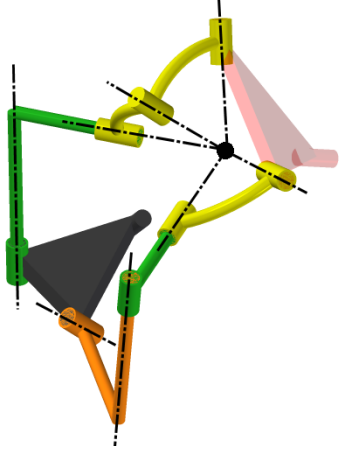
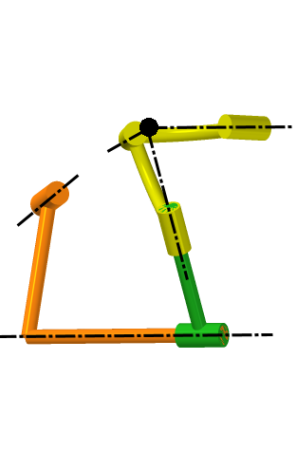
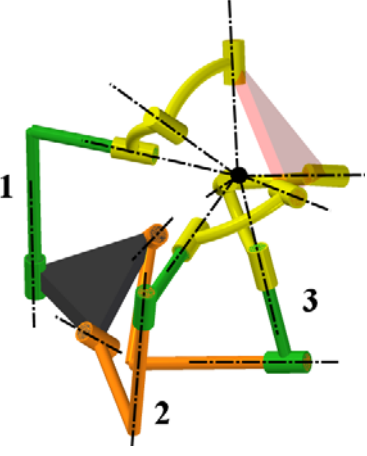
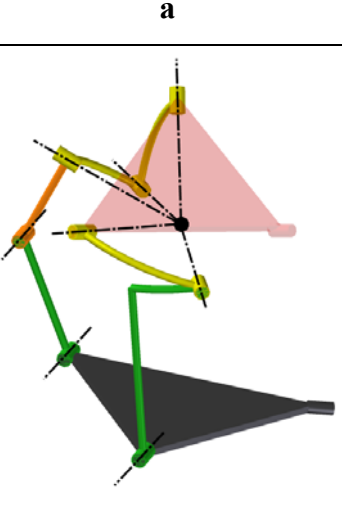
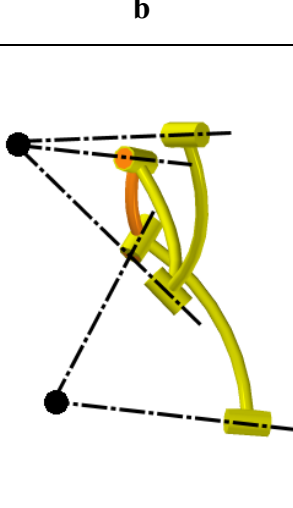
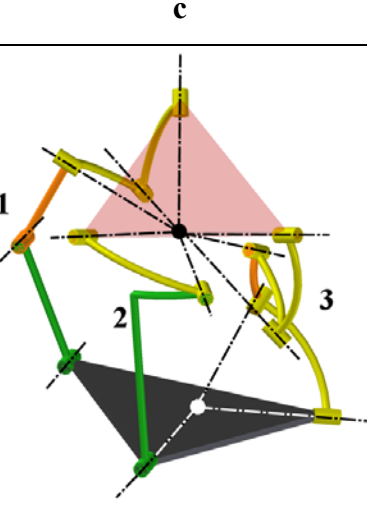


Figure 4.2. The Motion of End Effector.

During the design of this manipulator if the distribution of joints on legs is selected as 3-5-5 then another design can be introduced. For the loop that composed by legs 1 and 2 assembled with the condition shown in Table 4.4b for 3 DoF as $\text{---}(\text{---})$, shown in Table 4.8d. And for the second loop which is formed by legs 2 and 3 have the condition of intersecting axes in 2 points as shown in Table 4.8e. It can be seen clearly that leg 2 fits the conditions of each loop. The actuated joints and the construction of manipulator are shown in Table 4.8f.

Table 4.8. Steps for Constructing Overconstrained Manipulators.

First loop	Added leg	Manipulator
 <p style="text-align: center;">a</p>	 <p style="text-align: center;">b</p>	 <p style="text-align: center;">c</p>
 <p style="text-align: center;">d</p>	 <p style="text-align: center;">e</p>	 <p style="text-align: center;">f</p>

The design procedure of overconstrained serial platform manipulators will be similar to those of overconstrained parallel platform manipulators. For overconstrained serial platform manipulators c in Equation (4.7) is described as the summation of the total number of legs and total number of hinges as shown in Equation (4.8).

$$c = c_l + c_h \quad (4.8)$$

As all the loops must belong to a subspace, hinges included in the loops should be adequate to the conditions of that subspace.

Example 3: Let us design an overconstrained serial platform manipulator with 4 DoF. The manipulator consists of two platforms hinged together and connected to ground by four legs. It is obvious that each platform should have at least two legs. The number of joints calculated as $\sum f_i = M + (c - B)\lambda = 4 + (5 - 2)5 = 19$. The joints could be distributed in a combination of either 5-5+4-4 (Figure 4.3a) or 5-4+5-4 (Figure 4.3b).

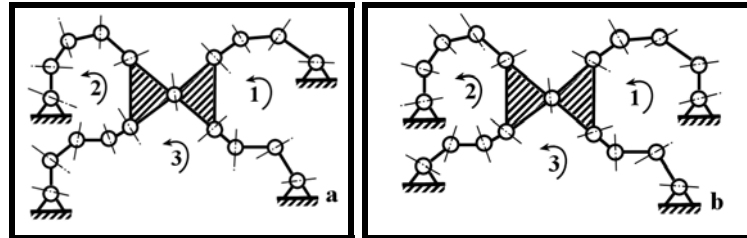
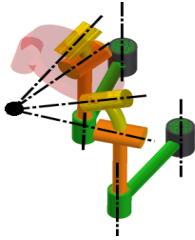
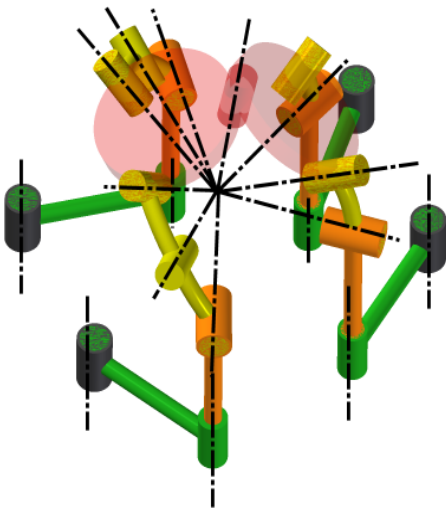
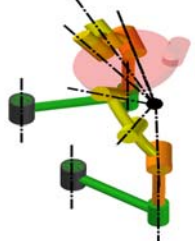


Figure 4.3. Structure of Overconstrained Serial Platform Manipulator.

The subspace selected for overconstrained manipulator is shown in Table 4.2c. For the combination 5-5+4-4 first loop is defined for 8 joints as $\overline{\text{$$$$}}-(\text{$$$$})$ (Table 4.9a). Then second loop is constructed for 10 joints as $\overline{\text{$$$$}}-(\text{$$$$})$ (Table 4.9b). The platforms are connected with a hinge which also fits the conditions of subspace. Finally the actuated joints are selected as shown in Table 4.9c.

Table 4.9. Construction Steps for Overconstrained Serial Platform Manipulator.

.First loop	Manipulator
	
<p data-bbox="470 1709 614 1742">Second loop</p> 	

CHAPTER 5

HAND WOVEN CARPET TECHNOLOGY PROCESS

To apply knowledge gained during the studies on robotics, the robotization of carpet technology process is selected. The research on hand made carpets is done by, not only examining publications written about hand woven carpets but also investigating the work places at Ghordes. After the literature search and investigations a carpet loom has been built up and the weaving of a carpet has started. Also during the research the ornaments in Turkish woven carpets were examined (Turkish Republic Ministry of State-Ministry of Culture and Tourism, 1987-90) and a carpet design has been introduced. In this chapter after giving some information about the terminology of hand woven carpets and explaining the process, information about the ornaments and patterns of Turkish carpets will be introduced

5.1 Terminology and Definitions

Before beginning to introduce hand woven carpet technology process, some definitions should be given for the ease of understanding. As seen in Figure 5.1 the lengthwise yarns, which are also shown in Figure 5.2 as placed between upper and lower beams of the loom, are warp yarns. They usually consist of cotton, silk, wool or mixture of those and they are tightly spun and plied for strength.

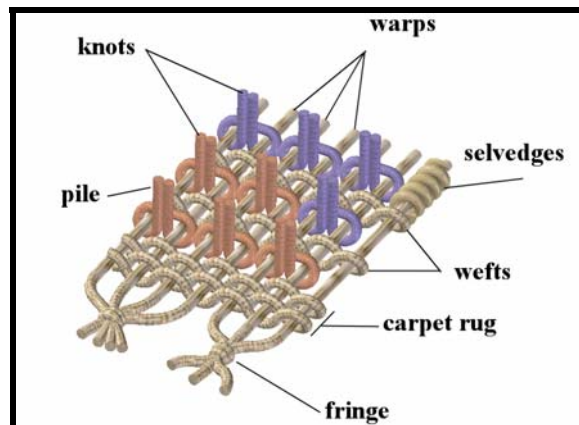


Figure 5.1. Carpet Structure.

The yarns diagonal to the warp yarns are called weft yarns and they pass through the warps and together with warp yarns form the base of the carpet with warp threads.

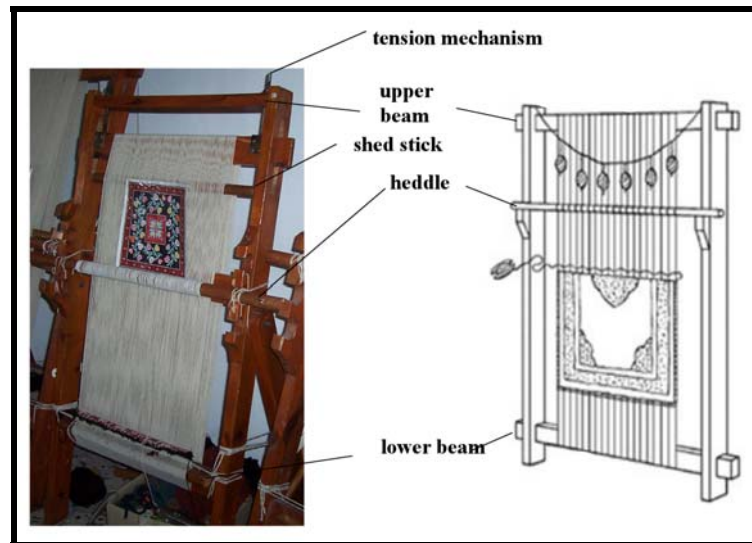


Figure 5.2. Loom Structure.

(Source: Hand Made Carpets 2007)

Heddle (Figure 5.3) is the system that distributes the warp threads in a line equally and separating front and back warps during the operation of wefting. Knots are tying of wool or silk yarns to the one, two or more threads of warp in different combinations.

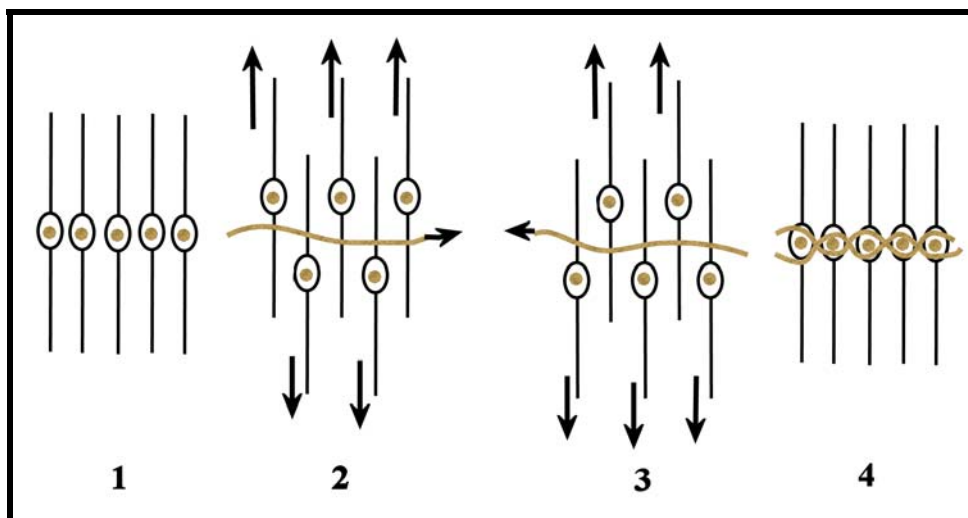


Figure 5.3. Heddle Motions.

As shown in Figure 5.4 there are lots of knot types and combinations but the well known and mostly used ones are symmetrical ones (Figure 5.4a) and nonsymmetrical (Figure 5.4b). The heights of knots are called piles and eaves are the remaining parts of warp threads of the two ends of the carpets. Changing with respect to the length of the carpet the lengths of the eaves are usually around ten centimeters. Chain is the chain type structure which is woven at the ends of the carpets parallel to the carpet rug. The rug is the straight weaving done up to the ends of the carpet to support pile height. Selvedges are the narrow parts of the sides of the carpet that are woven with the same color of the base carpet to strengthen the sides of carpet.

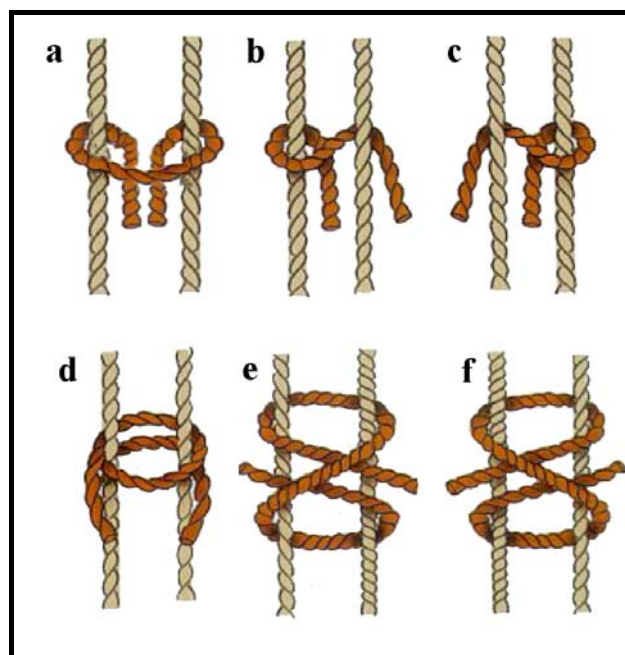


Figure 5.4. Knot Types.

5.2 Technology Process of Hand-Woven Carpets

The process of carpet making has many steps starting from the producing of yarn that is made of wool or silk to the cleaning of the carpet. These steps can be classified in three general groups such as pre-weaving operations, weaving and finishing operations.

the pre-weaving operations begins with the producing of yarns. Three types of materials are used in hand woven carpets. These are wool, silk, and cotton for warp and weft threads and only wool or silk for the knots. Use of industrial yarns such as nylon,

polypropylene and polyester decrease the quality of the carpet thus preferred neither by the producers nor by the customers. Dyeing process is then started after preparing the yarn. Natural dyes are preferred because of their shades of color can not be found in various synthetic dyes and natural dyes will mellow with time, and if left under the sun they will shine and radiate very good shades of color. Natural dyes are obtained from plants and animals, as dyes woad (blue,) madder red, ox-eye chamomile (yellow), walnut (brown), pomegranate tree (yellow).

After preparing and dyeing the yarn, next step is to construct a carpet base on a loom. Prepared yarns are attached to the loom's up and down shafts and then strained. Now the loom is ready to weave.

First operation before knotting is the preparation of the carpet rug with several wefts consecutively passed through the warp yarns. Wefting operation is done easily by the help of heddle system (Figure 5.3). The weft passed through the one side in first position then passed through its axis direction in second position. After each row of knotting these operations are repeated.

The knotting operation is the basis for the hand woven carpets. The weaver takes some yarn with the desired color in the pattern. Then pulls two neighbor warp threads, where the pile will be knotted. The yarn is passed between the warp threads, turned around left thread, passed to the right below the yarn, turned around right warp thread and get out between warps under the pile. Then the knot is pushed down to its place and surplus is cut. In each row, after the weft threads are passed, knots are hammered down to supply strength in the carpet

After the end of carpet weaving, weaved carpet is cut out from the loom and finishing operations start. These operations can be listed as washing, drying, shearing, dusting, stretching, repairing and finally quality control. In washing process firstly a singeing operation is applied to the carpet which is laid on a smooth floor then it is washed. During this operation pieces of yarns and unwanted surplus are removed from the carpet. After carpet is washed, it is dried in specially designed rooms. Then dried carpets are sheared with a single shearing machine in accordance with desired pile thickness. The sheared carpets are processed in dust board for purification form surplus and in order to eliminate the hardness of the carpet and provide a softer surface and same brightness. Next step is stretching. The carpet is stretched over the wooden panels to flatten the curls on edges, folds and inclinations on the surface. Besides these

processes the carpet is repaired for the errors occurred during the weaving or finishing processes. And now the carpet is ready for quality control.


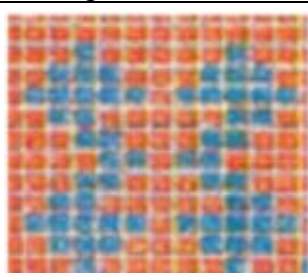


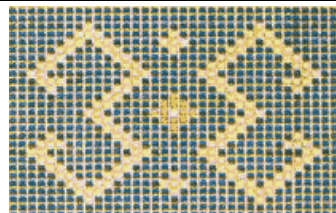
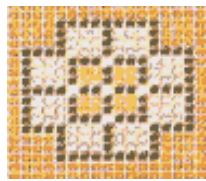
5.3 Pattern Study for the Turkish Hand Woven Carpets

Tremendous richness and variety of design combined with an effective use of color are the significant properties of oriental carpets. The colors in carpets are not only used for decoration but also used for the implementation of religious and emotional meanings with the use of patterns.

The design of carpets can be divided into two groups such as floral and geometrical. Persia and India are mostly using floral designs, Caucasian and Turkoman designs are always geometrical. In the Turkish carpets both geometrical and floral designs are seen.





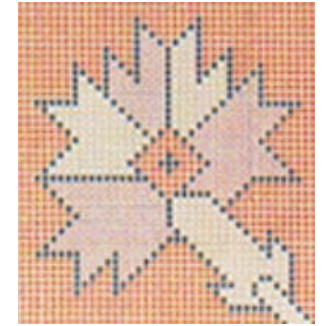

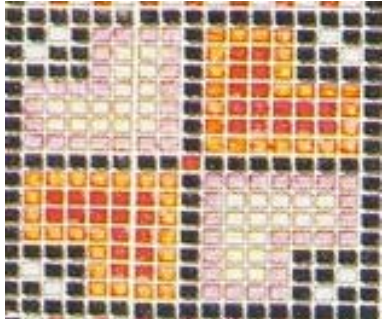
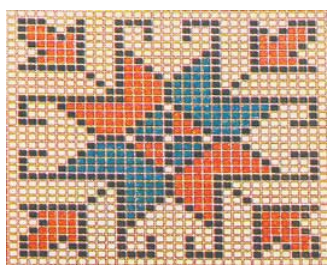
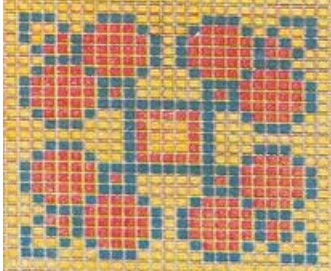
Animals, insects and birds are often featured in the design of hand woven carpets. Some ornaments for these animals are shown in Table 5.1 with the meanings they influenced to the carpet pattern.

Table 5.1. Animal Figures Seen in Turkish Carpets.(Source: Turkish Republic Ministry of State-Ministry of Culture and Tourism 1987-90)

Dragon	Birds	Camel
Animal guarding the tree of life	Souls flying over the garden of Eden	Importance of the animal
		
Dragon & Phoenix	Rams Horn	Scorpion
The unisons of earth and heaven	Symbolizes fertility and reproduction.	Protects the pregnancy against makice
		

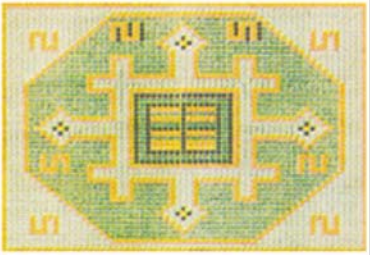




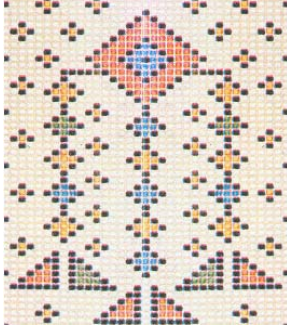
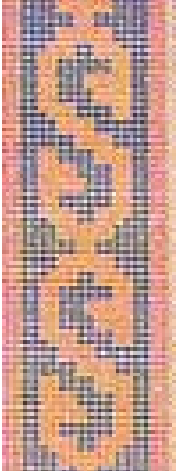

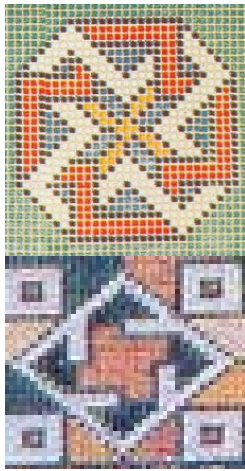
The most important symbols used in carpet designs are flowers, fruit and especially trees. Trees mostly stand for the tree of life which is the symbol for the immortality after life. The meanings of ornaments are listed in Table 5.2

Table 5.2. Plant Figures Seen in Turkish Carpets. (Source: Turkish Republic Ministry of State-Ministry of Culture and Tourism 1987-90)

Tree of life Reincarnation	Tulip Desire to have a child	Rose Marriage, purity of love
		
Acacia	Carnation	Plane tree leaves
To express Garden of Eden and tree of life		
		
Almond	Hyacinth	Clover
To express Garden of Eden and tree of life		
		

Some non-living figures are also symbolized in Turkish carpets such as chest, earrings, stars, etc. In Table 5.3, these are depicted with meanings.

Table 5.3. Non-Living Figures Seen in Turkish Carpets. (Source: Turkish Republic Ministry of State-Ministry of Culture and Tourism 1987-90)

Chest Trousseau chest and marriage	Star Happiness and eternity	Eye Protect against evil eye
		
Earring Desire for marriage	Tobacco bag Imply that the rug was woven for a certain man	Oil lamb Assign a religious characteristic to the rug
		
Hook Protection against evil eye	Hand Protection	Wheel of Fortune Control of destiny
		

The general design structure for a carpet can be seen in figure 5.5.

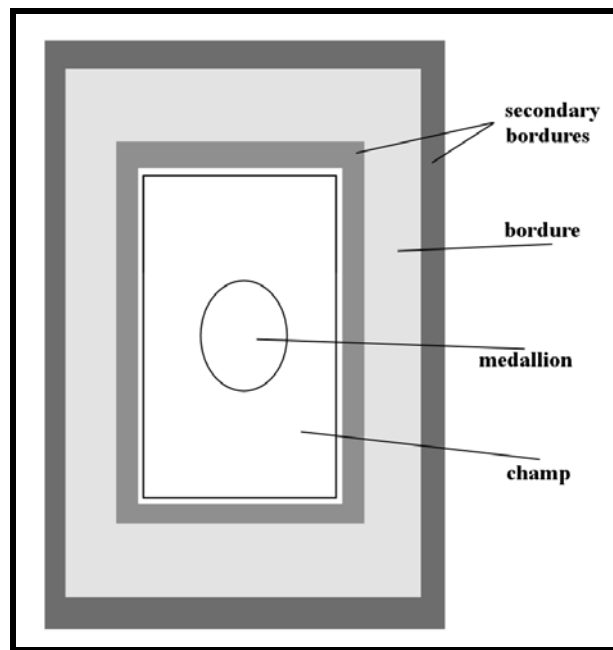


Figure 5.5. General Design Structure for Turkish Carpets.

By the combination of some ornaments and using the general design structure, the carpet with a unique design shown in Figure 5.6 is acquired.

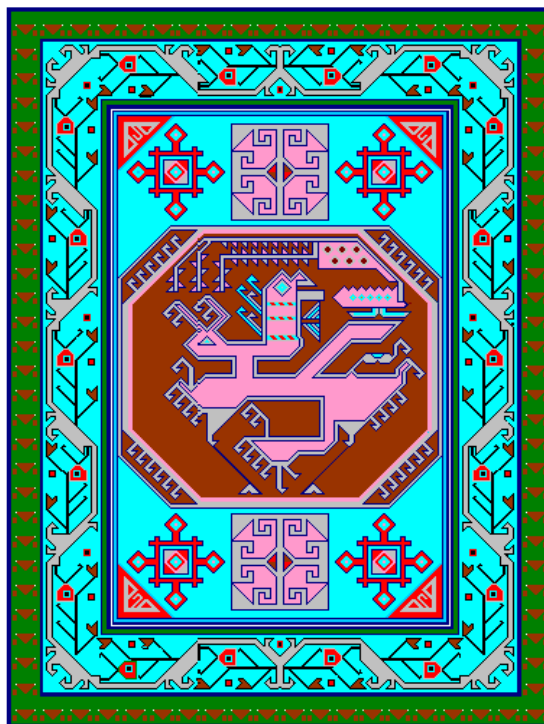


Figure 5.6. Unique Carpet Pattern.

CHAPTER 6

DESIGN OF MECHANISMS FOR HAND WOVEN CARPET TECHNOLOGY PROCESS

The hand woven carpet robot has to work by performing similarly when composed with the weaver in conventional hand carpet production process. The robotization will be applied to the weaving operations described in the previous section such as wefting, sley and knotting. For the operation of wefting two motions are needed as the manipulation of warp threads and the passing motion of the weft thread. After each weft is passed, a sley mechanism will pressure down the weft thread. After that the most important and complicated part of the process begin as the weaving of the knots. Knot weaving starts with the preparation of the pile yarn with the color defined in the pattern. Bringing the pile yarn to the weaver, it makes the knot and the knot is pressured down to weft threads. After each row of knots is finished, the procedure is repeated. As shown in Figure 6.1 the system will consist of a heddle mechanism, sley mechanism, weft mechanism, a robot arm and a weaver attached to this arm.

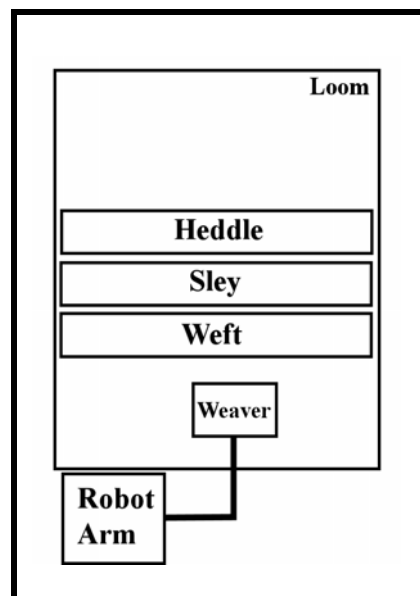


Figure 6.1. Schematic Structure of the Carpet Weaving Robot.

6.1. Structural Design of Carpet Robot

Before starting one must construct a loom that will carry the mechanisms and supply a work space to the robots. In the design of loom the forces on the beams should be considered. The forces acting on the beam are the weight of the beam itself (G) and the tension of the warp threads applied (F_r) as shown in Figure 6.2. and the Forces acting on the bearings of beams are denoted as F_b . If only one warp thread is considered the tension on that warp is nearly 15N that is a negligible force. However the majority of warps (800 in 2 meters) cause a large force to be considered. Note that the calculations for the beams are shown in Appendix A.

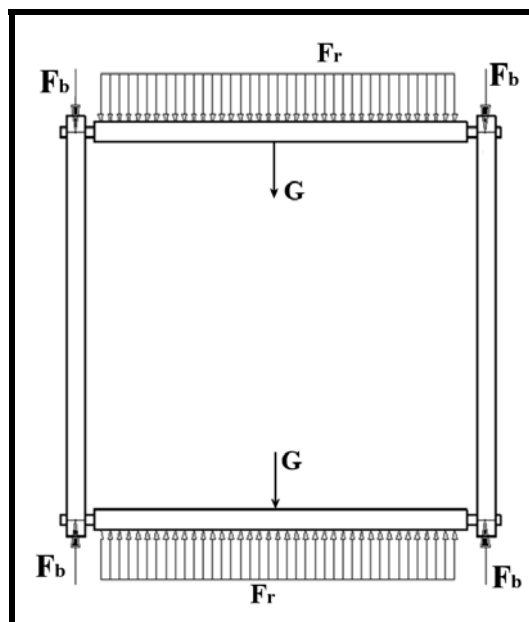


Figure 6.2. Forces Acting on the Loom.

The forces acting on the weft mechanisms are shown in Figure 6.2. Considering these forces, Forces acting on the Weft mechanisms are shown in Appendix A.

6.2. Design of Mechanisms for the Carpet Weaving Process

The motions in the Carpet weaving process can be defined as heddle motion for opening up the warps, weft motion for the weft thread pass through warps, sley motion for pressing the weft threads and the motions of weaving.

6.2.1. Design of Mechanisms for Heddle Motion

The motion of the heddle can be summarized as the movement of two parallel platforms in opposite directions. The rotational input must be converted to double linear outputs. The mechanisms that can be used for this process are double slider crank mechanism, rack and pinion mechanism, sprocket-roller chain system and cam mechanism. As shown in Figure 6.3 double slider crank mechanism consists of 2 slider cranks that are sharing the same input link. The sliders are the platforms themselves with linear guides.

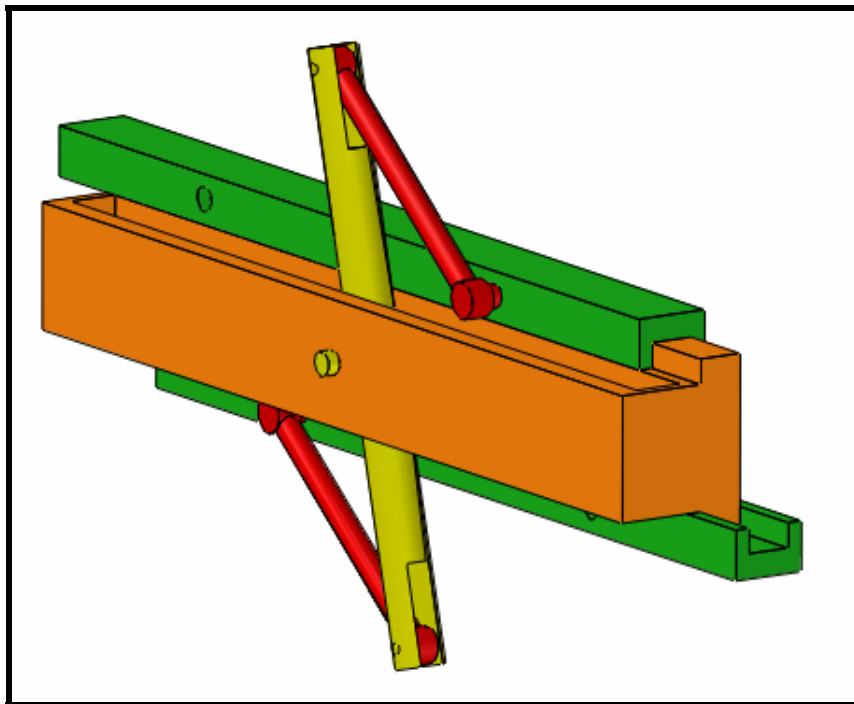


Figure 6.3. Double Slider Crank Mechanism.

Another mechanism proposed for the heddle movement is cam mechanisms. As seen in Figure 6.4 two pins are attached to the platforms, with sliders. A double slotted slider is connected to the input shaft. Thus, the orientation of the shaft transmits the motion to the platforms as linear motion.

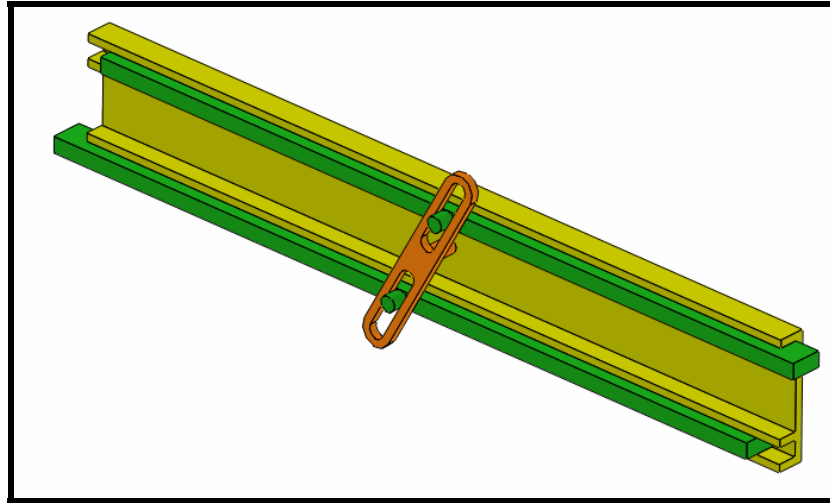


Figure 6.4. Slotted Slider Mechanism.

The next mechanism used for the motion of the heddle is sprocket and roller chain system as shown in Figure 6.5, the platforms are connected to the up and down lines of the roller chain.

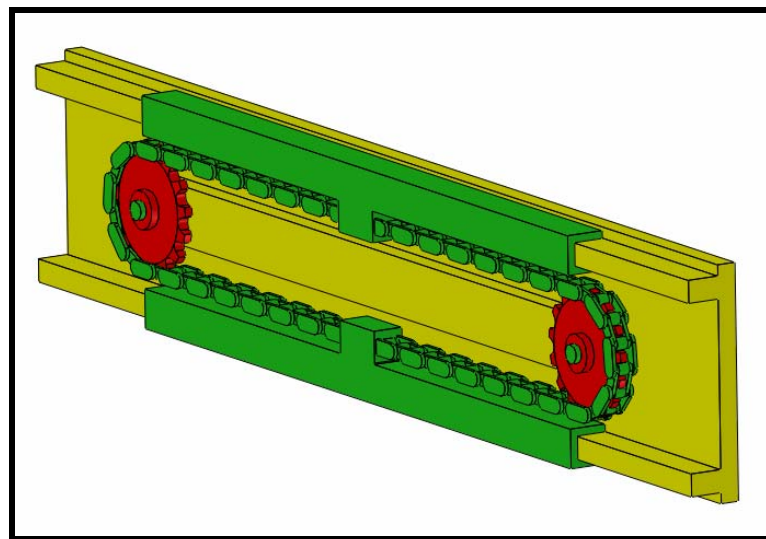


Figure 6.5. Sprocket and Roller Chain.

The last proposed mechanism is the rack and pinion system that is shown in Figure 6.6. This mechanism has the advantage of easy assembly and distribution of force more efficiently.

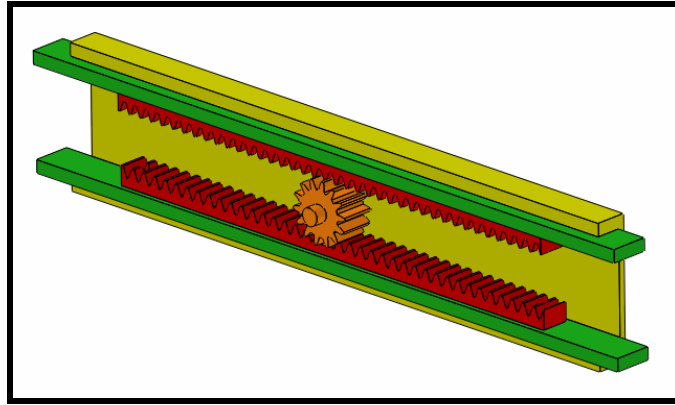


Figure 6.6. Rack and Pinion Mechanism.

6.2.2. Design of Mechanisms for Weft and Sley Motions

As described before weft threads are the yarns that are passing through the warp threads in each row of carpet, and sley is the comb movement that presses the weft threads down. During the design procedure these two movements can be considered as a whole or separate system. If considered together, the holder (Figure 6.7a) for the weft thread will be translated either on the sley mechanism (Figure 6.7b) or in a slot at the down side of the sley mechanism (Figure 6.7c)

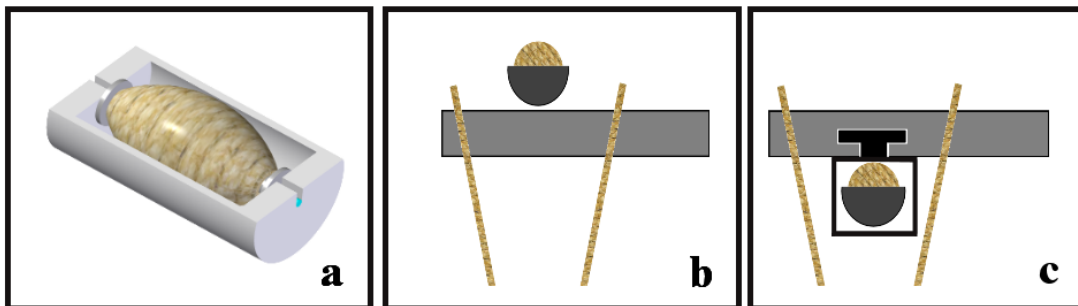


Figure 6.7. Holder and the Positions of the Holder.

The motion of the holder can be given by three ways as using a mobile robot that translates the holder along the loom, using two extensions mechanisms with grippers at the end or simply using a four bar to throw the holder from side to side. The four bar system as shown in Figure 6.8 consists of two four bars at each side of the loom. By applying a sudden force to the holder the translation from one side to other is supplied very quickly. Advantages of this system are speed and simplicity but the

disadvantages are need of high power and low reliability incase of struck of the holder in the middle of the loom.



Figure 6.8. Double Four-Bar Mechanisms.

Another mechanism is proposed as the extension mechanisms with grippers at the end. As seen in Figure 6.9a the holder is grasped by one gripper and the other remains open in first position. Then they both extended to the middle. When pushed towards, cam mechanisms with the gripper Figure 6.9b allows to swap the holder from one extension to other. At last both condensed.

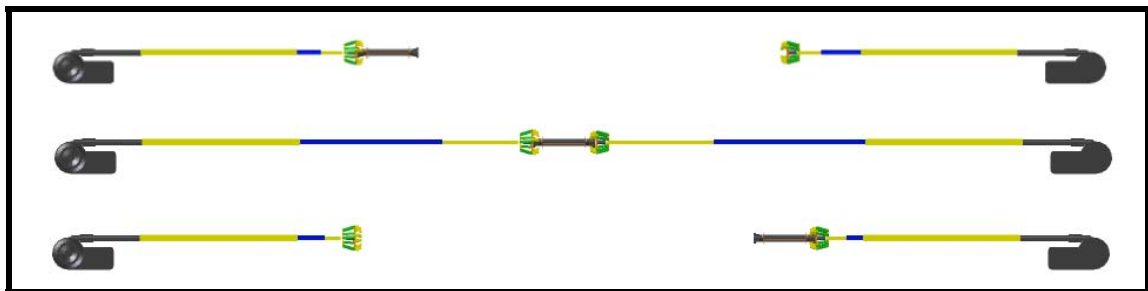
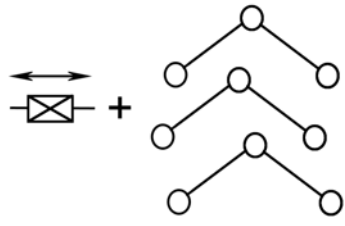
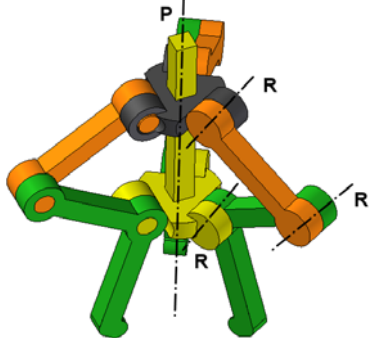
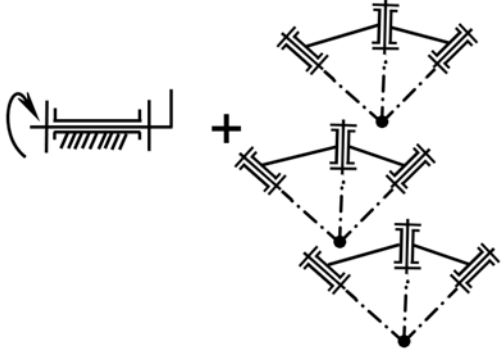
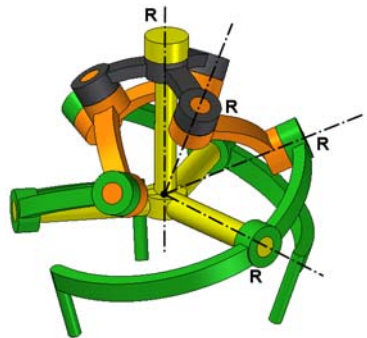
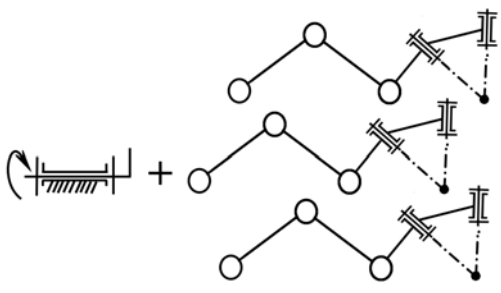
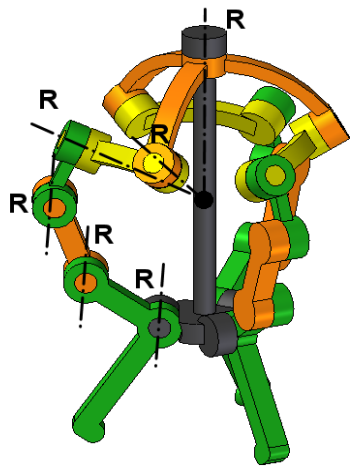


Figure 6.9. Extension Mechanisms.

For the structural design of the gripper Equation (6.1) is used and 3 types of grippers are presented. As seen in Table 6.1 first and second one have legs within the subspace $\lambda=3$ and the last one is constructed with legs in subspace $\lambda=5$

$$M = \lambda + \sum_{l=1}^{c_l} (f_l - \lambda_l) \quad (6.1)$$

Table 6.1. Gripper Designs for the Holder.

#	λ_l	Structural Bonding	Gripper
1	3		
2	3		
3	5		

As the process is carrying the holder from one side to another, it can also be done by using a mobile robot attachment. The path of the mobile robot can be either the warp threads or the comb as shown in Figure 6.10.

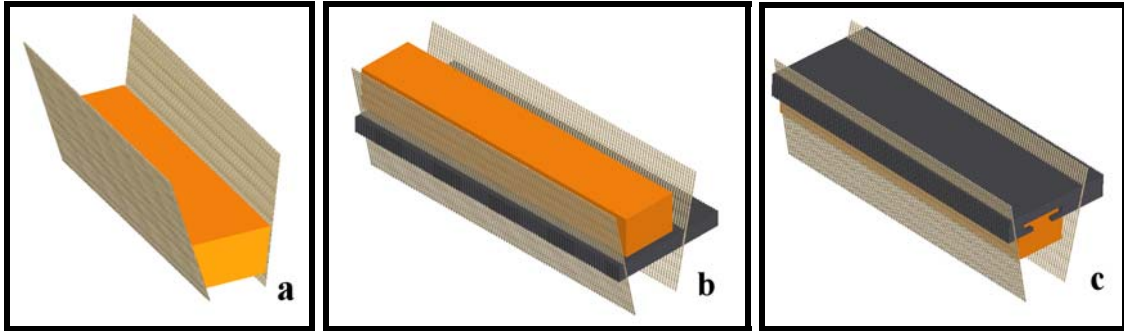


Figure 6.10. Paths of the Mobile Robot System.

If the robot is moving on warp threads (Figure 6.10a), the wheels must be either spherical or conical with the same angle as warp threads. If the robot is moving on or under the comb it must be guided by it. The usage of the comb as a path comes with the advantage of reliability but increases the cost of sley mechanism. The proposed drawings for the robots for all three paths can be seen in Figure 6.11.

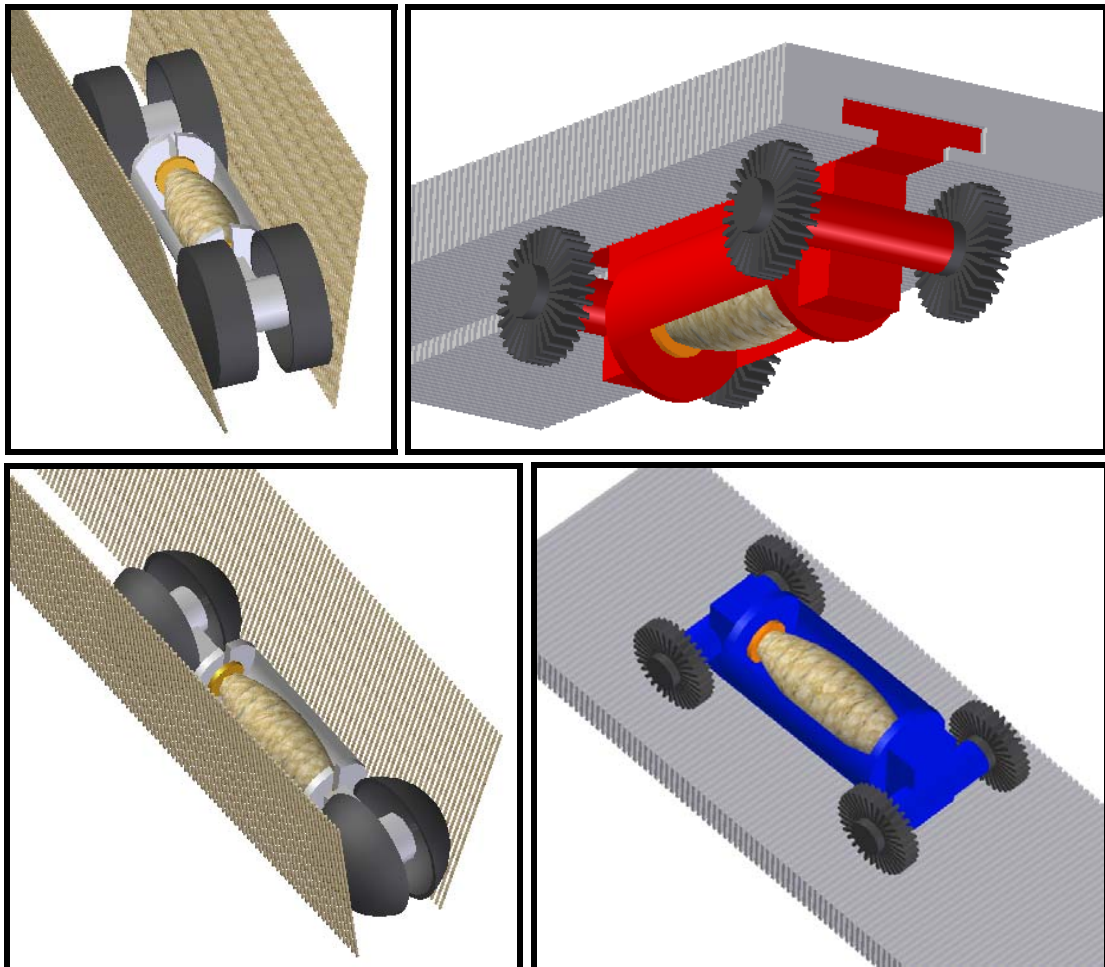


Figure 6.11. The Robots for Wefting.

Sley mechanism, if used with the weft mechanism will have a full body in the length of the loom that will carry the holder as shown in Figure 6.1a. The motion is given with four bar mechanism shown in Figure 6.13. If the sley is independent from weft it can be made by prismatic actuator and four bar in Figure 6.13 that is attached to it as shown in Figure 6.12b.

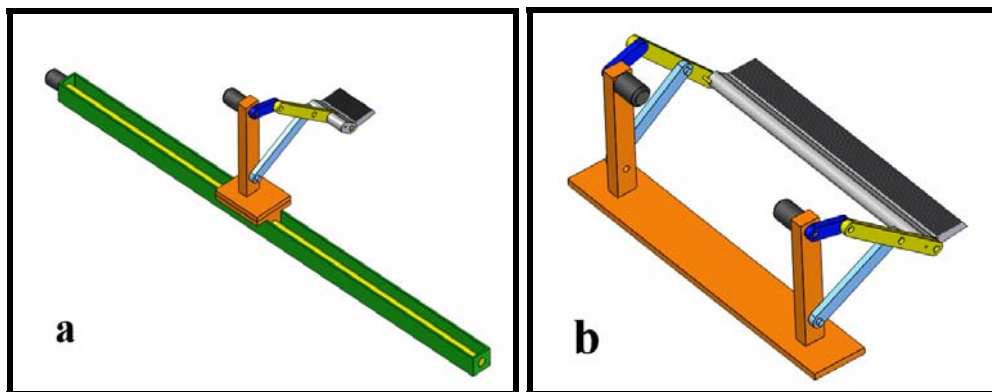


Figure 6.12. Sley Mechanisms.

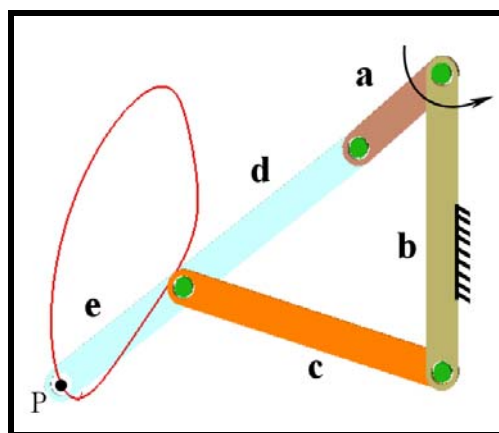


Figure 6.13. Path for Sley Mechanism.

6.2.3. Design of Weaver Arm

Before starting to describe the weaving operation, the end effector must be displaced in its work space with the robotic arm. This arm will make Cartesian motion. Serial, parallel or hybrid manipulators will be considered throughout this section. The serial arms can be PPP type or PRRR type as seen in Figure 6.14

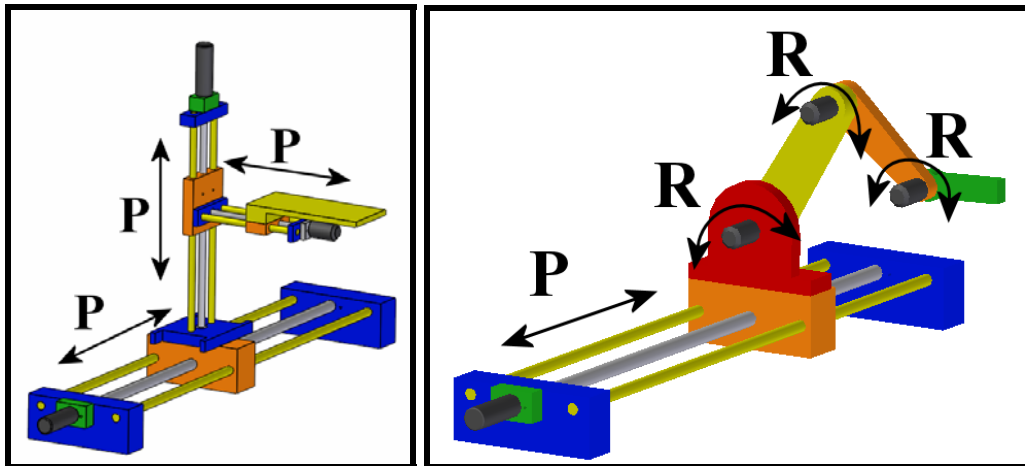


Figure 6.14. Serial Robot Arms.

Another type parallel robot that can be used for Cartesian motion is shown in Figure 6.15. The advantage of this robot is that it can carry higher loads or apply higher forces but the workspace is not wide enough for a big carpet loom.

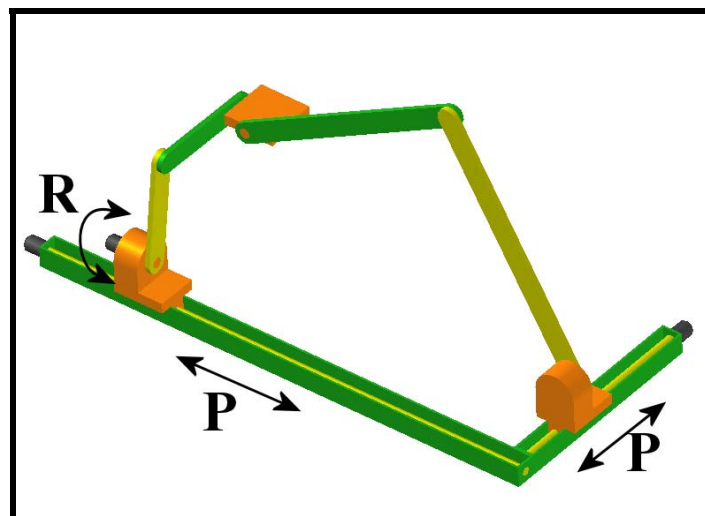


Figure 6.15. Parallel Manipulator.

The hybrid manipulators are the combination of serial and parallel types. As seen in Figure 6.16 the parallel part of the manipulator is connected to ground with a prismatic actuator. In this configuration high precision and large workspace properties can be achieved. Note that the positions of the motors are near to the ground.

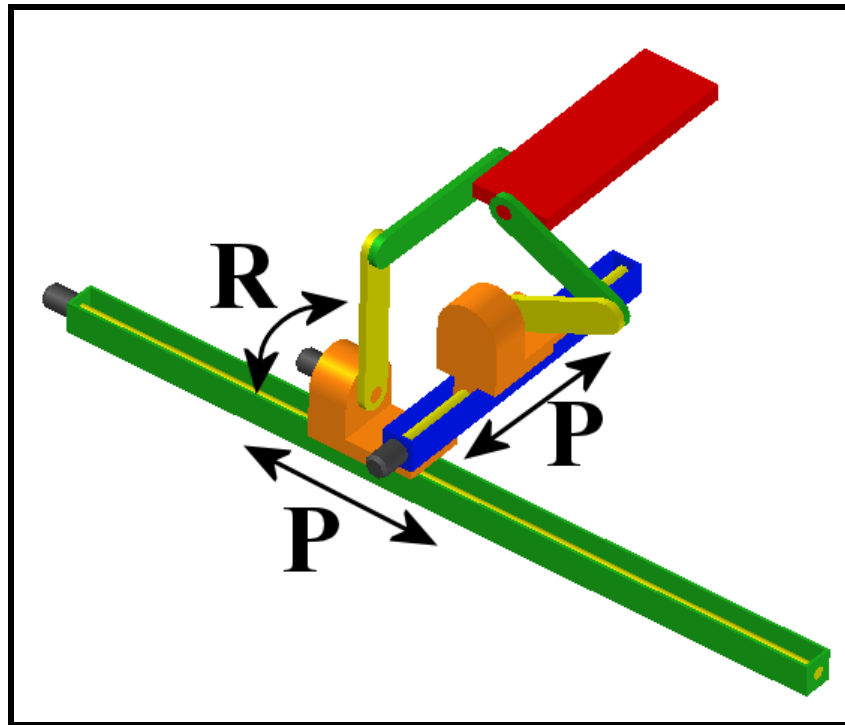


Figure 6.16. Hybrid Manipulator.

6.2.4. Design of Weaver System

The end effector of the arm, called as the weaver, is an electro mechanical system for tying a symmetrical knot. The process of weaver can be defined in 4 steps as, preparing the pile for knotting, getting some workspace by opening up the warp threads, knotting phase and grasping the knotted pile. After these processes the arm will push all the system downwards.

Before starting the knotting process the pile with the color in order must be prepared for the weaver. Preparation of the pile for weaving starts with the selection of the color. The data comes to the stepper motor and the tube of the selected color come inline with the handler. Then the handler starts to turn one step where a step is defined as $2\pi / (\text{number of handlings})$. The knife cuts the pile. Note that one way rollers in each tube avoids the retreat of piles backwards. After that, the handler turns enough to bring the pile in front of the weaver grippers as shown in Figure 6.17. However before the start of turning the yarn selection box moves so that the handler and tubes should not be aligned. The exact step of the movement is supplied with a Geneva wheel.

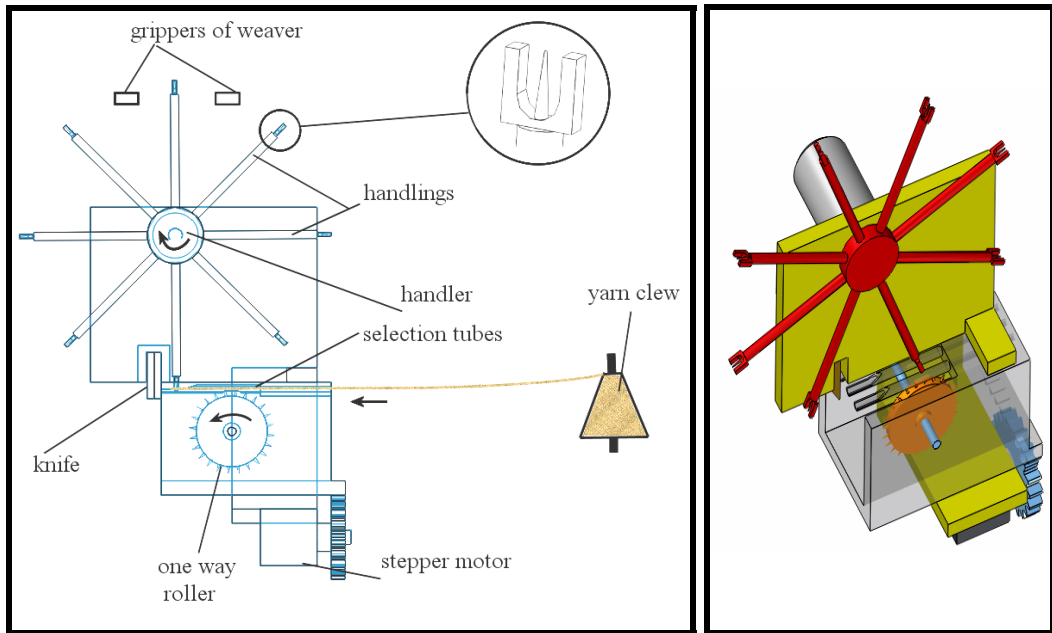


Figure 6.17. System for Preparing the Pile.

Two mechanisms are investigated for opening some workspace for the weaver. The first one is a double slider crank mechanism shown in Figure 6.18. It gets through the decided warps and opens up its ends a little for holding the warps. Afterwards, warps are taken out to widen the distance between them. Another mechanism is a cylindrical motion manipulator with an arrow head end effector as shown in Figure 6.19. In first position it gets through the warp threads and turns a little to hold the warps then take out warps by the help of backwards motion. Posterior to this, end effector turns more to widen the distance between warp threads.

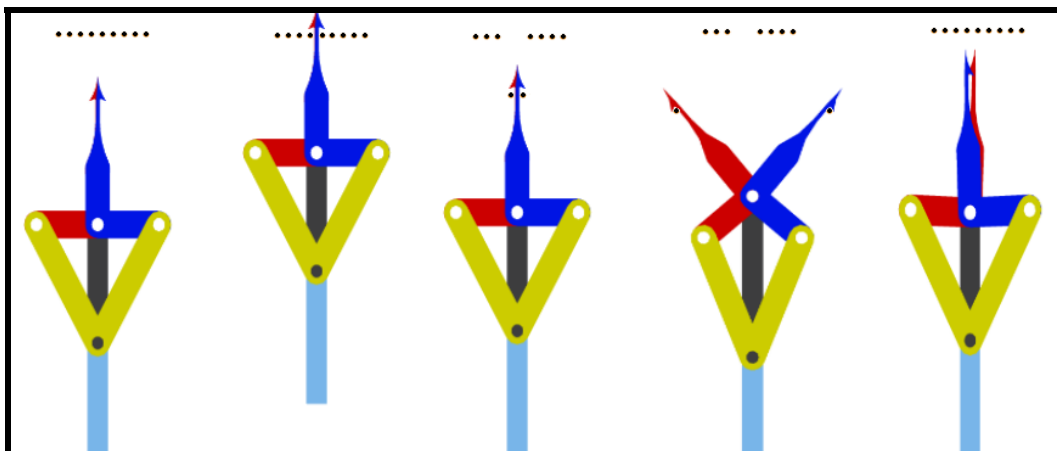


Figure 6.18. Mechanism for Holding the Warps.

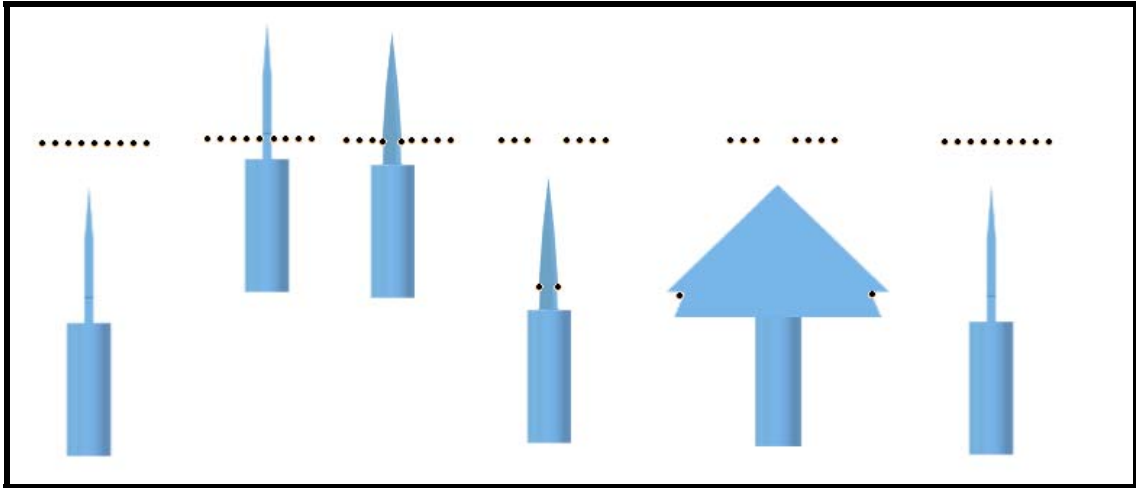


Figure 6.19. Mechanism for Holding the Warps.

Sequential to the bringing of the pile, the grippers of the knotting mechanism will grasp the pile. Then they will follow a path around the warp threads for knotting that are presented in Figure 6.20. This motion can be obtained by a four bar mechanism (planar, spherical), tendon driven serial fingers or a cylindrical motion parallel mechanism.

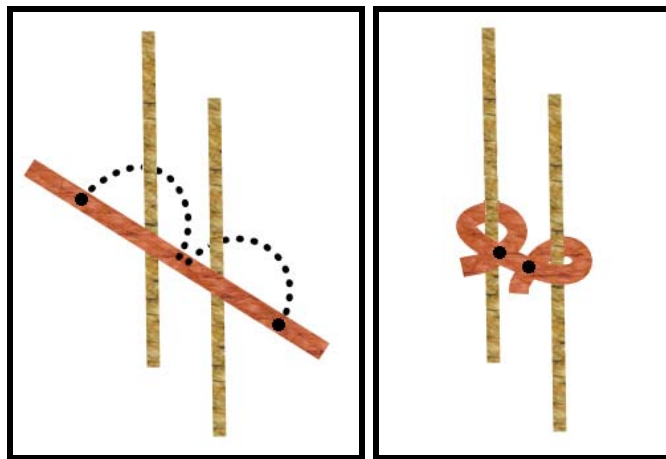


Figure 6.20. The Path of the Pile.

The advantage of spherical four-bar is the fact that it can both guide the point and the body of the pile for better grasping of pile ends.

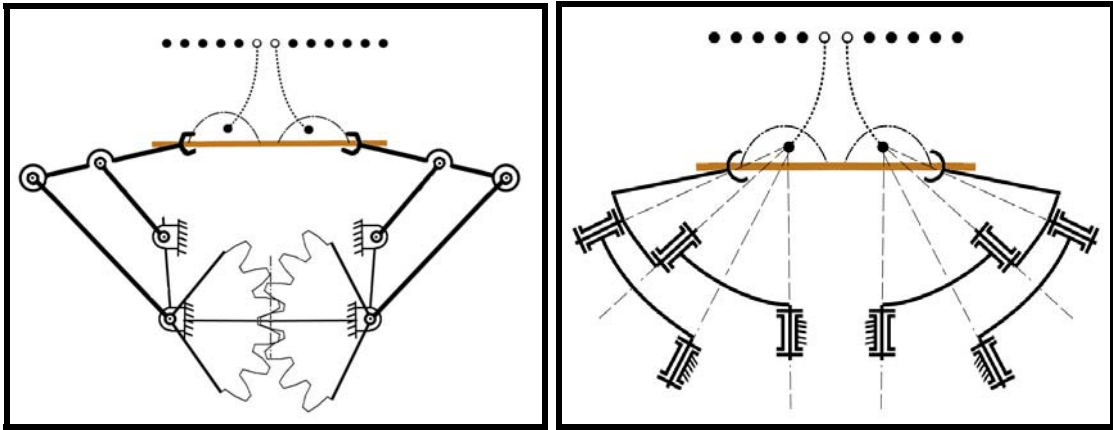


Figure 6.21. Four-Bar Mechanisms.

Tendon driven serial fingers can also be used as shown in Figure 6.21. The advantage of these grippers is that they can pass from all points of the trajectory. However it comes with the disadvantage as the redundant mobility and increased control complexity.

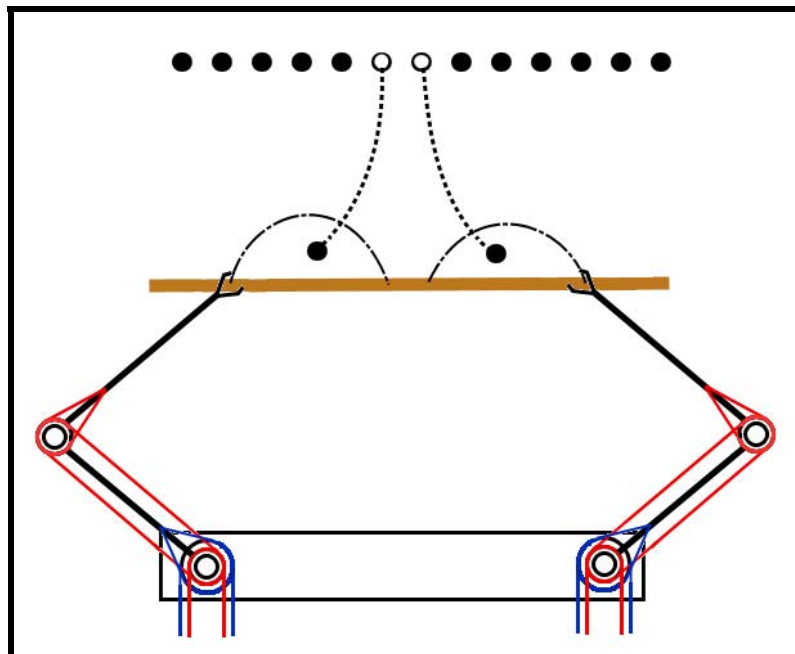


Figure 6.22. Serial Fingers.

The cylindrical manipulators have 2 DoF and their advantage is the fact that they can pose the pile ends such a way that it is easy for grippers to grasp.

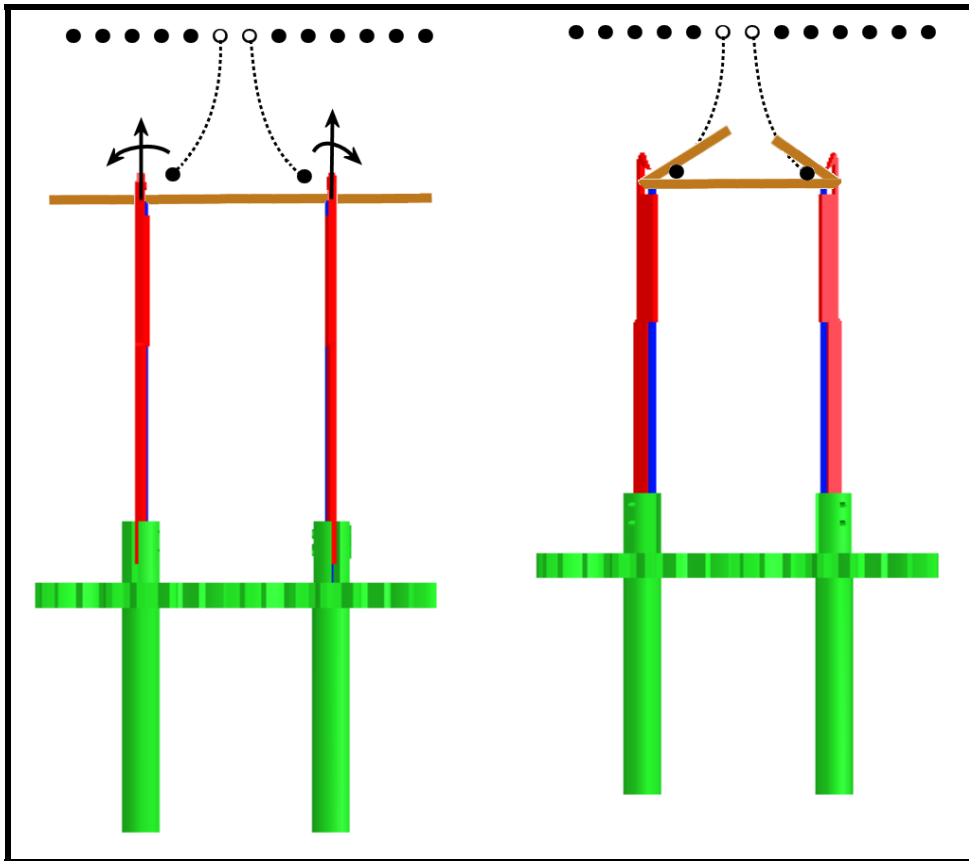


Figure 6.23. Cylindrical Manipulator.

Final work of the weaver is to grip pile ends between the warp threads and pull back. A slider crank or double slider crank mechanisms are proposed for this action as seen in Figure 6.24

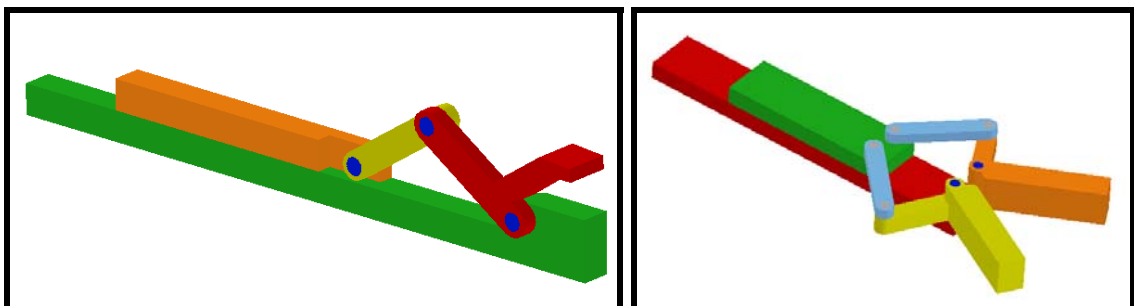


Figure 6.24. Gripper for Grasping the Pile Ends.

6.3. Design of Carpet Weaving Robot

The robot of carpet weaving consists of mechanisms for the motions of heddle, weft, sley and knotting. After giving the structure of the carpet robot and presenting suitable mechanisms for the stages of carpet weaving, the assembly and the interaction between them will be introduced. During the design of carpet robot, tie in and coordination of mechanisms have vital importance. The positions of the mechanisms on carpet loom are shown in Figure 6.25.

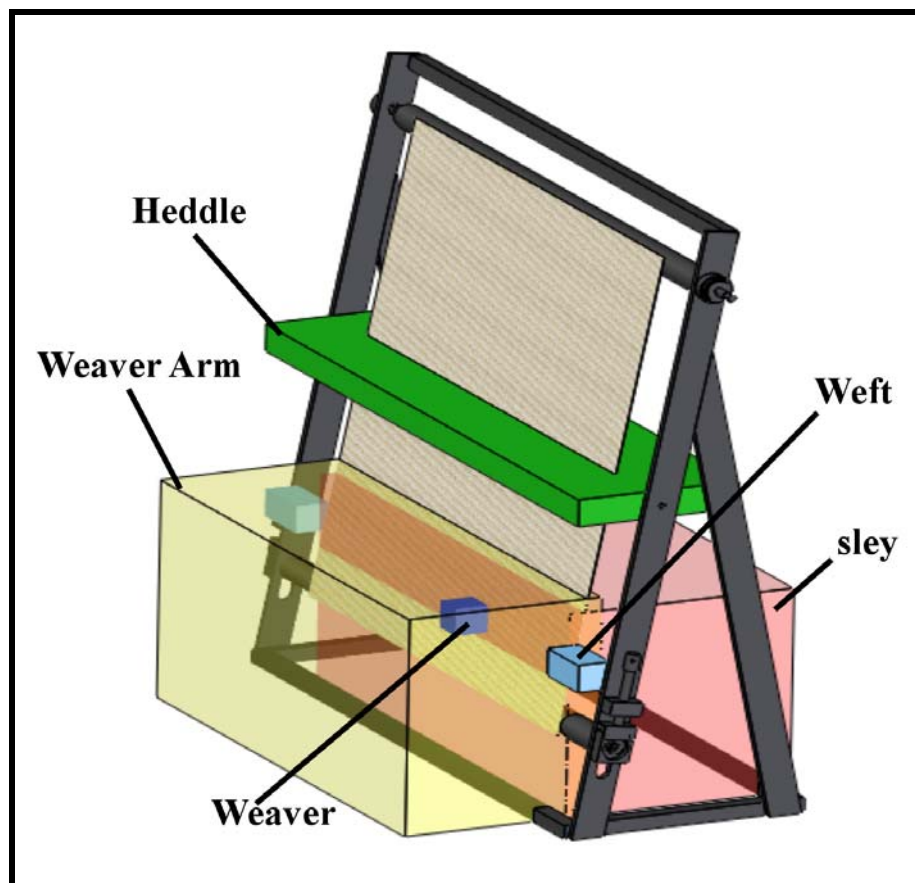


Figure 6.25. Positions of Mechanisms on the Loom.

The work order for the system is shown schematically in Figure 6.26.

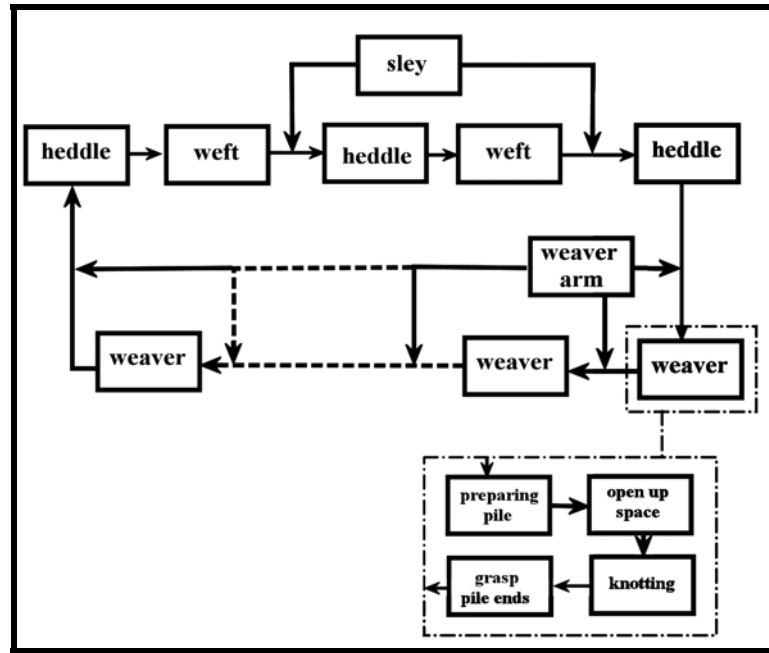


Figure 6.26. Work Order of the Carpet Robot.

Now the details of the selected designs of mechanisms will be given. For the heddle motion the rack and pinion system is selected, because of the properties, ease of manufacturing and ease of assembly. The mechanism will be attached to the both sides of the loom and will be driven by 2 motors with gear boxes. The calculations for the torque applied to shaft of the gear boxes by warp threads is in Appendix A. The mechanisms for weft and sley motions are decided as independent. For the weft motion the mobile robot with conical wheels is selected. The detail of the robot is given in Figure 6.27.

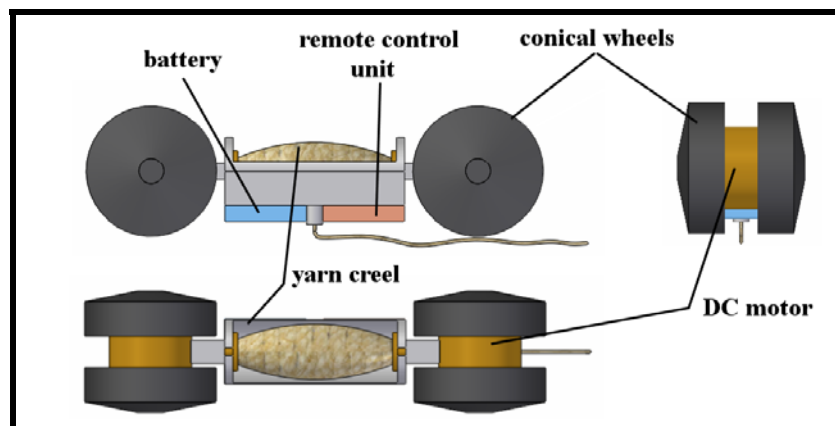


Figure 6.27. Detail of the Mobile Robot.

The desired mechanism for sley motion is selected as the robot shown in Figure 6.12 with a prismatic actuator and a four bar. The advantage of this system, it can be used for any carpet loom fits in its work space and light weight structure.

Due to the ease of control and ease of manufacture properties the weaver arm is selected as PPP serial robot manipulator (Figure 6.14). The system for the preparation of the pile for knotting is shown in Figure 6.17. For opening up workspace for knotting mechanism with double slider crank motion (Figure 6.18) is decided. The knotting operation will be by cylindrical manipulators. The gripper motion is supplied to ends of the manipulators by a wire and a gear distributes the motion equally to the both ends. Two motors for motion and one motor for gripping are used as shown in Figure 6.28.

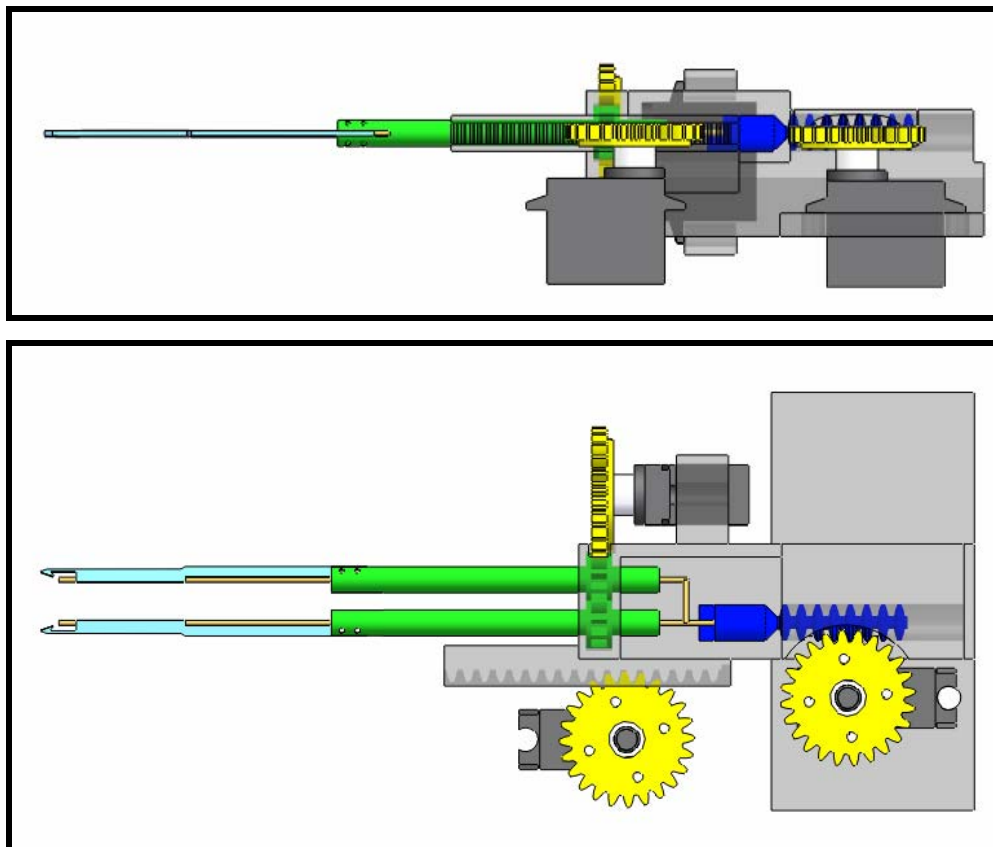


Figure 6.28. Cylindrical Manipulators.

Lastly for the weaver, grasping of pile ends is done with the slider crank mechanism shown in Figure 6.22. The whole system for the weaver is shown in Figure 6.29

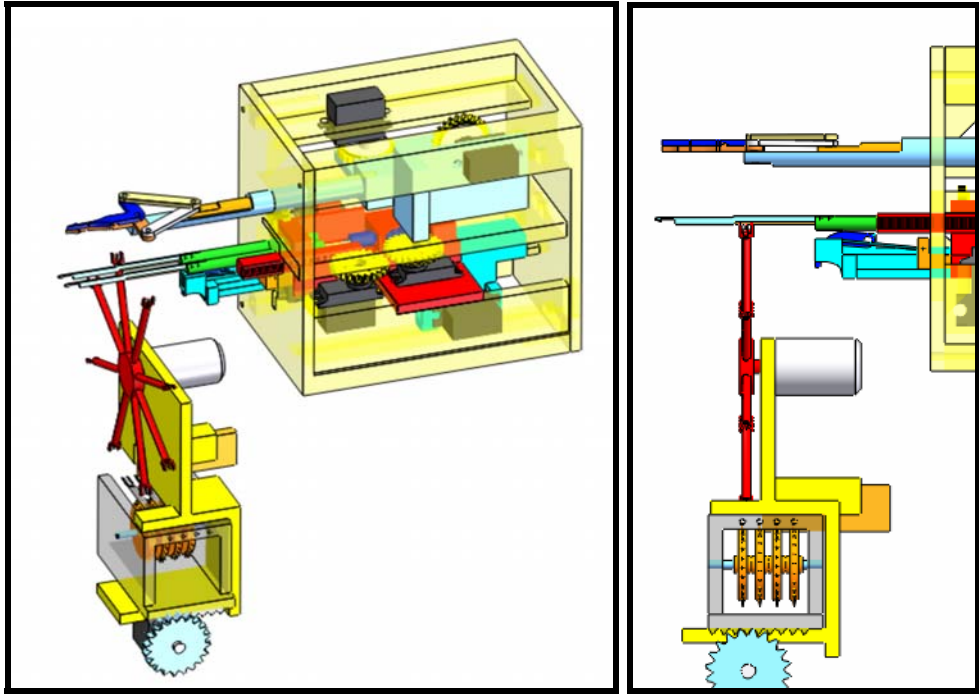


Figure 6.29. The Weaver.

After selecting all mechanisms the robot should be constructed as shown in Figure 6.30

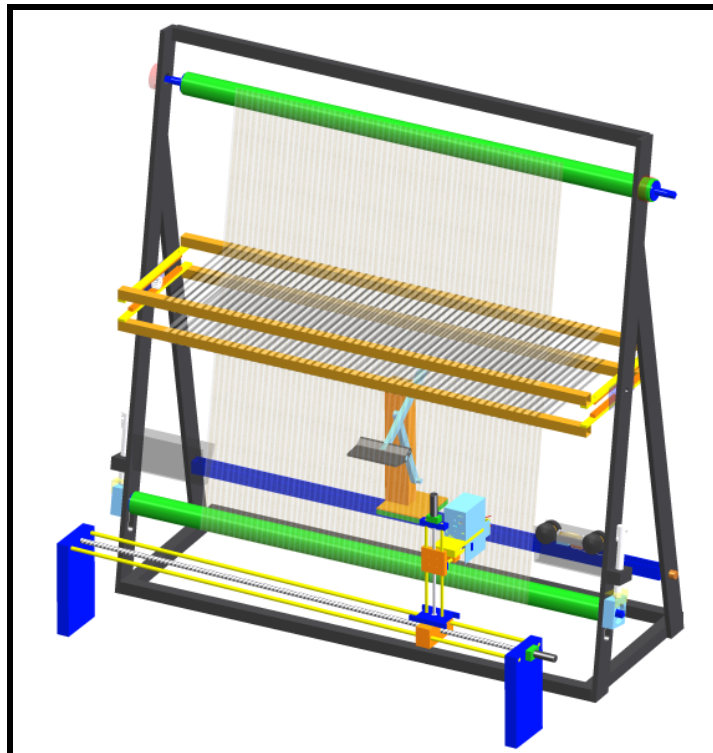


Figure 6.30. Carpet Weaving Robot.

CHAPTER 7

CONCLUSIONS

In this thesis structural design of overconstrained mechanisms and manipulators are investigated and their application to the robotization process is carried out. The unit vector algebra is improved and recurrent unit vector equations are presented for the analysis of linkages. An analytical method for finding new overconstrained mechanisms with general constraint one is given, all the mechanisms with general constraint one with revolute joints are given by using this method new mechanisms are build up. Found mechanisms are the only linear-angular constrained mechanism given by analytical formulations since Bennett proposed his spatial four bar linkage in 1903.

Moreover, in this study rigid body displacements in subspace with general constraint one are presented. Structural groups with revolute joints in subspace $\lambda=5$ are listed. After defining all single loop parallel manipulators and expressing the way to construct overconstrained parallel manipulators with defined structural groups, the proposed method is applied to the serial and parallel platform manipulators with loops of same or different conditions. Theory is detailed with examples.

Furthermore, the terminology and the definitions of the carpet technology process are summarized. The steps of the process of weaving are detailed in three main groups. Furthermore, the ornaments of Turkish hand woven carpets are tabulated with definitions to describe a way of combining these ornaments and getting new patterns. After investigating hand woven carpets, the motions of carpet weaving process are defined. The information gained during the structural synthesis of mechanism is used for the decision of mechanisms for robotization of hand woven carpet technology process. Finally, design of carpet weaving robot is introduced.

REFERENCES

- Alizade, R.I. and Bayram, Ç. 2004. Structural synthesis of parallel manipulators. *IFToMM Mechanism and Machine Theory* 39:857-870.
- Alizade, R.I., Bayram, Ç. and Gezgin, E. 2006. Structural synthesis of serial platform manipulators. *IFToMM Mechanism and Machine Theory* 42 (5):580-599.
- Alizade, R.I., Can, F.C., Gezgin, E. and Selvi, O. 2007. Structural synthesis of new parallel and serial platform manipulators. *12th IFToMM World Congress, Besancon, France, June*:18-21.
- Alizade, R.I., Can, F.C. and Gezgin, E. 2007. Structural synthesis of Euclidean platform robot manipulators with variable general constraints. *IFToMM Mechanism and Machine Theory*, <http://ees.elsevier.com/mechmt/> (accessed December 30, 2008)
- Alizade, R.I., Gezgin, E. and Selvi, O. 2007. Analytical approach for the mechanisms with one general constraint. *IFToMM Mechanism and Machine Theory*, <http://ees.elsevier.com/mechmt/> (accessed December 30, 2008)
- Altmann, P.G. 1954. Communications to Grodzinski, P. and M'Ewen, E, Link mechanisms in modern kinematics. *Proceedings of the Institution of Mechanical Engineers* 168 (37):889-896.
- Angeles, J. 2002. The qualitative synthesis of parallel manipulators. *Proceedings of the WORKSHOP on Fundamental Issues and Future Research Directions for Parallel Mechanisms and Manipulators October 3-4*:1-10.
- Baker, J.E. 1993. A geometrico-algebraic exploration of Altmann's linkage. *Mechanism and Machine Theory* 28 (2):249-260.
- Baker, J.E. 1997. The single screw reciprocal to the general plane-symmetric six screw linkage. *Journal for Geometry and Graphics* 1:5-12.

- Baker, J.E. 2000. On equivalent motions in spatial linkages. *Mechanism and Machine Theory* 35:1641-1649.
- Baker, J.E. 2002. Displacement-closure equations of the unspecialized double-Hooke's-joint linkage. *Mechanism and Machine Theory* 37:1127-1144.
- Baker, J.E. 2003. Overconstrained six-bars with parallel adjacent joint-axes. *Mechanism and Machine Theory* 38:103-117.
- Baker, J.E. 2005. A curious new family of overconstrained six-bars. *Transactions of the ASME* 127:602-606.
- Bennett, G.T. 1903. A new mechanism. *Engineering* 76:777-778.
- Bennett, G.T. 1905. The parallel motion of Sarrus and some allied mechanisms. *Philosophical Magazine 6th Series* 9:803-810.
- Bricard, R. 1927. Leçons de cinématique. *Gauthier-Villars* 2:7-12.
- Bode, Wilhelm and Ernst Kühnel. 1958. *Antique rugs from the near east*. Berlin :Klinkhardt and Biermann.
- Dai, J.S., Huang, Z. and Lipkin, H. 2006. Mobility of overconstrained parallel mechanisms. *Transactions of the ASME* 128:220-229.
- Dietmeier, P. 1995. A new 6R space mechanism. *Proceedings of Ninth World Congress on the Theory of Machines and Mechanisms, Milano* 1:52-56.
- Deniz , Bekir. 2000. *Türk dünyasında halı ve düz dokuma yaygıları*. Ankara:Atatürk Kültür Merkezi.
- Ellis, Charles G. 1976. *Early caucasian rugs: the textile museum fiftieth anniversary 1925-1975*. Washington. The Textile Museum.

- Fang ,Y. and Tsai, L.W. 2004. Structure synthesis of a class of 3-dof rotational parallel manipulators. *IEEE transactions on robotics and automation* 20(1):117-121.
- Fang ,Y. and Tsai, L.W. 2004. Analytical identification of limbs structures for translational parallel manipulators. *Journal of Robotic Systems* 21(5):209-218.
- Franke, R. 1951. Vom Aufbau der Getriebe. *Deutscher Ingenieur, Düsseldorf* 97-106.
- Freudenstein, F. and Alizade, R.I. 1975. On the degree of freedom of mechanisms with variable general constraint. *IV World IFToMM Congress England* 51-56.
- Gao, F., Li, W., Zhao, X., Jin, Z. and Zhao, H. 2002. New kinematic structures for 2-, 3-, 4-, and 5-dof parallel manipulators designs. *Mechanism and Machine Theory* 37:1395-1411.
- Gogu, G. 2005. Fully isotropic overconstrained parallel wrists with two degrees of freedom. *Proceedings of the 2005 IEEE International Conference on Robotics & Automation, Barcelona Spain April* 4014-4019.
- Goldberg, M. 1943. New five-bar and six-bar linkages in three dimensions. *Transactions of the ASME* 65:649–663.
- Grawshaw, Geoffrey H. 1987. *The manufacture of wool carpets*. Manchester: The Textile Institute.
- Gregorio, R.D. 2002. Translational parallel manipulators new proposals. *Journal of Robotic Systems* 19(12):595-603.
- Guest , S.D. and Fowler, P.W. 2005. A symmetry-extended mobility rule. *Mechanism and Machine Theory* 40:1002-1014.
- Harrisberger, L. and Soni, A.H. 1966. A survey of three dimensional mechanisms with one general constraint. *ASME 66-Mech-4:1-10*

- Herve , J.M. 2007. The planar-spherical kinematic bond: implementation in parallel mechanisms. <http://www.parallemic.org/Reviews/Review013.html>. (accessed November 21, 2007)
- Huang, C. and Sun, C.C. 2000. An investigation of screw systems in the finite displacements of Bennett-based 6R linkages. *Transactions of the ASME* 122:426-430.
- Huang, Z. and Li, Q.C. 2002. General methodology for type synthesis of symmetrical lower mobility parallel manipulators and several novel manipulators. *The International Journal of Robotics Research* 21(2):131-145.
- Jin, Q. and Yang, T. 2002. Overconstraint analysis on spatial 6-link loops. *Mechanism and Machine Theory* 37:267-278.
- Karger, A. 1998. Classification of 5R closed kinematic chains with self mobility. *Mechanism and Machine Theory* 33:213-222.
- Lee, C.C. and Herve, J.M. 2006. Translational parallel manipulators with doubly planar limbs. *Mechanism and Machine Theory* 41: 433-455.
- Lerbet. J. 2005. Coordinate-free kinematic analysis of overconstrained mechanisms with mobility one. *Zeitschrift fur Angewandte Mathematik und Mechanik* 85(10):740-747.
- Li, W., Sun, J., Zhang, J., He, K. and Du, R. 2006. A parallel 2 dof spherical mechanism with one-to-one input-output mapping. *Proceedings of the 6th WSEAS International Conference on Robotics. Control and Manufacturing Technology, Hangzo, China, April 16-18:6-11.*
- Making Carpets. http://www.handmadecarpets.net/carpet_store_kilims.htm (accessed December 17, 2007).

- Mavroidis, C. and Roth, B. 1994. Analysis and synthesis of overconstrained mechanisms. *Proceedings of the ASME Design Technical Conferences DE-70*:115-113.
- Mavroidis, C. and Roth, B. 1995. Analysis of overconstrained mechanisms. *Transactions of the ASME* 117:69-74.
- Mavroidis, C. and Roth, B. 1995. New and revised overconstrained mechanisms. *Transactions of the ASME* 117:75-82.
- Mavroidis, C. and Roth, B. 1995. Method to Determine Uncertain Configurations of 6R Manipulators. *Proceedings of the 9th World Congress on the Theory of Machines and Mechanisms, Milano, Italy* 3:1987-1992.
- Mavroidis, C. and Roth, B. 1995. New and revised overconstrained mechanisms. *Transactions of the ASME* 117:75-82.
- Mavroidis, C. and Beddows, M. 1997. A spatial overconstrained mechanism that can be used in practical applications. Proceedings of the 5th Applied Mechanisms and Robotics Conference, Cincinnati, OH, October 12-15
- Meng, J., Liu, G.F. and Li, Z. 2005. A geometric theory for synthesis and analysis of sub-6 dof parallel manipulators. *Proceedings of the 2005 IEEE international Conference on Robotics & Automation, Barcelona, Spain, April*: 2938-2943 .
- Neville, A.B. and Sanderson, A.C. 1996. Tetrobot family tree modular synthesis of kinematic structures for parallel robotics. *Proceedings of the IROS 96 IEEE* 382-389.
- Persian Rugs. <http://www.bestirantravel.com/culture/arts/rugs.html> (accessed December 17, 2007)

- Sarrus, P.T. 1853. Note sur la transformation des mouvements rectilignes alternatifs. en mouvements circulaires. et réciproquement. *Comptes Rendus Hebdomadaires des Séances de l'Académie des Sciences* 36:1036–1038.
- Schatz, Paul. 1998. *Rhythmusforschung und Technik*. Stuttgart:Verlag Freies Geistesleben.
- Shih . A.J. and Yan, H.S. 2002. Synthesis of a single-loop overconstrained six revolute joint spatial mechanism for two-position cylindrical rigid body guidance. *Mechanism and Machine Theory* 37:61-73.
- Tischler, C., Samuel, A. and Hunt, K. 2001. Selecting multi-freedom multi loop kinematic chains to suit a given task. *Mechanism and Machine Theory* 36:925-938.
- Topalbekiroğlu, M., Kireççi, A. and Dülger, L.C. 2005. Design of a pile-yarn-manipulating mechanism. *Proceedings of the IMechE, Part B Journal of Engineering Manufacture* 219:539-545.
- Topalbekiroğlu, M., Kireççi, A. and Dülger, L.C. 2005. A study of weaving Turkish knots in handmade carpets with an electromechanical system. *Proceedings of the IMechE, Part J Journal of System and Control Engineering* 219:343-347.
- Topalbekiroğlu, M. 2005. Kinematic analysis and synthesis of the knotting mechanisms can be used in the production of handmade carpet a case study. *Proceedings of the IMechE, Part C Journal of Mechanical Engineering Science* 219:987-1005.
- Turkish Republic Ministry of State-Ministry of Culture and Tourism. 1987-90. *Turkish hand woven carpets*. Ankara: Turkish Republic Ministry of State-Ministry of Culture and Tourism.
- Waldron, K.J. 1967. A family of overconstrained linkages. *Journal of Mechanism* 2:201-211.

- Waldron, K J. 1968. Hybrid overconstrained linkages. *Journal of Mechanisms* 3:73-78.
- Waldron, K J. 1969. Symmetric overconstrained linkages. *Transactions of the ASME. Journal of Engineering for Industry* B91:158-164.
- Wohlhart, K. 1987. A new 6R space mechanism. *Proceedings of the Seventh World Congress on the Theory of Machines and Mechanisms, Sevilla, Spain* 1:193–198.
- Wohlhart, K. 1991. Merging two general Goldberg 5R linkages to obtain a new 6R space mechanism. *Mechanism and Machine Theory* 26(2):659–668.
- Yetkin, Şerare. 1981. *Historical Turkish Carpets*. İstanbul: Türkiye İş Bankası.
- Yi ,Y., McInroy, J.E. and Jafari, F. 2004. Generating classes of orthogonal gough-stewart platforms. *Proceedings of the 2004 IEEE International Conference on Robotics & Automation*. New Orleans. LA April . 4969-4974

APPENDIX A

Force and Strength Calculations for Carpet Loom

In this appendix, force analysis of carpet loom will be given. Design of the beams under the loading, selection of the bearings and force on weft mechanism will be explained. The beams in the carpet mechanism can be taken as a beam under a distributed load with clamped-clamped ends. The value of the distributed load has been calculated as 15 N/mm. This calculation is also given in Figure A.1. In order to find the deflection of the beam under given loading integration method is used since the distributed load is known. According to integration method, the following non-homogeneous fourth order ordinary differential equation can be written in terms of deflection of the beam and loading.

$$EI \frac{d^4 y}{dx^4} = -w(x) \quad (\text{A.1})$$

where, E is Elastic or Young's modulus of the beam material, I is Moment of inertia of the cross-sectional area of the beam, $y(x)$ represents deflection, $w(x)$ is distributed load.

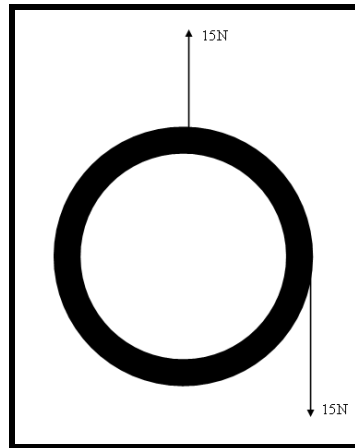


Figure A.1 Free Body Diagram of the Cylindrical Beam

Solution of any of these equations requires successive integrations to obtain the deflection, $y(x)$, of the elastic curve. In this case, the problem can be written as the following form

$$EI \frac{d^4 y}{dx^4} = -15 \quad (\text{A.2})$$

For each integration it is necessary to introduce a constant of integration and then solve for the entire constant to find an analytical solution for particular problem. By taking integral both sides of Equation (A.2), Equation (A.3) is obtained

$$EI \frac{d^3 y}{dx^3} = -15x + c_1 \quad (\text{A.3})$$

Using the similar procedure, deflection function is found as in Equation (A.4)

$$y(x) = \left(-\frac{5x^4}{8EI} + c_1 x^3 + c_2 x^2 + c_3 x + c_4 \right) \quad (\text{A.4})$$

In order to define the four integration constants in Equation (A.4), it can be used the following boundary conditions for clamped-clamped support beam shown in Figure A.2

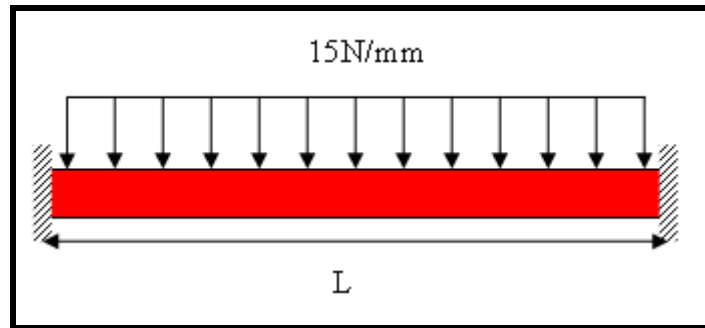


Figure A.2. Beam Loading and Boundary Conditions

$$y(0) = y(L) = 0, \frac{dy}{dx}(0) = \frac{dy}{dx}(L) = 0 \quad (\text{A.5})$$

Using the condition $y(0) = 0$, c_4 becomes 0. The condition $y(L) = 0$, gives

$$-\frac{5L^4}{8EI} + c_2 L^2 + c_3 L + c_1 L^3 = 0 \quad (\text{A.6})$$

Using condition $\frac{dy}{dx}(0) = 0$, c_3 becomes 0. The condition $\frac{dy}{dx}(L) = 0$ gives

$$\frac{-5L^3}{2EI} + 2Lc_2 + 3L^2c_1 = 0 \quad (\text{A.7})$$

Solving coupled equations, Equation (A.6) and Equation (A.7), integration constants are found to be

$$c_1 = \frac{5L}{4EI}, c_2 = -\frac{5L^2}{8EI}, c_3 = 0, c_4 = 0 \quad (\text{A.8})$$

Now, deflection function can be written by using Equation (A.4) and Equation (A.8) as

$$y(x) = -\frac{5(L-x)^2 x^2}{8EI} \quad (\text{A.9})$$

From the beam theory, it is known that the maximum deflection occurs in the middle of the beam for this type of loading and boundary conditions configurations. The formulation given in Equation(A.9) is valid, y_{\max} must be obtained at $x=L/2$. To check this, it can be used first derivative of $y(x)$ as

$$y'(x) = \frac{-5x(L^2 - 3Lx + 2x^2)}{4EI} \Rightarrow L^2 - 3Lx + 2x^2 = 0 \quad (\text{A.10})$$

The roots of Equation (A.10) give the point which causes the maximum deflection. From Equation (A.10) it is found $x = L/2$. Therefore the strength analysis is valid. In this structure, the length of the beam L is taken as 2 meters. Then for $L=2\text{m}$ Equation (A.9) becomes

$$y(x) = -\frac{5(2-x)^2 x^2}{8EI} \quad \text{and} \quad y_{\max}|_{x=L/2} = \frac{-5}{8EI} \quad (\text{A.11})$$

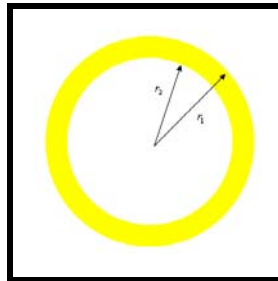


Figure A.3. Outer and Inner Radius of the Cylindrical Beam

$$I = \frac{\pi}{4} (r_1^4 - r_2^4) \quad (\text{A.12})$$

By using Equation (A.12), inner and outer radii for different materials can be found for $L=2m$. These are tabulated in Table A.2. In the calculation, maximum bending is taken as 1 mm for $L=2m$. Formulation given in Equation(A.11) is used in Tables A.1 and A.2 and steel is selected for production.

Table A.1. Moment of Inertia and Elastic Modulus Values for Different Materials
($L = 2m$)

Material	y_{\max} (mm)	E (Pa)	I (mm^4)
Steel	1	$200 \cdot 10^9$	$2.08333 \cdot 10^6$
Cast Iron(ASTM A-48)	1	$69 \cdot 10^9$	$6.03865 \cdot 10^6$
Aluminum Alloy 1100-H14	1	$70 \cdot 10^9$	$5.95238 \cdot 10^6$
Aluminum Alloy 2014-T6	1	$75 \cdot 10^9$	$5.55556 \cdot 10^6$
Copper	1	$120 \cdot 10^9$	$3.47222 \cdot 10^6$
Yellow Brass	1	$105 \cdot 10^9$	$3.96825 \cdot 10^6$
Tin Bronze	1	$95 \cdot 10^9$	$4.38596 \cdot 10^6$
Aluminum Bronze	1	$110 \cdot 10^9$	$3.78788 \cdot 10^6$

Table A.2. Alternatives of Inner and Outer Radiuses for Different Materials ($L = 2m$)

$L=2m$	r_1 (mm)	r_2 (mm)	r_1 (mm)	r_2 (mm)
Steel	43.14	30	60	56.7
Cast Iron(ASTM A-48)	54	30	60	48
Aluminum Alloy 1100-H14	53.8	30	60	47.9
Aluminum Alloy 2014-T6	53	30	60	48.17
Copper	47.82	30	60	49.27
Yellow Brass	49.2	30	60	54
Tin Bronze	50.3	30	60	53
Aluminum Bronze	48.7	30	60	52

For the calculations of force applied on weft mechanisms firstly the vertical force of one warp thread is found as shown below.

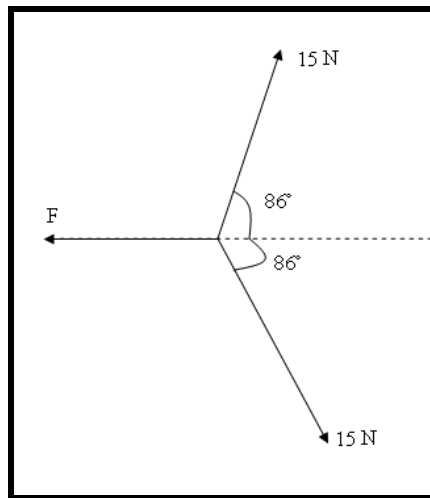


Figure A.4. Equilibrium of warp thread at working position

The force F can be calculated from the following equilibrium equation $15\cos 86^\circ + 15\cos 86^\circ = F$, $F = 2.1\text{N}$, for 400 warp threads, we obtain 840 N

In order to choose the bearing at the ends of the beam, the radial forces given in Figure 6.2 must be determined. Neglecting the weight of the beam, the forces F_b can be found as, $2F_b = 15\text{N} / \text{mm} \times 2000\text{mm}$, $F_b = 15\text{kN}$. Therefore 15kN must be in the bearing working interval. By using the Table A.3 we choose the UC 206 or UC 207.

Table A.3. Bearing Types from ORS Catalog

Bearing Type	Dimensions						Load Rating		Speed Limit	
	d (mm)	D (mm)	B_o (mm)	B_i (mm)	r_{omin} (mm)	r_{imin} (mm)	C_{ISO} (kN)	$C_{0,ISO}$ (kN)	Grease n_g (rpm)	Oil
UC 205	25	52	34.1	17	0.4	1	14.02	7.88	12 500	16 000
UC 206	30	62	38.1	19	0.5	1	19.45	11.26	10 000	12 500
UC 207	35	72	42.9	20	0.5	1.5	25.67	15.30	9 000	11 000
UC 208	40	80	49.2	21	0.5	1.5	29.11	17.90	8 000	10 000
UC 209	45	85	49.2	22	0.5	1.5	32.71	20.46	7 500	9 000
UC 210	50	90	51.6	23	0.5	1.5	35.07	23.18	6 800	8 200
UC 211	55	100	55.6	24	0.75	2	43.38	29.22	6 200	7 400
UC 212	60	110	65.1	26	0.75	2	52.42	36.17	5 600	6 700